



Cite this: *Chem. Soc. Rev.*, 2015,  
44, 6187

## Centrifugal microfluidic platforms: advanced unit operations and applications

O. Strohmeier,<sup>†ab</sup> M. Keller,<sup>†ab</sup> F. Schwemmer,<sup>†b</sup> S. Zehnle,<sup>†a</sup> D. Mark,<sup>ab</sup>  
F. von Stetten,<sup>ab</sup> R. Zengerle<sup>abc</sup> and N. Paust<sup>\*ab</sup>

Centrifugal microfluidics has evolved into a mature technology. Several major diagnostic companies either have products on the market or are currently evaluating centrifugal microfluidics for product development. The fields of application are widespread and include clinical chemistry, immunodiagnostics and protein analysis, cell handling, molecular diagnostics, as well as food, water, and soil analysis. Nevertheless, new fluidic functions and applications that expand the possibilities of centrifugal microfluidics are being introduced at a high pace. In this review, we first present an up-to-date comprehensive overview of centrifugal microfluidic unit operations. Then, we introduce the term “process chain” to review how these unit operations can be combined for the automation of laboratory workflows. Such aggregation of basic functionalities enables efficient fluidic design at a higher level of integration. Furthermore, we analyze how novel, ground-breaking unit operations may foster the integration of more complex applications. Among these are the storage of pneumatic energy to realize complex switching sequences or to pump liquids radially inward, as well as the complete pre-storage and release of reagents. In this context, centrifugal microfluidics provides major advantages over other microfluidic actuation principles: the pulse-free inertial liquid propulsion provided by centrifugal microfluidics allows for closed fluidic systems that are free of any interfaces to external pumps. Processed volumes are easily scalable from nanoliters to milliliters. Volume forces can be adjusted by rotation and thus, even for very small volumes, surface forces may easily be overcome in the centrifugal gravity field which enables the efficient separation of nanoliter volumes from channels, chambers or sensor matrixes as well as the removal of any disturbing bubbles. In summary, centrifugal microfluidics takes advantage of a comprehensive set of fluidic unit operations such as liquid transport, metering, mixing and valving. The available unit operations cover the entire range of automated liquid handling requirements and enable efficient miniaturization, parallelization, and integration of assays.

Received 3rd November 2014

DOI: 10.1039/c4cs00371c

www.rsc.org/chemsocrev

### 1. Introduction

Microfluidics enables the miniaturization, integration, and automation of laboratory processes ranging from basic operations to complex biochemical assays. Obviously, an increase in the research activities in this field has been accompanied by a much slower conversion of microfluidic approaches into products. The reasons for this tardy technology transfer have been extensively discussed in previous studies,<sup>1,2</sup> stating for instance a lack of flexibility of the microfluidic implementations, which allow for a very limited number of applications for a single microfluidic device.

All of the research, development, and certification expense would have to be paid off by these very limited number of applications developed for a small market segment.

As one possible solution, microfluidic platform-based approaches have been suggested.<sup>3,4</sup> A microfluidic platform provides a set of microfluidic unit operations such as liquid transport, metering, mixing and valving. The unit operations are validated, scalable, and standardized, and can be combined in an easy and consistent manner. In some cases, it might be possible that a fixed set of unit operations is implemented within a generic disposable cartridge, in which different applications can be processed, simply by adjusting chemistry. In general, the key advantage of using platforms is the possibility to make use of building blocks from existing solutions to implement new applications with reduced effort and risk, and to address an increased market, which can be as large as the number of applications implemented within a platform.

The company Cepheid impressively demonstrated platform based automation of biochemical analysis. An application specific cartridge was introduced, but the cartridge is capable of

<sup>a</sup> Hahn-Schickard, Georges-Koehler-Allee 103, 79110 Freiburg, Germany.  
E-mail: Nils.Paust@Hahn-Schickard.de; Tel: +49 761 203 73245

<sup>b</sup> Laboratory for MEMS Applications, IMTEK – Department of Microsystems Engineering, University of Freiburg, Georges-Koehler-Allee 103, 79110 Freiburg, Germany

<sup>c</sup> BIOS Centre for Biological Signalling Studies, University of Freiburg, Schanzlestr. 18, 79104 Freiburg, Germany

† Authors contributed equally.



performing analysis for many different targets by changing the analysis chemistry. Thus, a single cartridge covers a large range of products for nucleic acid-based sample-to-answer testing with high market penetration (e.g., \$411 million annual turnover by Cepheid, 2014).<sup>5</sup> Based on one cartridge format, 22 different tests are currently available, covering applications in the fields of healthcare-associated infections, critical infectious diseases, sexual health, and oncology. In dependency of the desired throughput, processing devices for 1, 2, 4, or 16 cartridges in parallel are available.<sup>5</sup> Another success story for *in vitro* diagnostics testing at the point-of-care is the handheld device and the microfluidic cartridges from Abbott's i-STAT system, for which more than 35 million tests were sold in 2014.<sup>6</sup> Cartridges are available for measuring blood chemistries and electrolytes, hematology, blood gases, coagulation, or cardiac markers.<sup>6</sup> It has been predicted that the market for microfluidic automation will continue to grow. The market for microfluidic devices for point-of-care applications alone is expected to grow

from US\$200 million today to a US\$800 million turnover in 2019.<sup>7</sup> In order to be successful, a microfluidic platform has to fully cover the functionalities from sample input to data analysis for the desired range of applications. Several recent publications e.g. by Mark *et al.*, Sin *et al.* or Madou *et al.*, provide criteria to select an appropriate microfluidic platform.<sup>8–10</sup>

This review intends to deepen the understanding of platform-based microfluidic automation. It focuses exclusively on platforms making use of centrifugal microfluidics in order to provide detailed insight into this obviously emerging technology. When compared to other microfluidic platforms, centrifugal microfluidics has several strengths: the centrifugal propulsion mechanism allows for a closed fluidic system, free of any interfaces to external pumps. The removal of any bubbles that may interfere with the proper performance of an assay is particularly simple due to the scalable buoyancy in the centrifugal gravity field. In addition, residual liquids that may be trapped due to surface forces can be removed from channels, chambers and sensor matrixes, again, simply by adjusting



**O. Strohmeier**

*Oliver Strohmeier studied Microsystems Engineering, majoring in life sciences at IMTEK. In 2008, he finished his studies with a diploma thesis on enzymatically catalyzed biofuel cells. For dissertation, he afterwards joined the Lab-on-a-Chip division at the Laboratory for MEMS Applications mainly working on the integration of molecular biological tests on the centrifugal microfluidic platform. Since December 2011, he is heading the joint research group*

*for centrifugal microfluidics – LabDisk at Hahn-Schickard and at the Laboratory for MEMS Applications together with Mark Keller.*



**M. Keller**

*Mark Keller studied Microsystems Engineering majoring in life sciences at IMTEK. In 2011 he graduated as a Master of Science with a master's thesis in the field of neuroprosthetics at the Laboratory for Biomedical Microtechnology. For dissertation, he afterwards joined the Laboratory for MEMS Applications. There he works as an R&D engineer on the integration of nucleic acid analyses in the centrifugal microfluidic platform group of the Lab-on-a-Chip*

*division. Since March 2013, he is heading the joint research group for centrifugal microfluidics – LabDisk at Hahn-Schickard and at the Laboratory for MEMS Applications together with Oliver Strohmeier.*



**F. Schwemmer**

*Frank Schwemmer studied physics at the University of Würzburg and the University of Texas at Austin, where he received his master's degree in physics in 2010 for his work on energy landscapes of ligand-receptor interactions. He currently works as an R&D engineer and PhD candidate within the Laboratory for MEMS Applications at the University of Freiburg. His research focuses on the development of Lab-on-a-chip systems, new unit operations and prototyping processes in centrifugal microfluidics.*



**S. Zehnle**

*Steffen Zehnle studied Microsystems Engineering at the University of Freiburg and the Technical University of Denmark. He received his master's degree in 2012 with a master's thesis on pneumatic unit operations on centrifugal microfluidic platforms. Since 2012 he works as an R&D Engineer and PhD candidate in the Lab-on-a-Chip division at Hahn-Schickard. His research focuses on the development of new unit operations and assay automation on both LabDisk and LabTube platforms.*



the volume forces by rotation. The strength of centrifugal microfluidics is reflected by an enormous breadth of available unit operations and initiated an increase in research activity on the one hand and an increasing commitment by major diagnostic companies on the other hand. Panasonic, Roche, Samsung, 3M, and Abaxis already have centrifugal microfluidic-based products on the market and a considerable number of additional companies are currently evaluating the use of centrifugal microfluidics for their applications.

The last published comprehensive review on centrifugal microfluidics focused on the history and individual biomedical applications.<sup>11</sup> Since then, more than 300 papers have been published on centrifugal microfluidics. An overview of the scientific journal publications and selected milestones in technology transfer is depicted in Fig. 1. Among the scientific publications, a clear trend toward the full integration of a complex sample-to-answer analysis can be observed. In addition, ground breaking novel unit operations have been developed that have the potential of making significant contributions to the field in the near future. Consequently, our review highlights these recent innovations. Special focus is directed towards the process of translating the assay step by step into a microfluidic layout, particularly the method used for combining unit operations to facilitate the miniaturization, integration, and automation of laboratory processes on centrifugal microfluidic platforms. Whereas basic fluidic functionalities are called unit operations, for a concatenation of such basic functionalities representing a laboratory workflow, we introduce the term “process chain.” In this context, we propose to standardize fluidic unit operations for the implementation of basic stand-alone functionalities such as metering, valving, and mixing. For the integration of frequently applied complete laboratory workflows, process chains should be standardized to allow for their efficient implementation without the need to deal with the basic functionalities. Examples of process chains

are chemical cell lysis, nucleic acid purification and amplification, blocking to avoid unspecific binding, washing, immunocapture, *etc.* The terms used to describe the centrifugal microfluidic platform-based approach are defined in Table 1. Application examples for the hierarchy of a fluidic layout using process chains are depicted in the respective application chapter. Throughout this review, wherever suitable, we attempt to explain the implemented centrifugal microfluidic applications using the categories “process chains” and the underlying “unit operations.”

This review is structured as follows. First, the physics of centrifugal microfluidics is briefly outlined, followed by a comprehensive review of the established and recently proposed centrifugal microfluidic unit operations. Based on the review of microfluidic unit operations, we reach conclusions about how some of the described developments will foster the integration of more complex applications. Subsequently, we review centrifugal microfluidic implementations of nucleic acid-based analysis; immunodiagnosics; clinical chemistry; and the analysis of food, water, and soil. Specific embodiments of centrifugal microfluidic systems, *e.g.*, specific platforms using centrifugal microfluidics that are commercially available or under development are briefly outlined thereafter. Finally, we summarize the strengths and limitations and identify and discuss future trends.

### 1.1 Physics of centrifugal microfluidics

In order to understand the unit operations used in centrifugal microfluidics, we hereby introduce the forces that are exploited on this platform, as illustrated in Fig. 2. In general, we differentiate between intrinsic forces—sub-classified into pseudo-forces and non-pseudo forces—that are induced merely by the presence or absence of centrifugation, and extrinsic forces resulting from the use of external means.

**1.1.1 Intrinsic forces.** Pseudo-forces are inertial body forces acting on fluids or particles in rotating systems. In centrifugal



**R. Zengerle**

*Dr Roland Zengerle is full professor at the Department of Microsystems Engineering at the University of Freiburg and director at the “Hahn-Schickard-Institut für Mikro- und Informationstechnik”. The research of Dr Zengerle is focused on microfluidics and specialises in Lab-on-a-chip solutions, non-contact microdispensing, medical MEMS, bio fuel cells as well as micro- and nanofluidics in porous media. Dr Zengerle co-authored more than 300 papers. He is a*

*member of the German national academy of sciences, Leopoldina, a board member of the Chemical and Biological Microsystems Society (CBMS) as well as an international steering committee member of the International Conference on Solid-State Sensors, Actuators & Microsystems (Transducers).*



**N. Paust**

*Dr Nils Paust studied energy and process engineering at the Technical University of Berlin with a focus on fluid mechanics, thermodynamics and control engineering (degree: diploma). He received his PhD with the dissertation entitled “Passive and self-regulating fuel supply in direct methanol fuel cells” at the University of Freiburg in 2010. Since February 2010, he is head of the group LabTube at Hahn-Schickard in Freiburg. Main*

*research interest of Nils Paust is the centrifugal microfluidic system integration. This comprises new microfluidic functionalities, the interface between fluidics and scalable cost-efficient mass fabrication and the implementation of complete laboratory workflows on centrifugal microfluidic platforms.*



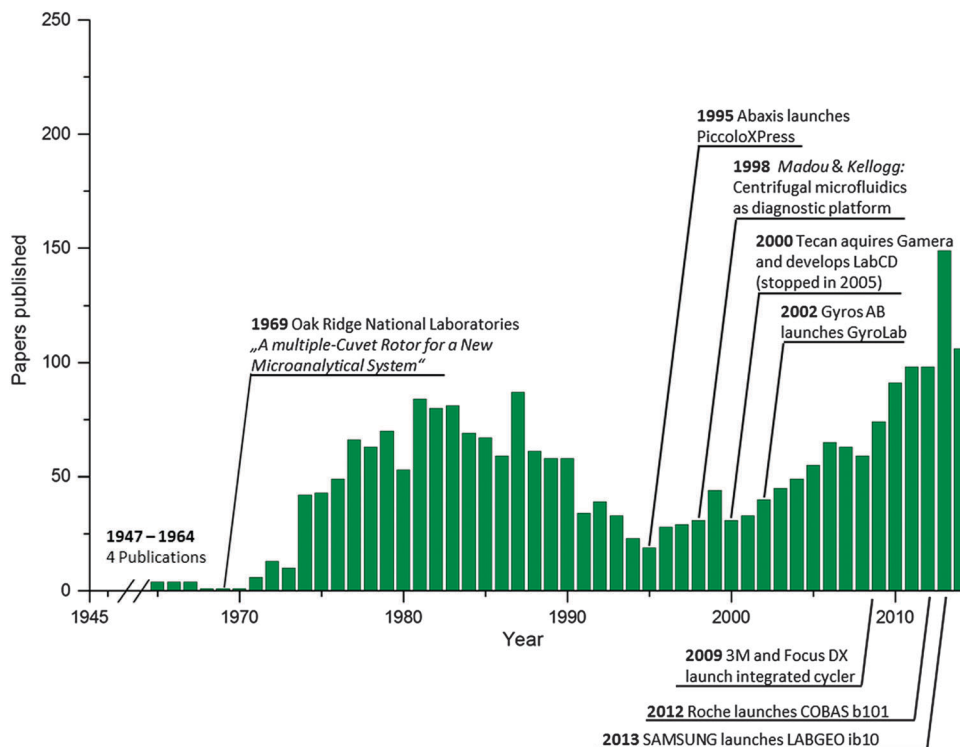


Fig. 1 Annual number of publications related to centrifugal microfluidics (source: Thomson Reuters ISI web of science); search term: "centrifug\* AND (microfluid\* OR analyzer\* OR analyser)" in the category "topic" accessed on March 15, 2015) and landmarks in technology transfer. The highlighted landmarks were selected based on their importance for the field starting from the basic idea in 1969 through the era of centrifugal analyzers, the launch of the first diagnostic product in 1995 (Abaxis Piccolo XPress) and companies that generated basic IP in the field (such as Tecan and Gyros), to the market entry of several global players (3M, Roche, Samsung). Further information on the history of centrifugal microfluidics is given in Section 4 "Embodiments of centrifugal microfluidic platforms".

microfluidics, they arise from the centripetal acceleration of the rotor and are therefore easily controllable. Pseudo-forces comprise the centrifugal force ( $F_c$ ), Coriolis force ( $F_{Co}$ ), and Euler force ( $F_E$ ). The forces exerted on a point-like body (mass  $m$ ) at position  $r$  in a system rotating with an angular rotational frequency  $\omega$  are given by eqn (1)–(3):

$$F_c = -m\omega \times (\omega \times r) \quad (1)$$

$$F_{Co} = -2m\omega \times \frac{d}{dt}r \quad (2)$$

$$F_E = -m\frac{d}{dt}\omega \times r \quad (3)$$

For the basic design of fluidic elements, it is convenient to use scalar differential pressures  $\Delta p$  rather than vectorial forces  $F$ , so that the centrifugal pressure over a liquid column (density  $\rho$ ) yields

$$\Delta p_c = \frac{1}{2}\rho\omega^2(r_2^2 - r_1^2) \quad (4)$$

where  $r_1$  is the inner radial point, and  $r_2$  is the outer radial point of the liquid column.

Non-pseudo forces are present in rotating systems, as well as in non-rotating systems. Hence, they are not limited to centrifugal platforms, but still play a major role in many centrifugal unit operations. The most dominant and most exploited non-pseudo forces and their corresponding differential pressures

are the viscous force ( $\Delta p_v$ ) (eqn (5)), pneumatic force ( $\Delta p_{pneu}$ ) (eqn (6)) exerted by a pressurized gas, capillary force ( $\Delta p_{cap}$ ) (eqn (7)), and fluidic inertia ( $\Delta p_i$ ) (eqn (8)).

$$\Delta p_v = -R_{hyd}q \quad (5)$$

$$\Delta p_{pneu} = p_0 \left( \frac{V_0}{V} - 1 \right) \quad (6)$$

$$\Delta p_{cap} = \sigma\kappa \quad (7)$$

$$\Delta p_i = -\rho la \quad (8)$$

Here,  $R_{hyd}$  is the hydraulic resistance, which is proportional to the dynamic viscosity  $\mu$ ;  $q$  is the volumetric flow rate;  $p_0$  denotes the ambient pressure;  $V_0$  is the volume of a gas bubble at  $p_0$ ; and  $V$  is the gas volume in a compressed (or expanded) state. Furthermore, we define  $\sigma$  to be the surface tension of a processed liquid, and  $\kappa$  to be the curvature of its meniscus, while  $l$  is the length of a fluidic channel filled with the liquid, and  $a$  is the acceleration of the liquid.

In the case of particle transport in fluids, such as in sedimentation processes, the particles are subject to a viscous force: the drag force ( $F_d$ ). It is given by

$$F_d = C_d \frac{\rho_{fluid}}{2} u^2 A_{particle} \quad (9)$$

where  $\rho_{fluid}$  and  $u$  are the density and velocity of the fluid relative to a particle, respectively;  $A_{particle}$  is the particle's cross



**Table 1** Definitions. The terms microfluidic platform, microfluidic chip, processing device, fluidic unit operations, and process chains are used throughout the review and defined accordingly

Term	Definition
Microfluidic platform	A microfluidic platform provides a set of validated fluidic unit operations, which are designed for easy combination within a standardized fabrication technology. <sup>8</sup> The platform approach enables efficient implementation of various laboratory workflows and/or applications.
Microfluidic chip/ microfluidic cartridge	A microfluidic chip, which is often referred to as a microfluidic cartridge, is a substrate that provides structures like chambers, channels, <i>etc.</i> for the hardware implementation of the fluidic unit operations. For most applications, microfluidic chips are disposed of after use to avoid cross contamination and/or save regeneration cost.
Fluidic unit operations	...are basic fluidic functionalities such as the following: <ul style="list-style-type: none"> <li>• sample and reagent supply</li> <li>• reagent pre-storage and release</li> <li>• liquid transport</li> <li>• valving and switching</li> <li>• metering and aliquoting</li> <li>• mixing</li> <li>• separation</li> <li>• droplet generation</li> <li>• detection</li> <li>• ...</li> </ul>
Processing device	The processing device (often also called the “instrument”) is a piece of reusable hardware that provides additional means to operate the microfluidic chip. This may comprise the main actuator ( <i>e.g.</i> , spinning drive) to control the fluids, as well as external means such as temperature control and/or magnetic, electric, optic, pneumatic, or mechanical features, including a means for detection/read-out.
Process chains	...are assemblies of fluidic unit operations and external means that represent laboratory workflows on a higher level of integration. Examples of process chains are... <ul style="list-style-type: none"> <li>• blood plasma separation</li> <li>• cell lysis</li> <li>• nucleic acid purification</li> <li>• nucleic acid amplification</li> <li>• immunocapture</li> <li>• washing</li> <li>• blocking</li> <li>• ...</li> </ul>

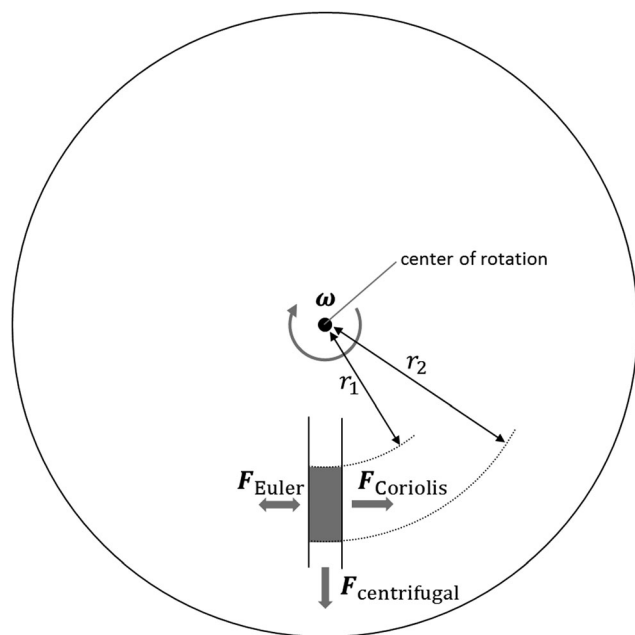


**Fig. 2** Pseudo-forces acting in centrifugal microfluidics. While the centrifugal force always acts radially outward, the Coriolis force acts perpendicular to both  $\omega$  and the fluid velocity, and the Euler force is proportional to the angular acceleration.

sectional area; and  $C_d$  is the drag coefficient. For the laminar flow regime (Stoke's drag), the drag coefficient is proportional

to the fluid viscosity  $\mu$  and inversely proportional to its velocity  $u$  relative to the particle, such that for a spherical particle with radius  $r$ , the drag force yields

$$F_s = 6\pi\mu ru. \quad (10)$$

**1.1.2 Extrinsic forces.** Extrinsic forces are used whenever centrifugation alone cannot fulfill the tasks to be accomplished in a centrifugal microfluidic cartridge. Such forces can be magnetic, electric, or pneumatic forces that bring fluids or particles into motion. The intentions of exploiting extrinsic forces are manifold and range from the mixing of liquids using magnetic beads or pneumatic stirring to the pumping of liquids and magnetophoretic or dielectrophoretic separation.

Paramagnetic beads are commonly used in suspensions and attracted by external magnets on- or off-chip. The magnetic force  $F_{\text{mag}}$  acting on a spherical paramagnetic bead exposed to a magnetic flux density  $B$  is given by

$$F_{\text{mag}} = V_{\text{bead}} \frac{\chi_{\text{bead}}}{\mu_0} (\nabla B) B \quad (11)$$

where  $V_{\text{bead}}$  is the volume of the magnetic bead,  $\chi_{\text{bead}}$  is its magnetic volume susceptibility, and  $\mu_0$  is the magnetic vacuum permeability. The susceptibility of the surrounding medium is neglected.

Electric forces can be applied in centrifugal systems *via* electrodes, which are preferably integrated into the microfluidic cartridge.



This ensures the permanent and proximal exposure of samples to an electric field to perform electrolysis, dielectrophoresis, and other separation processes. The use of an external pneumatic pressure in centrifugal microfluidics can be realized in a non-contact fashion such as by directing a pressurized gas jet at certain openings of a rotating platform. Thus, the impact pressure of the gas is applied to the microfluidic network.<sup>12</sup>

## 2. Unit operations

A microfluidic platform provides a set of validated fluidic unit operations, which are designed for easy combination within a standardized fabrication technology.<sup>8</sup> Unit operations are defined as the basic fluidic functionalities of a microfluidic platform. Examples of unit operations include sample and reagent supply, reagent pre-storage and release, liquid transport, valving and switching, metering, aliquoting, mixing, and detection. Assemblies of unit operations enable the efficient implementation of various process chains, which are laboratory workflows and/or applications on a higher level of integration. Examples of such process chains include blood plasma separation, cell lysis, nucleic acid purification, nucleic acid amplification, immunocapture, washing, and blocking. In the following, prominent unit operations are introduced and discussed in the light of their applications.

### 2.1 Sample and reagent supply

It is inherently necessary to load the sample material and certain reagents for sample processing and analysis into the centrifugal microfluidic cartridge, either prior to or during processing. In more advanced applications and commercially available products, reagents are typically prestored in the cartridge to facilitate handling. Despite their importance, sample supply and reagent prestorage are seldom considered in academic publications. The following section will give an overview of the relevant concepts for sample loading and prestorage and the release of reagents in centrifugal microfluidic cartridges.

**2.1.1 Sample supply.** In the majority of academic studies and some commercially available products (*e.g.*, Abaxis Piccolo Xpress), centrifugal microfluidic cartridges are loaded with the sample by manually pipetting them into microfluidic chambers *via* inlet holes using pipettes<sup>13</sup> or syringes.<sup>14</sup> Conversely, solutions for automated sample addition have been demonstrated using pipetting robots.<sup>15</sup> Both approaches to reagent supply, however, require open connections to the environment and can only be performed while the cartridge is not rotating. The latter can be avoided by applying concepts for the non-contact addition of reagents onto rotating cartridges.<sup>16–18</sup>

The direct uptake of whole blood *via* a cartridge-integrated capillary was demonstrated by Rombach *et al.*<sup>19</sup> An integrated capillary primes upon contact with a fingerprick blood sample and fills up with a defined volume. Subsequently, the blood is centrifuged to downstream processing chambers and directly processed by the cartridge to detect cholesterol. The uptake of whole blood by capillary forces was also integrated into the Roche Cobas b 101 system.<sup>20</sup>

**2.1.2 Integrated reagent prestorage.** For the commercialization of centrifugal microfluidics, it is important to facilitate the ease of use and reduce the hands-on time and cross contamination (*e.g.*, *via* openings to the environment). This requires the integration of on-board reagent prestorage, and the controlled release of liquid reagents or rehydration of dry reagents at a certain assay step.<sup>21</sup> Furthermore, on-board reagent prestorage eliminates the risk associated with mixing reagents from different production batches, which facilitates quality control. Prestorage in general can be subdivided into the prestorage of liquids, dried reagents, and functional immobilisation of reagents onto surfaces. Whereas the prestorage of dried reagents and surface functionalizations are rather biochemical challenges and intensively discussed elsewhere,<sup>22,23</sup> this review focuses on liquid reagent prestorage and their release in centrifugal microfluidic cartridges. For a deeper insight into reagent prestorage in microfluidics in general, the interested reader is directed to Hitzbleck *et al.*<sup>21</sup>

The prestorage of liquid reagents allows complete hands-off automation obviating the need for manual reagent addition during processing. The diverse nature of chemical and biochemical reagents, including alcohols, solvents, aqueous solutions, *e.g.*, with a high salt concentration<sup>24</sup> or proteins and enzymes, renders their long-term stable prestorage extremely challenging. Alcoholic reagents evaporate easily and therefore need to be prestored in materials with low vapor transmission rates. Solvents and aqueous solutions might chemically interact with the surrounding material. Proteins and enzymes can degrade over time, with a loss in activity or change in concentration in the solution as a result of adsorption to the cartridge and container material.

The concepts for the prestorage of liquid reagents can be roughly divided into two groups: (1) prestorage in suitable containers that are placed in the cartridge or (2) prestorage directly in microfluidic chambers on the cartridge. The prestorage of reagents in additional containers might be a superior way to reduce physical and chemical interactions between the reagent and the cartridge material (mainly polymers) and is less critical with respect to swelling, water uptake, and vapor transmission.<sup>24</sup> However, the required technologies for container fabrication and the mechanisms for releasing the reagents from the containers into the fluidic networks are more complex. Because of its advantages, commercially available centrifugal microfluidic systems like the Abaxis Piccolo Xpress<sup>25</sup> or Roche Cobas b 101<sup>20</sup> use reagent prestorage in additional containers.

The long-term stable prestorage of liquid reagents for DNA extraction has been demonstrated by Hoffmann *et al.*<sup>24</sup> Washing- and elution-buffers were encapsulated in glass ampoules, which were placed in the cartridge. To release the reagents into the microfluidic structures, the glass ampoules were crushed manually prior to processing. Ethanol and water have been prestored for time periods of up to 300 days without any noticeable losses. Glass ampoules have further been used to prestore rehydration buffer for lyophilized polymerase pellets (Fig. 3b).<sup>26</sup> A prestorage concept with a release mechanism that



solely relies on centrifugal forces was presented by van Oordt *et al.* Liquid reagents were packed in miniature stick packs, which were fabricated from vapor-tight aluminum composite foil. Liquid was released *via* a peelable seal<sup>27</sup> on the outer side of the stick pack by exceeding a defined centrifugal force (Fig. 3a). A 250  $\mu\text{L}$  quantity of 10% v/v isopropanol in water did not show any significant evaporation after storage at 70  $^{\circ}\text{C}$  for 21 days, which corresponded to 18 months of storage at room temperature.<sup>28</sup> This concept has later been used by Czilwik *et al.* for prestorage and on-demand release of a rehydration buffer for PCR reagents.<sup>29</sup> The reagent release by centrifugation would furthermore enable the handling of highly wetting reagents, such as alcoholic buffer solutions, which could cause unwanted capillary priming of the microfluidic channel network if loaded to the disk in absence of centrifugal forces. The prestorage of highly reactive bromine water in inert Teflon or glass tubes sealed by ferrowax plugs was demonstrated by Hwang *et al.* The reagent release was controlled by melting the wax plugs *via* laser irradiation allowing the bromine to diffuse out while the diffusion was stopped after resolidification of the wax. This principle allowed the release of reagents in small increments depending on the progress of the chemical reaction.<sup>30</sup> Kawai *et al.* presented a rotatable reagent cartridge that was placed in a centrifugal microfluidic disk. Different reagents for an enzymatic L-lactate assay with volumes between 230 nL and 10  $\mu\text{L}$  were sequentially released by rotating the container, and thereby connecting the respective compartment with the microfluidic channel network. The recovery of more than 96% of the prestored reagents was reported.<sup>31</sup>

Liquid reagent prestorage directly within a cyclic olefin polymer (COP) cartridge has been demonstrated with fluid reservoirs connected to the microfluidic system *via* optofluidic valves. Prestorage without noticeable fluid loss was demonstrated for a period of one month.<sup>32,33</sup> The prestorage of tetramethyl benzidine (TMB), washing buffer, and detection antibody solution directly in the cartridge was

demonstrated by Kim *et al.* The single reservoirs were connected to the microfluidic network *via* ferrowax valves that were opened by laser irradiation.<sup>34</sup> A similar concept was used to connect the prestored liquids to the microfluidic channel network *via* wax valves with different melting temperatures, thereby making it possible to sequentially release liquids into the network by melting the valves using infra-red heating.<sup>35</sup>

Recently, the LabTube was introduced as a new concept for centrifugal microfluidics based on stacked microfluidic elements.<sup>36</sup> A centrifugally actuated ballpen mechanism enables the simultaneous axial and rotatory movement of the stacked elements “revolvers” relative to each other. A first revolver comprises cavities for the storage of reagents with pierceable aluminum foil. A second revolver is equipped with lancing structures. The serial release of reagents is controlled by the ballpen mechanism, which lances the reagent cavities either in parallel or one after the other.

The prestorage of dry reagents is mostly conducted by drying reagents to the surface or placing dry/lyophilized pellets or functional beads into microfluidic chambers during fabrication. Drying of reagents directly onto the cartridge surface has successfully been demonstrated for polymerase chain reaction (PCR) primers and probes<sup>37–40</sup> and genomic DNA.<sup>41</sup> In another work, dry enzyme pellets for the detection of nitrite and hexavalent chromium were prestored in microfluidic chambers on the cartridge. After a storage period of 31 days in a desiccator, the relative standard deviation of the concentration adjusted absorbance was 7.91%.<sup>42</sup> The prestorage of lyophilized enzymes for DNA amplification was demonstrated by Lutz *et al.*<sup>26</sup> and Strohmeier *et al.*<sup>43</sup>

## 2.2 Transport of liquids

A fundamental unit operation in centrifugal microfluidics is the transport of liquids within a fluidic network of channels and chambers. Typically, centrifugal forces, created by a defined rotation,

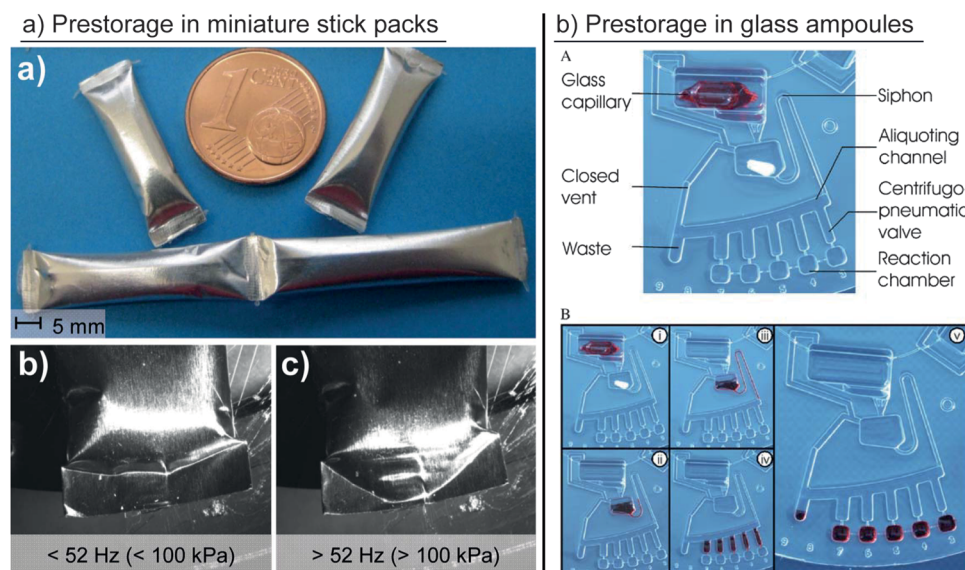


Fig. 3 Different concepts for liquid reagent prestorage in containers. (a) Prestorage of liquids in miniature stick packs and release *via* peelable seal.<sup>27,28</sup> (Reproduced with permission from The Royal Society of Chemistry.) (b) Prestorage of liquid in glass ampoules and release by crushing the ampoules.<sup>26</sup> (Reproduced with permission from The Royal Society of Chemistry.)



have been exploited to transport fluids from a radially inward position (high level of potential energy) to a radially outward position (low level of potential energy). Because of the flow directed from the cartridge center radially outward, the number of cascaded unit operations and process chains is limited by the radius of the cartridge. In many cases, the available radius may not be large enough for the integration of all the process chains that are needed for a desired application. As a consequence, alternatives to the use of centrifugal forces to drive liquid transport in any direction—particularly radially inward—have been required and have recently been developed to enable the integration of larger and more complex fluidic networks.

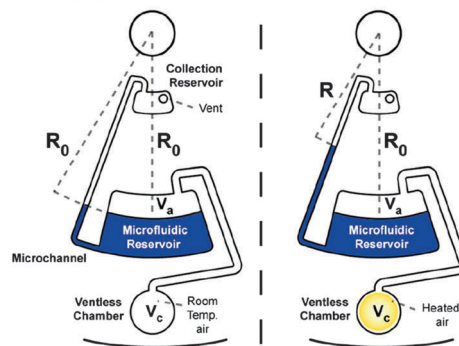
A straightforward approach for pumping liquids radially inward was demonstrated by Kong *et al.*, and involved directing an external gas stream through orifices into a rotating microfluidic cartridge.<sup>12</sup> At closely defined spinning frequencies and gas flow rates, the gas displaces a liquid within the cartridge radially inward. Similar approaches for displacement pumping have been presented, employing an additional liquid that is introduced into a microfluidic cartridge. When the displacer liquid is pumped radially outward, it forces the sample liquid to move to a position situated closer to the center of rotation.<sup>44,45</sup>

Other approaches have exploited on-chip gas generation or expansion to displace and pump liquids. For this purpose, external heat sources have been used to heat up a gas volume entrapped in a microfluidic chamber, causing it to expand thermally. Thereby, water was transferred radially inward at constant spin frequencies between 5 and 20 Hz (Fig. 4a).<sup>46</sup> The same principle was applied in reverse. A decrease in temperature was used for the thermal contraction of an entrapped gas volume. The resulting underpressure “pulled” the liquid into a chamber located at a radially inward position.<sup>47</sup> Instead of thermal expansion, the on-chip electrolysis of water has been used to generate a gas volume that displaces liquids radially inward (Fig. 4c).<sup>48</sup> All of the methods described so far require additional external or disk-integrated means for operation (Table 2).

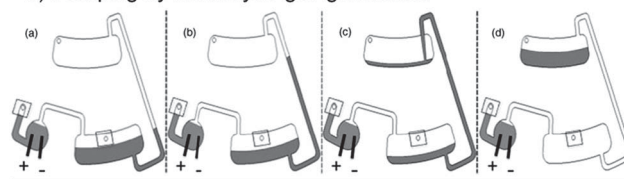
Recently, centrifugo-dynamic pumping has been presented, which does not require any external means but relies solely on the dynamics of deceleration from higher to lower spin frequencies.<sup>49</sup> At high spin frequencies, a sample liquid is directed into a microfluidic dead-end chamber, where it entraps and compresses an air volume. The access channel to this dead end chamber branches into a narrow inlet channel, through which the liquid enters and into a wider outlet channel. The fast deceleration to a low spin frequency (6 Hz) leads to a fast expansion of the compressed air volume and, because of the lower flow resistance, most of the liquid is pumped from the dead-end chamber through the wider outlet channel to a radially more inward position (Fig. 4b).

Other methods for temporary liquid displacement to a radially inward position include capillary priming,<sup>50,51</sup> pneumatic pumping,<sup>52</sup> magneto-pneumatic pumping,<sup>53</sup> and suction-enhanced siphon priming.<sup>54</sup> These pumping techniques do not transfer liquids permanently to a position situated radially more inward. Instead, they can be used for enhanced fluid control. In combination with

#### a) Pumping by thermal expansion



#### b) Pumping by electrolytic gas generation



#### c) Centrifugo-dynamic inward pumping

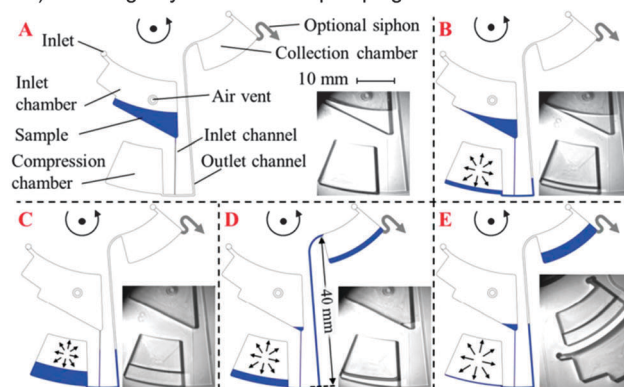


Fig. 4 Liquid transport on centrifugal microfluidic platforms exploiting (a) gas-overpressure generated by heat<sup>46</sup> (with kind permission from Springer Science and Business Media) and (b) electrolytic gas generation.<sup>48</sup> (Reproduced with permission of the Electrochemical Society.) In (c), air compression at high centrifugation, followed by air expansion at a low spin frequency is used in combination with different hydraulic resistances of the inlet and outlet channels to pump liquids radially inward.<sup>49</sup> (Reproduced with permission from The Royal Society of Chemistry.)

siphon valves for example, these pumping techniques are used to prime the siphon for subsequent transfer of liquid to a radially outward position.

### 2.3 Valving and switching

Valving is regarded as one of the most essential unit operations on the centrifugal microfluidic platform<sup>35</sup> because it controls the flow of the fluid through the fluidic network. Typical requirements include rapid liquid passage at a distinctive point in the spatio-temporal domain, compatibility with a broad range of physicochemical liquid properties, and low dead-volumes.<sup>55</sup> Valves can be grouped into active and passive valves, the latter referring to an actuation principle solely controlled by centrifugal forces.<sup>55</sup> Obviously, passive actuation is advantageous to reduce the need for external means, which add to the complexity of the entire





**Table 2** Pumping methods for liquid transfer radially inward.  $\Delta p_c$  = centrifugal pressure (eqn (4));  $\Delta p_v$  = pressure loss due to viscous dissipation (eqn (5)) and  $\Delta p_{pneu}$  = pneumatic pressure (eqn (6))

Ref.	Actuation principle	External means	Actuation pressures	Pumping rate <sup>a</sup> ( $\mu\text{L s}^{-1}$ )	Pump efficiency <sup>a</sup> (%)
Zehnle S. <i>et al.</i> <sup>49</sup>	Centrifugo-dynamic	—	$\Delta p_c, \Delta p_{pneu}, \Delta p_v$	18.2	91
Kong M. C. R. <i>et al.</i> <sup>44</sup>	Displacer liquid	—	$\Delta p_c, \Delta p_{pneu}$	0.6	60
Noroozi Z. <i>et al.</i> <sup>48</sup>	Electrolytic gas generation	Electrical connection	$\Delta p_c, \Delta p_{pneu}$	9.0	100
Abi-Samra K. <i>et al.</i> <sup>46</sup>	Thermal gas expansion	Radiation source	$\Delta p_c, \Delta p_{pneu}$	17.6	100
Kong M. C. R. <i>et al.</i> <sup>12</sup>	Pneumatic (external)	Pressurized gas	$\Delta p_c, \Delta p_{pneu}$	1.1	100

<sup>a</sup> Maximum values reported in the cited publication.

centrifugal microfluidic system.<sup>11</sup> The initial state of a valve can be normally closed (NC) or normally open (NO). An overview of the implementations of valves in centrifugal microfluidics is given in Table 3. Embodiments of valves that feature more than one outlet and allow a liquid flow to be directed to a defined outlet are referred to as “switches”. The following sections discuss valves and switches, starting with passive ones.

**2.3.1 Passive valves.** All embodiments of integrated passive valves in centrifugal microfluidics are implemented as normally closed. The burst or opening of a normally closed passive valve is triggered either by centrifugal pressure (eqn (4)), capillary forces (eqn (7)), or in rare cases the Rayleigh–Taylor instability on a

liquid/gas interface. To describe valves using a reproducible model, the centrifugal pressures are recommended for all valves. The often-used rotational frequency is not sufficient without knowing the radial position, radial length of the liquid column, and density of the liquid. A graphical depiction of different implementations of passive valves is given in Fig. 5.

Early implementations of passive valves used the effect of liquid meniscus pinning at abrupt and sharp channel widenings. To pass the valve, the centrifugal pressure (eqn (4)) has to exceed the capillary counter pressure (eqn (7)). As the pinning effect of the fluid flow is solely based on the capillary counter pressure, these valves are referred to as “capillary valves” (Fig. 5a). Capillary valves

**Table 3** Overview of implementations of passive and active valves in centrifugal microfluidics. NC = normally closed; NO = normally open;  $\Delta p_c$  = centrifugal pressure (eqn (4));  $\Delta p_{cap}$  = capillary pressure (eqn (7));  $\Delta p_{cap\text{ hydrophobic}}$  = counter pressure of hydrophobic capillary (eqn (7)), and  $\Delta p_{pneu}$  = pneumatic counter pressure (eqn (6))

Ref.	External means	Actuation principle	Mode	Vapor-tight
Lai S. <i>et al.</i> <sup>59</sup>	—	$\Delta p_c > \Delta p_{cap}$	NC	—
Duffy D. C. <i>et al.</i> <sup>58</sup>	—	$\Delta p_c > \Delta p_{cap}$	NC	—
Gorkin R. <i>et al.</i> <sup>74</sup>	—	Integrated film dissolves when brought into contact with liquid. Fluidic pathway is opened.	NC	✓
Mark D. <i>et al.</i> <sup>73</sup>	—	$\Delta p_c > \Delta p_{cap} + \Delta p_{pneu}$	NC	—
Andersson P. <i>et al.</i> <sup>69</sup>	—	$\Delta p_c > \Delta p_{cap\text{ hydrophobic}}$	NC	—
Siegrist J. <i>et al.</i> <sup>81</sup>	—	$\Delta p_{cap} > \Delta p_c$	NC	—
Gorkin R. <i>et al.</i> <sup>54</sup>	—	Pressure drop at T-junction caused by auxiliary liquid pulls sample liquid over siphon crest.	NC	—
Hwang H. <i>et al.</i> <sup>79</sup>	—	Integrated membrane valve opens above critical centrifugal pressure. Fluidic pathway is opened.	NC	✓ <sup>b</sup>
Gorkin R. <i>et al.</i> <sup>52</sup>	—	$\Delta p_{pneu} > \Delta p_c$	NC	—
LaCroix-Fralish A. <i>et al.</i> <sup>66</sup>	—	$\Delta p_c > \Delta p_{cap}$	NC	—
Hoffmann J. <i>et al.</i> <sup>78</sup>	—	Delamination of weakly bonded interface by exceeding critical centrifugal pressure. Fluidic pathway is opened.	NC	✓
Ukita Y. <i>et al.</i> <sup>57</sup>	—	Time-dependent decrease of fill level opens connection to venting. <sup>a</sup>	NC	—
Zhang H. <i>et al.</i> <sup>65</sup>	—	$\Delta p_c > \Delta p_{cap\text{ hydrophobic}}$	NC	—
Kinahan D. J. <i>et al.</i> <sup>56</sup>	—	Integrated film dissolves when brought into contact with liquid on paper strip. Air vent is opened. <sup>a</sup>	NC	✓
Kinahan D. J. <i>et al.</i> <sup>86</sup>	—	First liquid dissolves a film to trigger valving of the a next liquid	NC	✓ <sup>b</sup>
Siegrist J. <i>et al.</i> <sup>76</sup>	—	$\Delta p_c > \Delta p_{pneu}$	NC	—
Abi-Samra K. <i>et al.</i> <sup>35</sup>	Active: stationary halogen lamp	Integrated wax valves melted by infrared heating. Fluidic pathway is opened.	NC	✓
Park J. M. <i>et al.</i> <sup>87</sup>	Active: mobile laser diode	Integrated ferrowax valves are melted by laser. Fluidic pathway is opened or closed.	NO/NC/reversible	✓
Amasia M. <i>et al.</i> <sup>90</sup>	Active: thermo-electric module	Freezing of a liquid plug blocks fluidic pathway.	NO	✓
Garcia-Cordero J. L. <i>et al.</i> <sup>33</sup>	Active: laser	Laser melts orifices in polymer separation layer. Fluidic pathway is opened.	NC	✓
Al-Faqheri W. <i>et al.</i> <sup>55</sup>	Active: hot air gun	Integrated wax valves are melted by heat gun. Connection to venting is opened. <sup>a</sup>	NO/NC	✓

<sup>a</sup> Valving principle based on reduction of under pressure after defined opening of air vents. <sup>b</sup> Vapor-tightness has not been demonstrated, but valve is expected to be vapor-tight.



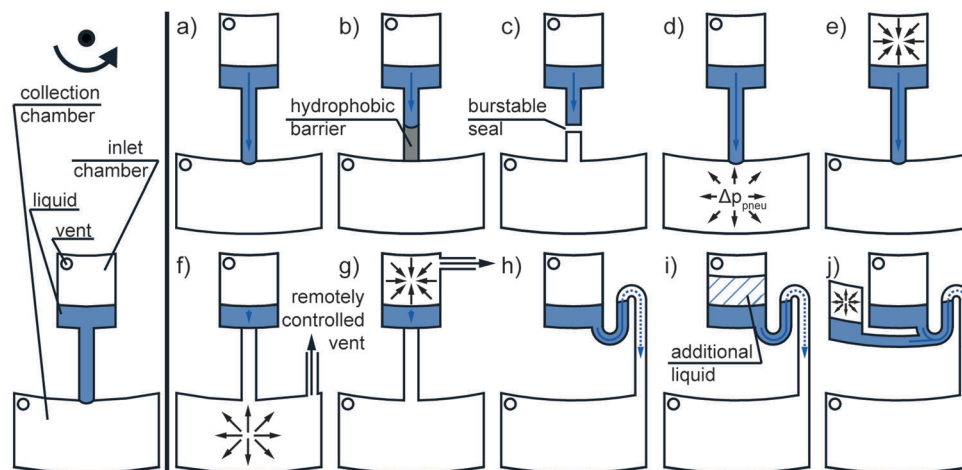


Fig. 5 Passive valves solely actuated by centrifugal forces (eqn (1)): (a) capillary, (b) hydrophobic, (c) burstable seal, (d) centrifugo-pneumatic overpressure, (e) centrifugo-pneumatic under pressure, (f) remotely vented collection chamber (e.g., by wetting a dissolvable film<sup>56</sup>), (g) remotely vented inlet chamber (e.g., by a clepsydra structure<sup>57</sup>), (h) capillary siphon, (i) overflow siphon, and (j) pneumatic siphon valve.

have been demonstrated in complex fluidic networks, e.g., by Duffy *et al.*<sup>58</sup> and Lai *et al.*<sup>59</sup> Later, the flow sequencing of five different liquids using capillary valves with different burst pressures (as a result of defined channel cross sections at different radial positions) and parallel valving of up to 120 single 40 nL aliquots were successfully demonstrated by Madou *et al.*<sup>60</sup> and Schwemmer *et al.*,<sup>61</sup> respectively. Multiple studies have investigated the dependency of the burst pressure on the micro-channel dimensions, surface tension, and contact angle of the liquid using analytical modeling.<sup>62–65</sup> In that context, deviations in the dimensions and low surface quality have been identified as critical parameters for burst pressure prediction and reproducibility.<sup>58,62,64</sup> To circumvent stringent manufacturing requirements, the implementation of fused silica capillaries instead of monolithically integrated capillary valves was reported.<sup>66</sup> Different burst pressures were realized by integrating fused silica capillaries with different inner diameters ranging from 12 to 100  $\mu\text{m}$ . The concept of integrated fused silica capillaries was later adopted by Kong *et al.*<sup>44</sup> and Kazarine *et al.*<sup>67</sup>

Geometric capillary valves become increasingly unstable for wetting liquids when the contact angles drop below 45°. <sup>68</sup> To increase the reproducibility for liquids with low contact angles, local hydrophobic surface coatings have been applied. The valving principle is then based on stopping a liquid flow at the hydrophobic coating, and corresponding valves are referred to as “hydrophobic valves” (Fig. 5b). The flow continues when the centrifugal pressure (eqn (4)) overcomes the capillary pressure (eqn (7)). The demonstrated surface coatings include mostly fluorinated polymer solutions, which are applied by spraying<sup>69</sup> or dispensing.<sup>70</sup> An example of the highly parallel integration of 208 hydrophobic valves was given by Honda *et al.*<sup>71</sup> Another approach demonstrated rapid surface modification for hydrophobic valves by means of a laser printer. Printed toner spots in a microchannel led to an increase in the contact angles from 51° to 111° (measured for DI-water). Depending on the density of the toner spots, a broad range of

burst pressures, ranging from 158  $\pm$  18 Pa to 573  $\pm$  16 Pa, was realized.<sup>72</sup>

Another approach to circumvent the need for local surface coatings and high-precision manufacturing, termed “centrifugo-pneumatic valve” (Fig. 5d), was demonstrated by Mark *et al.* Here, the liquid flow is stopped by a combination of the capillary counter pressure (eqn (7)) at the interface of a channel to a dead-end chamber and the pneumatic counter pressure (eqn (6)) of the compressed air inside the dead-end chamber. Valving is triggered by the centrifugal pressure (eqn (4)) overcoming the counter pressures. After the breakthrough, the complete release of the liquid is ensured by the Rayleigh–Taylor instability of the liquid/air interface. Centrifugo-pneumatic valving makes it possible to handle highly wetting/low surface tension liquids with reported burst pressures of 1300  $\pm$  400 Pa for ethanol and 14 000  $\pm$  2800 Pa for water.<sup>73</sup> The centrifugo-pneumatic valve was later combined by Gorkin *et al.* with an integrated water-dissolvable membrane. The membrane was applied to close an outlet of the dead-end chamber, which allowed centrifugo-pneumatic valving. After contact with the liquid, the membrane dissolved in as little as 10 seconds, which allowed for downstream fluidic post processing.<sup>74</sup> Subsequently, microfluidic networks have been presented with multiple integrated dissolvable films to allow the auto-cascading of valving sequences.<sup>75</sup> An inversion of the centrifugo-pneumatic valve, representing a centrifugo-pneumatic under pressure valve (Fig. 5e), was reported by Siegrist *et al.* The liquid is initially allocated in an unvented inlet chamber, and a retaining pneumatic under pressure (eqn (6)) in the enclosed air volume is generated when the liquid is forced radially outward through the centrifugo-pneumatic under pressure valve during rotation.<sup>76</sup> Al-Faqheri *et al.* demonstrated that burst pressures in both centrifugo-pneumatic over- and under pressure valves can be controlled by blocking air vents with an auxiliary liquid.<sup>77</sup>

To handle evaporating reagents, vapor-tight valves are required. Hoffmann *et al.* presented a valve that applied centrifugal pressure (eqn (4)) for the well-defined delamination of the sealing foil of a



centrifugal microfluidic cartridge, thereby opening up the fluidic pathway. This valve is called a “burstable seal valve” (Fig. 5c). For centrifugal pressures of 2 bar, release times of 31 s were reported.<sup>78</sup> In another approach, polydimethylsiloxane (PDMS) membranes were integrated into a microfluidic network to close the fluidic pathway by bonding the PDMS membrane to the thermoplastic cartridge. With increasing centrifugal pressure (eqn (4)), the membrane is deflected and opens up the fluidic pathway. Depending on the membrane thickness and spin speed, various flow rates were achieved.<sup>79</sup>

In contrast to passive valves that open with an increase in centrifugal pressure, “capillary siphon valves” (Fig. 5h) require a temporary state of low centrifugal pressure (eqn (4)) to trigger the burst event.<sup>80</sup> This valving principle is based on the capillary priming of an S-shaped siphon channel and thus requires advancing contact angles  $< 90^\circ$ . The siphon channel connects an inlet reservoir and outlet reservoir and has to fulfill the following requirements: (a) the inlet of the siphon is located radially inward of the outlet and (b) the crest of the siphon is situated radially inward of the filling level of the inlet reservoir.<sup>3</sup> The siphon channel is thus primed by capillary forces (eqn (7)) against the direction of the centrifugal forces at a low spin speed, while at higher spin speeds, the centrifugal forces dominate and prevent capillary priming.<sup>80</sup> After priming the siphon, the inlet reservoir is emptied through the outlet at a sufficiently high centrifugal pressure. Siegrist *et al.* demonstrated flow sequencing based on serial siphon valving, *i.e.* the concatenation of multiple capillary siphons with integrated capillary valves. The integrated capillary valves prevent the premature priming of the capillary siphon and allow for the release of liquid after a defined number of rotate-and-halt cycles. However, this results in a minor dead-volume of liquid that does not reach the outlet. In this approach, plasma treatment has been recommended to render the surface hydrophilic for liquids with contact angles  $> 90^\circ$ .<sup>81</sup> Because many of the materials used for centrifugal microfluidic cartridges exhibit hydrophobic properties and surface treatment adds to the complexity of cartridge fabrication, Godino *et al.* demonstrated the integration of paper-based siphons as a low-cost alternative.<sup>82</sup> Alternatively, siphon valves can be primed by increasing the filling height inside the inlet chamber above the siphon crest by adding additional liquid. Such valves are referred to as “overflow siphon valves” (Fig. 5i).<sup>83</sup>

To circumvent the demand for hydrophilic coatings, siphon priming by the release of pneumatic energy (eqn (6)) from an enclosed and compressed air bubble was exploited in the so-called “pneumatic siphon valve” (Fig. 5j).<sup>52</sup> Later, the cascading of pneumatically actuated siphons for sequential release was employed.<sup>84</sup> Another approach demonstrated suction-enhanced siphon priming by creating an under pressure at the siphon outlet through an auxiliary liquid. However, in this approach, the siphoned reagent inevitably mixes with the auxiliary liquid.<sup>54</sup>

A small group of passive valves does not rely on centrifugal pressure but provides a time-dependent release of liquids. Recently, Schwemmer *et al.* introduced a microfluidic timer that could be used to trigger liquid actuation independent from

the spinning speed: the timer employs temporary storage of pneumatic energy (eqn (6)), which is suddenly released after a pre-defined period of time. The timer is set by overfilling a first pneumatic chamber, which results in liquid flowing into a secondary pneumatic chamber through a narrow channel at high rotational frequencies. Upon decrease of centrifugal pressure (eqn (4)), emptying of the secondary chamber and channel results in a delay before the pneumatic energy is released.<sup>85</sup> Kinahan *et al.* demonstrated the integration of a paper strip into a centrifugal microfluidic cartridge. This paper strip is “connected” to multiple integrated dissolvable films that sequentially open fluidic pathways as soon as the part of the paper strip in contact with the dissolvable film is wetted<sup>56</sup> (Fig. 5f). Kinahan *et al.* also demonstrated event-triggered valving, where the completed valving of one liquid opens an air vent by dissolving a film to trigger the valving of a next liquid. By combination of a fluidic network with dissolvable films 10 sequential valving events at one rotational frequency were demonstrated in a single cartridge.<sup>86</sup> Ukita *et al.* reported a microfluidic clepsydra structure connected to the venting of a loading structure for the sequential release of liquids. Over time, the liquid level in the clepsydra decreases and thereby sequentially opens the venting for the single loading structures<sup>57</sup> (Fig. 5g).

**2.3.2 Active valves.** Active valves are controlled by external means and therefore require additional interfaces to the processing device or user. Active valves have the advantage of being either normally open or normally closed during fluidic processing. In rare cases, the normally open and closed states are reversible.<sup>87</sup>

Optofluidic valves actuated by a solid state laser were reported by Garcia-Cordero *et al.* Printed toner spots on a polymer separation layer, COP or polyethylene terephthalate (PET) film, were used to increase the light absorbance to melt orifices (30–280  $\mu\text{m}$  in diameter) into the separation layer, thereby opening the fluidic pathway. When using 100 and 300 mW of laser power, the response time of the valve was reported to be 0.5 seconds. A fluidic network with 106 laser printed single addressable optofluidic valves has been presented. Contact between the liquid and valve had to be avoided during melting because the liquid could be contaminated by combustion products and absorb thermal energy.<sup>33</sup>

Instead of melting the cartridge substrate, paraffin wax valves have been integrated into centrifugal microfluidic cartridges. Stationary infrared sources were used to melt the wax under rotation, thereby opening the fluidic pathway. The sequential opening of valves has been demonstrated by using waxes with different melting temperatures. Response times of 25 seconds were reported for the simultaneous actuation of nine valves.<sup>35</sup> Another approach used handheld heat guns instead of infrared lamps to melt wax valves.<sup>88</sup> However, it has to be considered that the molten wax and heat input to the cartridge could have a negative effect on the reagents used.<sup>35</sup> As an improvement to overcome these limitations, Al-Faqheri *et al.* relocated the wax valves away from the reagents, thereby preventing direct contact. Instead of opening the fluidic pathway, connections to the air vents were opened or closed by melting the valves<sup>55</sup> (Fig. 6b).



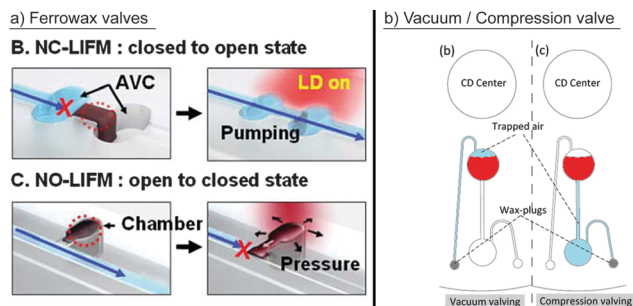


**Fig. 6** Prominent concepts for active valving. (a) Park *et al.* demonstrated laser irradiated ferrowax microvalves (LIFM) to open and close the fluidic pathways of normally closed LIFM (NC-LIFM) and normally opened LIFM (NO-LIFM), respectively, activated by a laser diode (LD).<sup>87</sup> The layout includes assistant valve chambers (AVC). (Reproduced with permission from The Royal Society of Chemistry.) (b) Al-Faqheri *et al.* used wax plugs to open connections to the ventilation.<sup>55</sup> (Reproduced under the Creative Commons Attribution License O.)

Aiming at minimizing the energy input, single addressable, laser-irradiated ferrowax microvalves (LIFM) were introduced by Park *et al.*<sup>87</sup> and later implemented for different applications.<sup>89</sup> For efficient heating, iron oxide nanoparticles were mixed into the wax, which allowed valve actuation *via* low-power lasers (1.5 W) and a response time of only 0.5 seconds. The laser ensured that only the nanoparticles were heated and not the surrounding liquids. The LIFM were reported to be leak-free at a centrifugal pressure of up to  $403.0 \pm 7.6$  kPa. Normally closed, normally open, and even reversible valve actuation has been demonstrated (Fig. 6a).

Amasia *et al.* demonstrated ice valving to avoid evaporation during PCR thermocycling. Liquid plugs were frozen in defined channel areas when the disk was at rest using thermoelectric modules. The response time for these ice valves was 30 seconds.<sup>90</sup>

An alternative to using thermal energy for active valving has been demonstrated by Swayne *et al.* A focused air stream opens a fluidic path for the liquid, which had previously been blocked by a gel. Postulated advantages of the valve are the small footprint and ease of fabrication.<sup>91</sup>

**2.3.3 Passive flow switches.** Similar to passive valves, passive switches are solely controlled by centrifugation (centrifugal pressure (eqn (4)) and the direction of rotation). Early approaches for flow-switching were presented by Brenner *et al.* using an inverse Y-channel with one inlet channel and two outlets. At low spin-frequencies, the liquid from the inlet channel is equally distributed between the two outlet channels and is only affected by the manufacturing tolerances of the channels. At increased spin speeds, the liquid is directed toward one of the outlet ports as a result of the transversal Coriolis force (eqn (2)). Hence, switching the liquids depends on the direction and speed of the rotation and the corresponding Coriolis force.<sup>92</sup> The functionality of the Coriolis switch was later investigated extensively by analytical means.<sup>93</sup> Thuy *et al.* presented a passive flow switch consisting of an inlet channel branching into two outlet channels, one with a hydrophobic valve that could be controlled by the rotational speed of

the cartridge. At high rotational frequencies, liquid is routed through the channel with the hydrophobic valve. At low spin speeds, the hydrophobic valve does not break and liquid overflows into the other channel.<sup>94</sup>

Other approaches for passive flow switching have been demonstrated, including that based on fluidic capacitance by Kim *et al.*<sup>93</sup> and that based on the pneumatic counter pressure (eqn (6)) of an enclosed air volume by Mark *et al.* The latter exploits centrifugal pressures (eqn (4)), depending on the speed of rotation to direct liquids to either one of the outlets.<sup>95</sup> Later, Müller *et al.* demonstrated passive unidirectional switching by closing the connection to the venting with the overflow volume of one of the assay reagents.<sup>96</sup>

**2.3.4 Active flow switches.** Active flow switches are controlled by other means than centrifugal pressure. They have the obvious disadvantage of requiring external means. Al-Faqheri *et al.* demonstrated the use of wax plugs to block or unblock connections to the venting hole when heated. However, the outlet chamber for a liquid is predefined by the microfluidic network because the liquid is always directed into the vented microfluidic chamber. Heating times of 8 minutes were reported to open the melt wax plugs.<sup>55</sup> Another active flow switch was demonstrated by Thio *et al.* By heating up enclosed air volumes with a hot air gun and then cooling them, liquids could be pumped and pulled into different microfluidic chambers. Liquid transfer times of 3.7–8.3 minutes were reported.<sup>47</sup> Kong *et al.* demonstrated active flow switching by directing a gas stream from outside the disk through one of two orifices into the microfluidic network. A liquid could thereby be directed to one of two fluidic chambers.<sup>97</sup> Switching based on the use of heat to melt wax plugs<sup>55</sup> or for thermal air expansion<sup>47</sup> clearly lacks actuation speed, while gas pressure-based<sup>97</sup> systems require an open hole within the cartridge, which might be critical in terms of cross contamination.

## 2.4 Metering and aliquoting

Most microfluidically integrated applications require precise input volumes of liquids in order to obtain quantitatively reproducible results. Consequently, unit operations for the metering of liquid volumes are widely employed. Splitting an input liquid volume into multiple defined sub-volumes is referred to as aliquoting, which mostly involves multiple parallel metering steps. Aliquoting itself was subcategorized by Mark *et al.* into one-stage and two-stage aliquoting (Fig. 7b). The latter refers to a microfluidic aliquoting process in which single aliquots are transferred into fluidically separated chambers after metering.<sup>98</sup> The embodiments of centrifugal microfluidic unit operations for metering and aliquoting are listed in Table 4. In the simplest case, a metering structure consists of a connection channel to an inlet, a metering chamber with a defined volume, and an overflow to a waste chamber for excess volume (Fig. 7a). The metering can be combined with valves at the radially outer end of the metering chamber to allow for further fluidic processing. The demonstrated valves include hydrophobic,<sup>69</sup> capillary siphon,<sup>99</sup> and centrifugo-pneumatic valves.<sup>73</sup> The metering accuracy is mainly affected by the variation of the



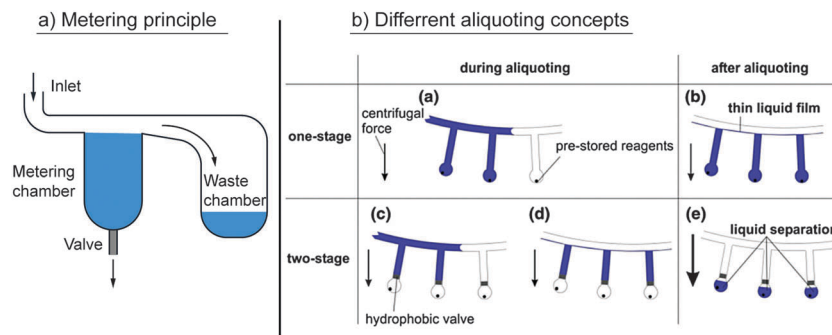


Fig. 7 Centrifugal microfluidic unit operations for metering and aliquoting. (a) Basic principle of metering. A liquid fills a metering chamber with a defined volume. The excess is gated into a waste chamber. The metered volume can subsequently be transferred into the microfluidic network via suitable valves. (b) Different aliquoting concepts.<sup>98</sup> (With kind permission from Springer Science and Business Media.)

cavity size within the fabrication tolerances<sup>98</sup> and the wicking effects at liquid interfaces due to capillary forces.<sup>100</sup> Capillary forces (eqn (7)) can be counteracted by centrifugal forces (eqn (4)), which produces a high metering accuracy in centrifugal microfluidics even at nanoliter volumes.

In single-stage aliquoting, fluid volumes are metered directly into the receiving chamber. Thus, the aliquoting process simply involves the transport of the liquid from an inlet into multiple receiving chambers, while the excess is gated into an overflow. As mentioned by Mark *et al.*, single stage aliquoting bears the problem of cross contamination between adjacent aliquots, because they might still be connected by a liquid film.<sup>98</sup> To avoid cross contamination, Sundberg *et al.* used a mineral oil to fill the microfluidic channel and separate the aliquoted volumes after the aliquoting process.<sup>101</sup>

Two-stage aliquoting allows for full fluidic separation between adjacent aliquots, and therefore is usually applied when cross contamination is an issue,<sup>37</sup> or when further fluidic processing of the individual aliquots is required. Two-stage aliquoting combines the parallel metering of one-step aliquoting with normally closed valves at the radial outer side of each metering finger. After metering, the single aliquots can pass the valve and be used for further fluidic processing.<sup>30,69</sup>

## 2.5 Mixing

The purpose of mixing in microfluidics is to reach a sufficiently high distribution and homogeneity of sample and reagent molecules such that chemical reactions are accelerated. Conventional mixing in macroscopic standard laboratory processes is mostly performed by stirring, shaking, or vortexing. However, on a centrifugal microfluidic platform, mixing becomes difficult because the cartridge is rigidly attached to a motor shaft, which rotates the cartridge with a relatively high moment of inertia. The artificial gravity generated by this rotation makes the centrifugal microfluidic platform particularly useful for the separation of phases with different mass densities, but not for mixing. Moreover, for liquid volumes ranging from several hundred nanoliters to a few milliliters, purely diffusive mixing is rather inefficient.<sup>103,104</sup> Since mixing is nevertheless crucial for many biochemical assays, several methods have been researched to mix fluids on the centrifugal microfluidic platform.

A concept for the batch-wise “shake-mode” mixing of liquids that relied on continuous changes in the spin speed of the centrifugal microfluidic cartridge was demonstrated by Grumann *et al.* The angular momentum caused by the acceleration or deceleration induced Euler forces (eqn (3)) and resulted in layer inversion of the liquids in the microfluidic chamber (Fig. 8a). As a measure of the mixing quality, the standard deviation of all the recorded pixel grayscale values of a mixture containing dyed and undyed liquids was determined using image processing. The mixing time was defined as the time required to reach a  $1/e$  decay in the standard deviation. As a result, the mixing time in the reported embodiment could be reduced from 7 minutes for purely diffusive mixing down to 3 seconds for shake-mode mixing. It was found that the mixing quality depended on the acceleration and deceleration rates, as well as the azimuthal span of the rotation and radial position of the mixing chamber. Adding magnetic beads and pulling them through the mixing chamber further reduced the mixing time to 0.5 seconds. A deflection of the magnetic beads was induced by a set of external permanent magnets that attracted the beads radially in- and outward.<sup>103</sup>

Noroozi *et al.* presented another mixing concept that employs the interplay of centrifugal and pneumatic pressures (eqn (4) and (6)) to transport liquids between two chambers (Fig. 8c).<sup>105</sup> This mixing-by-reciprocation concept was later used to maximize the incubation and hybridization efficiency for the centrifugal microfluidic integration of an immunoassay and showed a reduction in the processing time and reagent consumption by one order of magnitude.<sup>106</sup> In this approach, mixing occurs due to micro-vortices and Taylor dispersions, which are both present in each mixing cycle. The use of the pneumatic counter-pressures of an entrapped air volume enables frequency oscillations at elevated spin speeds, thus making mixing by reciprocation easily combinable with pneumatic siphon valving.

Instead of pneumatic energy storage, Aeinehvand *et al.* recently integrated a latex membrane in a stack of PMMA layers and pressure sensitive adhesives. At the radial distal end of the mixing chamber, the latex membrane could freely expand out of the disk plane through a hole in the solid PMMA, thus forming a micro-balloon. The reciprocating flow of the reagents



Table 4 Centrifugal microfluidic unit operations for metering and aliquoting

Ref.	Integrated valve type	Aliquoted volume	CV (%)	Number of parallel aliquots
Schembri C. T. <i>et al.</i> <sup>80</sup>	No valve	Not reported	<2	4 or 21
Sundberg S. O. <i>et al.</i> <sup>101</sup>	No valve	33 nL	16	1000
Andersson P. <i>et al.</i> <sup>69</sup>	Hydrophobic valve	200 nL	0.75	112
Andersson P. <i>et al.</i> <sup>69</sup>	Hydrophobic valve	20 nL	1.90	1
Mark D. <i>et al.</i> <sup>98</sup>	Centrifugo pneumatic valve	6–10 $\mu$ L	2.2–3.6	8 or 16
Steigert J. <i>et al.</i> <sup>99</sup>	Capillary siphon	500 nL	<5	1
Schwemmer F. <i>et al.</i> <sup>61</sup>	Capillary valve	40 nL	1–5.5	120
Li G. <i>et al.</i> <sup>102</sup>	Capillary valve	31 nL	2.80	24
Hwang H. <i>et al.</i> <sup>30</sup>	Ferrowax-based microvalves	100 $\mu$ L	Not reported	5

to be mixed was induced by oscillations of the spin frequency. At a high spin speed, the centrifugal pressure drove the reagents into the inflating micro-balloon, thereby stretching the latex membrane. At rest, the absence of the centrifugal pressure allowed the latex membrane to return to its initial flat shape. This version of mixing by reciprocation was proven to be suitable for low operating frequencies in the range of 0–14 Hz and chamber depths in the range of a few hundred micrometers. For such shallow chambers, mixing by reciprocating the flow was shown to be a good alternative to shake-mode mixing.<sup>107</sup> This is because shake-mode mixing requires moderate aspect ratios in the range of one to provide sufficient advection.

Mixing based on Coriolis pseudo-forces (eqn (2)) was demonstrated by Haeberle *et al.* Here, two liquids were dispensed into two separate microfluidic inlets on the centrifugal microfluidic cartridge (Fig. 8b). These liquids merged within a Y-shaped channel, where they were mixed due to transversal convection as a result of the Coriolis forces acting perpendicular to the flow direction. After mixing, the product was spun from the cartridge into a receiving vessel, thereby allowing for continuous mixing.<sup>108</sup> Coriolis mixing was later improved by the multilamination of flows

via a split-and-recombine concept.<sup>109</sup> In another work, Coriolis mixing was used to fold laminar flows and thereby shorten mixing times by two orders of magnitude.<sup>110</sup> Further investigations on the mixing regimes of two fluids in a T-shaped microchannel showed Coriolis force-based mixing at intermediate spin speeds.<sup>111</sup> The channel geometry, speed of rotation, and flow rates were identified as key impact parameters on the mixing quality.<sup>109,112</sup> Recently, Coriolis mixers have been employed in serpentine configurations that also use the Dean effect in channel bends to improve the overall mixing efficiency.<sup>113,114</sup> The independence from changes in the spin speed makes Coriolis mixing suitable for applications on a wide range of processing devices, *e.g.*, standard laboratory centrifuges. A challenge for the integration of Coriolis mixing is that the flow rates of the fluids entering the mixing channels have to be accurately controlled.

Other approaches for mixing at a constant spin speed have recently been explored. Burger *et al.* used the disruption of continuous liquid flows to generate discrete droplets and create multiple alternating lamellae with two different liquids. In this way, the interface between the two liquid phases was significantly increased, and mixing by diffusion was supported. By generating

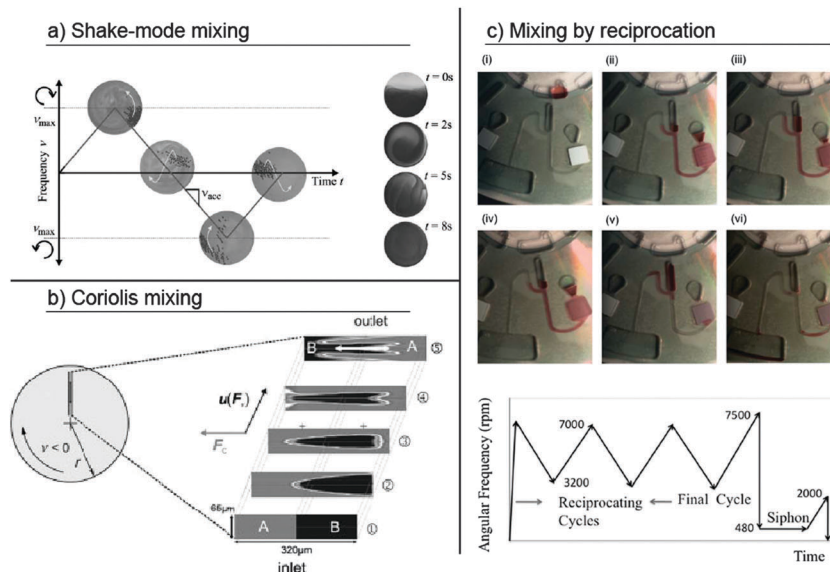


Fig. 8 Different concepts for mixing of liquids employed in centrifugal microfluidics. (a) Shake-mode mixing at alternating spin frequencies.<sup>103</sup> (Reproduced with permission from The Royal Society of Chemistry.) (b) Coriolis mixing exploiting Coriolis force induced transversal flow.<sup>108</sup> (Preprinted with permission of John Wiley and Sons.) (c) Mixing by reciprocating the flow at alternating spin frequencies.<sup>106</sup> (Reprinted with permission from AIP Publishing LLC.)



droplets with 60 nL volumes, blood plasma and PBS were mixed and divided into single aliquots. The protein concentrations in all of the aliquots showed good agreement with the value expected for a perfect mixture.<sup>83</sup>

Liebeskind *et al.* used the catalytic decomposition of H<sub>2</sub>O<sub>2</sub> to water and oxygen as an on-chip gas source to generate gas bubbles for mixing. The generated gas was pumped into a mixing chamber, where, due to the buoyancy force in the artificial gravitational field, the bubbles moved through the liquids to be mixed and caused perturbations. The mixer was used to perform the lysis and binding steps in the extraction of DNA from whole blood.<sup>115</sup>

Active mixing employing an external air stream was used by Kong *et al.* to stir liquids within a microfluidic chamber. The air stream was directed from outside the disk through an orifice into the microfluidic structures, which allowed mixing at constant and low spin frequencies. Within 11.2 seconds, a 30-fold increase in mixing quality was reported compared to diffusive mixing at a spin frequency of 7.5 Hz.<sup>116</sup>

## 2.6 Separation

The separation of different substances from each other is an essential unit operation in many (bio-) chemical processes. The target substances can be small molecules such as metabolites, macromolecules like nucleic acids and proteins, and larger elements such as cells or solid particles that have to be isolated from a surrounding medium. Typically, differences in the chemical or physical properties of these substances are exploited for the technical implementation. This review chapter is structured as follows. First, we review publications on physical separation techniques, including filtering and sedimentation, followed by a discussion of the implementations of chemical separation within centrifugal microfluidics.

**2.6.1 Separation based on differences in physical properties.** The majority of physical separation techniques that have been demonstrated on centrifugal microfluidic platforms are based on filtering and sedimentation. In microfluidic structures, filtering can be used to remove or concentrate solid particles from a liquid phase based on the particle size. Pre-filtering can be implemented to avoid clogging microfluidic channels<sup>66</sup> or to prevent negative interference with the assay if the permeate, the liquid that passes the filter, is processed in the downstream application. Other implementations employ filtering to enhance the assay sensitivity by concentrating cells or bacteria in the retentate, the substances that are retained by the filter. Instead of particle size, sedimentation exploits density differences between the separated element and the surrounding media. Driven by centrifugal forces (eqn (1)), denser objects sediment radially outwards along the centrifugal force vector, while the cleared supernatant can be transferred to downstream microfluidics. Typical applications for sedimentation include the removal of solid particles or blood cells. These are explained in more detail in the corresponding application section.

Filtering by cartridge-integrated geometric restrictions was demonstrated by Czugala *et al.* In this implementation, the

height of a microfluidic channel was decreased step-wise from 1500  $\mu\text{m}$  to 86  $\mu\text{m}$ . *Via* these restrictions, up to 94% of the particles were filtered from a river-water sample.<sup>117</sup> Instead of geometric restrictions, filter membranes have successfully been integrated into centrifugal microfluidic cartridges to remove bacteria from water samples<sup>18</sup> or particulates from soil.<sup>118</sup> Both publications report filtration efficiencies of 100% of the tested particulates. Also based on filter membranes, selective filtering of circulating tumor cells from a whole blood sample was demonstrated. Filtration efficiencies were reported to be up to 84%.<sup>119</sup>

Specific filtering by di-electrophoresis exploiting the electrical polarizability of molecules has been demonstrated by Martinez-Duarte and co-workers. Cartridge integrated carbon electrodes powered *via* electrical contacts with a slip-ring on the rotor shaft specifically filtered yeast cells from a mixture of yeast cells and latex particles.<sup>120</sup> Boettcher and colleagues presented the manipulation of particles and cells using a rotating microfluidic di-electrophoresis chip. Two co-rotating batteries powered the chip, while a co-rotating generator provided the required alternating currents. Using the described di-electrophoretic setup, sedimenting cells and particles could be directed to a defined branch of a Y-shaped channel.<sup>121</sup>

Burger *et al.* presented an implementation for capturing beads during sedimentation using arrays of V-shaped structures. The implementation aimed at a sharp peak in bead-distribution, *i.e.*, capturing exactly one bead per cup. The size and density of the V-cup structures, as well as the size of the beads, were identified as important parameters for the bead distribution and number of empty cups. Up to 99.7% single bead-occupancy per V-cup was reported with 5% of the cups remaining empty.<sup>122</sup>

Kirby *et al.* presented a concept for centrifugo-magnetophoretic particle separation. Magnetic particles sediment in a stagnant fluid due to centrifugal forces. Permanent-magnets integrated into the rotating cartridge cause a defined deflection of the magnetic particles perpendicular to the centrifugal forces while non-magnetic particles sediment in direction of the centrifugal force. Thereby, particles could be routed to one of three outlets depending on their size, density, and magnetic properties and on the spin speed.<sup>123</sup> This concept was later employed by Glynn *et al.* for separating beads with captured CD4+ cells from whole blood.<sup>124</sup>

A unit operation for the sedimentation of solid particles from turbid samples and the subsequent transfer of clear supernatant was demonstrated by LaCroix-Fralish *et al.* Fused silica capillaries (<110  $\mu\text{m}$  in diameter) were used as the connection between two microfluidic chambers. The liquid above the sedimented fraction of solid particles was decanted by placing one end of the capillary in the upstream chamber.<sup>66</sup> In another implementation, saw-toothed obstacles in an inlet chamber were used to hold back sedimented particles from seawater samples. After sedimentation, a wax valve was opened to release the clear seawater into an aliquoting structure.<sup>30</sup>

Similar concepts have been employed for blood-plasma separation based on the sedimentation of the denser cellular blood content from the cell-free blood plasma. The implementations



basically differ in the implemented unit operations for plasma transfer after sedimentation, which included centrifuge-pneumatic gating,<sup>125</sup> centrifuge-pneumatic siphon valving,<sup>126</sup> capillary siphon valving,<sup>99</sup> decanting,<sup>127</sup> or using an integrated Y-channel that allowed denser cell content to enter the radially outward branch of the Y-channel, while the plasma was transferred into the downstream microfluidics *via* the radial inward channel.<sup>128</sup> Because blood-plasma separation is a discrete process chain in many laboratory workflows, it is discussed in detail with respect to the reported performance parameters in Section 3.3.1.

**2.6.2 Separation based on chemical properties.** All centrifugal microfluidic implementations of chemical separation are based on the affinity of a target substance to a suitable mobile or non-mobile support. Mobile or non-mobile supports have to be brought in contact with the target substance and different assay reagents in a sequential order. Non-mobile supports have to be embedded into a network of microfluidic unit operations, valves, and switches, to allow for the sequential transport of the sample and reagents, while mobile supports can actively be moved to the location of a reagent or sample. The implementation of mobile or non-mobile supports and fluidic unit operations is discussed in the respective application chapters because their combination can be regarded as a process chain, while we report some commonly exploited affinity mechanisms here. The underlying principles for the manipulation of mobile supports, which are mostly based on magnetic interaction, are included in the description in this chapter.

A common affinity mechanism for the separation of nucleic acids exploits the binding of DNA and RNA to silica surfaces under high chaotropic salt conditions.<sup>129</sup> Implementations have been demonstrated using non-mobile cartridge-integrated silica membranes,<sup>24,96</sup> glass bead columns,<sup>130</sup> or silica sol-gel.<sup>131</sup> Other separation principles involve the hybridization of nucleic acids to complementary strands that are immobilized to the cartridge surface.<sup>132–134</sup> The affinity mechanism exploited for immunoassays and immunoseparation relies on the binding of antibodies to antigens. Antibodies (and in rare cases antigens) have been immobilized to a variety of non-mobile solid supports, including trapped antibody-coated polystyrene beads,<sup>71,135</sup> glass beads,<sup>136</sup> silica beads,<sup>137</sup> PMMA disks,<sup>59</sup> and nitrocellulose membranes,<sup>106</sup> which are then passed by the sample and other liquid reagents.

Demonstrated implementations with mobile support include a simple approach for the separation of nucleic acids using magnetic silica beads as the mobile support. Depending on the azimuthal position of the centrifugal microfluidic cartridge with respect to an external magnet, the beads could be transported through multiple reagent-filled microfluidic chambers.<sup>138</sup> Cho *et al.* used antibody-coated magnetic beads for pathogen capturing and immuno-magnetic separation from a whole blood sample. The beads were manipulated by a cartridge-integrated magnet and an external magnet on a linear gear. Thereby, the mixing of the beads or temporary immobilization of the beads in a dedicated location could be achieved while the surrounding media were exchanged.<sup>89</sup> Another approach for immunomagnetic separation was demonstrated by Chen and co-workers, where antibody-labeled magnetic beads were used to capture target cells. After binding, the beads were trapped by a co-rotating magnet,

while the cell sample was gated into a waste reservoir.<sup>139</sup> Glynn *et al.* and Kirby *et al.* demonstrated centrifugo-magnetophoretic separation to separate magnetic from non-magnetic particles or cells. In this approach, co-rotating disk-integrated magnets were used to deflect sedimenting magnetic particles with attached target cells to designated reservoirs.<sup>123,124</sup>

Schaff and Sommer demonstrated the sedimentation of beads through a density media for an immunoassay. Antibody-labeled beads were used to capture antigen and detection antibodies from a sample layered on top of a density medium. After capture, the beads were separated from the sample by sedimentation through the density medium.<sup>88</sup>

## 2.7 Droplet handling

While droplet-based microfluidics is a very active field in pressure-driven microfluidics, so far little work on droplet handling has been performed in centrifugal microfluidics. The reported unit operations are limited to the generation of droplets<sup>140</sup> or bubbles.<sup>141</sup> In these publications, both the droplets and bubbles were generated in oil.

With respect to applications, droplet generation in centrifugal microfluidics has been employed to create particles. Chitosan/alginate droplets<sup>142,143</sup> were generated at a nozzle in air and dispensed into a cross-linking solution. Upon contact with the hardening solution, the droplets became solid, forming micro-particles. The reported advantages compared to other microfluidic bead generation methods are low dead volumes, uniform droplets due to the pulse free propulsion, and possible parallelization by a straightforward and even distribution of hydrostatic pressure on an array of nozzles. In particular, the dispensing method using an air gap, which prevents contact between the nozzle and hardening solution and thus circumvents nozzle clogging, is reported to be a unique feature.

Dispensing through an air gap was later applied to form 3D multi-compartmental particles using a multi-barreled capillary as a nozzle.<sup>144</sup> Up to six-compartment body compositions with custom designed geometries were reported in this work. These were produced on a tabletop centrifuge equipped with a swinging bucket rotor.

Within centrifugal microfluidics, besides particle generation, we see the potential for the automation of highly parallel applications such as emulsion-based nucleic acid amplification as sample preparation for sequencing or digital amplification, or the implementation of digital immunoassays. The advantages include artificial gravity-based pulse-free propulsion, and thus the ability to form well-defined highly parallel micro-droplets with minimal dead volume. For example, centrifugal step emulsification can be employed for absolute quantification of nucleic acids by digital droplet RPA.<sup>145</sup> Furthermore, the integration of droplet-based operations, together with complex sample preparation such as nucleic acid purification, may enable sample-to-answer implementations of digital assays.

## 2.8 Detection

Although not a classical fluidic functionality, we consider detection to be a unit operation because it represents a basic





building block for the assessment or quantification of the result of an assay. With respect to fluidics, detection usually requires maintaining the analyzed volume at a certain position or defined flow rate. The more relevant aspect of detection, however, is the general principle with which the quantification is assessed. Therefore, we categorize the unit operations used for detection into optical, electrochemical, and other detection principles.

**2.8.1 Optical detection.** Optical detection is very common in centrifugal microfluidics for several reasons. (i) Costly optical detectors are usually integrated into the processing devices, which makes it possible to keep the disposable cartridges cheap. (ii) A multitude of azimuthal locations on a spinning disk can be analyzed sequentially by rotation, which only requires a single detector. (iii) The spinning rotors are capable of precisely positioning readout cavities relative to the detector position, which enables the alignment of the optical system at no additional cost. The optical detection section is structured as follows. First, we review systems that allow for the visual detection of the assay result, followed by methods for absorbance- and fluorescence-based detection. A final section is dedicated to publications that use commercially available CD or DVD drive pick-up heads for detection.

Kim *et al.* presented a centrifugal microfluidic cartridge with an integrated lateral flow strip. Gold nanoparticle-stained antibodies were bound to a DNA amplification product and created a visible line on the lateral flow strip.<sup>146</sup> Another molecular biological application exploited a color change from purple to blue during isothermal DNA amplification.<sup>147</sup> Riegger *et al.* presented a system for the visual detection of hematocrit. A disk-imprinted scale next to a dead-end channel allowed for the visual read-out of hematocrit after centrifugation by identifying the location of the interface between the sedimented red blood cells and the plasma.<sup>148</sup>

Grumann *et al.* employed the total internal reflection for absorbance measurements. A light beam directed onto the disk plane was deflected by a cartridge-integrated V-groove and gated through a microfluidic chamber in the azimuthal direction. A second V-groove deflected the light beam out of the disk

plane to the detector. Thereby, the path length for the absorption measurement (and thus the sensitivity) was increased from 1 mm to 10 mm compared to direct light incidence (Fig. 9a).<sup>149</sup> Czugała *et al.* used a paired emitter detector diode (PEDD) device for absorption detection. In the PEDD setup, two light emitting diodes were used. One diode served as the light source and was placed above the cartridge, while the second diode, operated in the reverse bias mode, served as the light detector for the transmitted light. An improved sensitivity and signal-to-noise ratio along with a low cost, small size, and low power consumption, were reported as the major advantages of the PEDD setup compared with the standard setup using an LED and a photodiode (Fig. 9b).<sup>117</sup> LaCroix-Fralish *et al.* presented the spectrophotometric detection of a bioassay using a halogen light source, which emitted light in the ultraviolet and visible regime, and a Czerny–Turner type spectrometer with a photodiode array for the detection of the transmitted light. For the detection, the disk had to be removed from the spinning device and mounted in the path of the spectrometer.<sup>42</sup>

Detection *via* fluorescence measurement is frequently conducted for nucleic acid analysis and in some cases also for immunoassays, and typically provides a more sensitive and specific detection<sup>150</sup> compared to other optical detection methods. Focke *et al.* presented a microfluidic cartridge with a line-up of reaction cavities close to the rim of the cartridge. Fluorescence signals from these reaction cavities were detected using a commercially available PCR thermocycler by exploiting the inbuilt fluorescence detection unit, *i.e.*, an LED excitation source and a photo-multiplier for detection.<sup>38</sup> The same concept was later adapted for other applications.<sup>26,37,39,41</sup> Nwankire *et al.* presented a microfluidic cartridge with an integrated supercritical angle fluorescence chip that allowed the selective measurement of fluorescent signals generated in close proximity to the surface. The optical setup was completed by a laser for fluorescence excitation and a photomultiplier for detection.<sup>150</sup> Various papers have reported the implementation of CCD cameras, especially for spatially resolved optical information. Riegger *et al.* demonstrated a detection concept for multiplexing *via* color-coding composed of an LED for excitation and a CCD camera for detection. In a

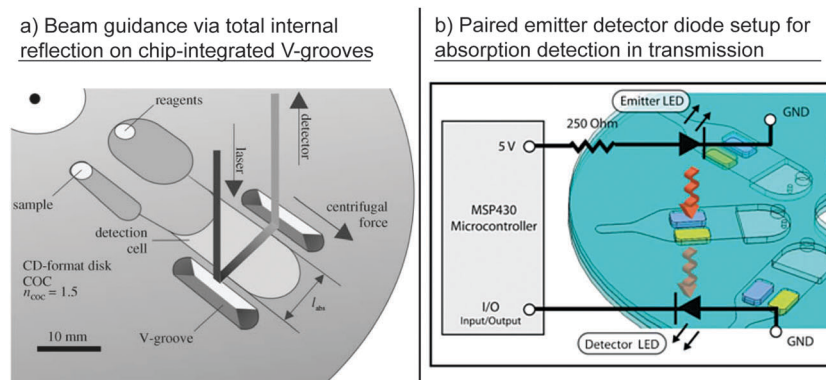


**Fig. 9** Different setups for optical detection. (a) Enhancement of sensitivity by on-chip beam guidance using chip-integrated V-grooves.<sup>149</sup> (With kind permission from Springer Science and Business Media.) (b) Paired emitter detector diode (PEDD) setup as sensitive and cheap alternative to common LED–photodiode setups for absorption measurement in transmission.<sup>117</sup> (Reproduced with permission from The Royal Society of Chemistry.)



first step, the camera acquired the spectral information of a layer of quantum dot beads for decoding the various bead types used and subsequently detected the fluorescence signals on the bead surfaces to quantify the bead-specific analyte reactions. The fluorescence on the bead surfaces was associated with the assay result, while the color of the beads corresponded to the assay target.<sup>151</sup> Ukita *et al.* presented a stroboscopic fluorescence microscope for observation of fluorescent objects such as 6  $\mu\text{m}$  particles on a spinning disk at a rotational frequency of up to 3000 rpm.<sup>152</sup> The detection of multiple ions using a cartridge-integrated optode array was demonstrated by Watts *et al.* The detection principle was based on a change in the fluorescence signal due to the exchange of cations from the sample with the hydrogen in the optode membrane.<sup>153</sup>

Otsuka and colleagues developed a cartridge-integrated surface plasmon resonance sensor for the detection of protein adsorption to a gold surface. The adsorption of proteins influenced the resonance frequency of the surface plasmons, which resulted in a shift in the light intensity distribution with respect to the wavelength. The light intensity was measured using a CCD camera.<sup>154</sup>

Recently, multiple papers have been published on the use of standard optical CD and DVD pick-up heads for detection. One of the driving forces for their implementation is the cost benefit<sup>155,156</sup> because they are already produced in large numbers for consumer electronics. Li and coworkers demonstrated the read-out of different binding assays using an unmodified CD read-out system by exploiting the error-signals in the detection because biomolecule/nanoparticle conjugates, bound to the surface of a CD, block the laser beam. The detected error-signal corresponded to a physical location or spot on the disk.<sup>157</sup> A similar principle for the detection of immobilized immunoreaction products based on the error distribution as a function of the “playtime” was presented by Morais *et al.* using a standard DVD drive. In the same work, another detection concept was introduced, where signal changes from the DVD drive-integrated detection photodiode were acquired, as the reflection of the laser beam was attenuated when striking the immunoreaction product.<sup>155</sup> Lange *et al.* used a modified CD pick-up head for the detection of silver grains on the CD surface, which were catalyzed by surface immobilized, gold-labeled antibodies. The silver grains caused a change in reflectivity.<sup>158</sup> A DVD pickup head for the detection of binding events was employed by Bosco *et al.* Binding biomolecules to gold-coated cantilevers caused a deflection, a change in the resonant frequency and optical roughness, which was detected by the DVD laser.<sup>159</sup>

**2.8.2 Electrochemical detection.** Multiple electrochemical instead of optical detection approaches have been demonstrated on centrifugal microfluidic platforms.<sup>34,160,161</sup> All these approaches used an integrated three-electrode setup, comprising a working electrode, reference electrode, and counter electrode, and were exploited for the chrono-amperometric quantification of liquid flow rates and visualization of flow patterns like droplet formation<sup>160</sup> or for measuring the concentration of a protein biomarker.<sup>34</sup> The latter application reported a 17-fold increase in sensitivity for the electrochemical

measurement compared to the conventional optical read-out. Both approaches used a slip ring around the axis to provide an electrical contact to the cartridge under rotation. Another implementation of a three-electrode setup, combined with an enzyme layer on the working electrode, was used to measure concentrations of hydrogen peroxide, that was generated by the enzymatic reaction of the working electrode with a set of metabolic parameters.<sup>161</sup>

**2.8.3 Other detection principles.** Surface acoustic wave (SAW)-based sensing was demonstrated by W. Lee and colleagues. Gold-stained antibodies, adsorbing to the surface of the SAW chip, produced a mass-dependent phase shift with respect to the cartridge-integrated reference SAW sensor. The SAW concept was demonstrated for the determination of certain biomarker concentrations.<sup>162</sup>

Steinert *et al.* promoted a system for protein structure analysis using X-ray crystallography as the detection principle. In this approach, X-rays from a beamline were transmitted to a cartridge-integrated crystallization chamber and produced characteristic diffraction patterns.<sup>163</sup> Schwemmer and colleagues later proposed a platform for the small-angle X-ray (SAXS) scattering-based analysis of protein structures based on the scattering of X-rays transmitted to reaction chambers on a centrifugal microfluidic cartridge.<sup>61</sup>

## 2.9 Conclusion of unit operations and introduction of process chains

Traditionally, centrifugal microfluidics has mainly used the interplay of centrifugal forces and capillary forces to control the liquid flow.<sup>62,64,80</sup> Both forces are present on centrifugal microfluidic platforms, because centrifugation is inherently available in rotating systems and capillary forces become dominant as dimensions shrink. Yet, the increasing demand on centrifugal microfluidic cartridges, namely for the integration of complex assays and high reliability/robustness, has led to an expansion of the means that are used to realize specific unit operations.

One of these means is on-chip air compression or expansion by the processing liquid, which enables new principles for valving and pumping.<sup>49,52,74,98</sup> Similar to centrifugation, this method is also intrinsically available, but compared to capillary action, it is less dependent on the surface tension and wetting properties, as well as the fabrication tolerances. Moreover, the pneumatic forces are usually orders of magnitude higher than the capillary forces, making pneumatic action particularly robust.

Another trend is the use of external radiation sources to selectively heat up areas of the cartridge or to perform optical measurements.<sup>35,46</sup> The simple implementation of radiation sources and detectors into processing devices, as well as their non-contact characteristic and applicability in numerous unit operations, make them exceedingly promising. Furthermore, such unit operations are widely independent of the liquid properties. These advantages also apply to external magnets, which are mostly used in combination with magnetic beads.<sup>138,164</sup> Another advantage of external active means is the extension of the degrees of



freedom in cartridge operation, which allows some unit operations to become independent of the rotational speed.

The portfolio of unit operations that has been discussed in this review article so far includes sample and reagent supply, liquid transport, valving and switching, metering and aliquoting, mixing, separation, droplet generation, and detection. Combining these fluidic unit operations makes it possible to implement tasks with higher complexity such as blood plasma separation, cell lysis, nucleic acid purification, and nucleic acid amplification. Here, we introduce the term “process chain” in order to refer to these tasks with higher complexity. “Process chains” can usually be implemented by combining “unit operations,” and they are very useful to describe assay implementations on a higher hierarchical level. Complex applications such as genotyping assays in molecular diagnostics can be implemented to a great extent in a straightforward manner by simply concatenating several of the above-mentioned “process chains” such as “cell lysis,” “nucleic acid purification,” and “nucleic acid amplification.” Developers may re-use validated “process chains” from other assay implementations within the same microfluidic platform without the need to know the underlying fluidic unit operations in great detail, which reduces the costs and risks of implementing new assays. In that context, applying “process chains” in an assay implementation is very similar to applying “modules” and/or “subroutines” in programming. Introducing process chains is advantageous for all kinds of microfluidic platforms.

In the following sections, the most relevant applications and underlying process chains that have been published so far are presented and discussed.

### 3. Applications

The review of the applications in centrifugal microfluidics starts with a discussion of nucleic acid-based analysis, which can be subdivided into sample preparation, amplification and detection, and the implementation of sample-to-answer nucleic acid-based analysis. Here, the term process chain is used to categorize how the lysis of cells, purification of nucleic acids, and subsequent amplification and detection are implemented in centrifugal microfluidics. Subsequently, immunoassay-based analysis is reviewed by separately discussing the largest group of enzyme-linked immuno-sorbent assays (ELISA) and other implementations of immunoassays. Thereby, the implementations of process chains for blocking, immunocapture, and washing are discussed. A review of clinical chemistry applications follows, including a discussion of the implemented process chains for blood plasma separation as an example. Then, we discuss centrifugal microfluidic cell handling; the analysis of food, water, and soil; and the analysis of protein structures and functions. Finally, applications are reviewed that do not fit into the above-listed categories such as the generation of photonic crystals.

#### 3.1 Nucleic acid analysis

Bench top nucleic acid analysis is applied to a wide range of applications where information on the DNA or RNA level is required. Because of the multiplicity of processing steps within

standard laboratory workflows, significant efforts have been put into automation by microfluidic integration, aiming at reducing the laboratory time as well as reagent and equipment costs.<sup>165</sup> The automation and integration of all the required steps on one cartridge, which can potentially be processed in a portable processing device, will facilitate complex nucleic acid testing at the point-of-care because minimal resources and no special laboratory training will be required to perform the test.

The standard laboratory workflow for a nucleic acid analysis can be roughly divided into two parts.<sup>166</sup> (1) The first part is sample preparation with the aim to make nucleic acids accessible. Process chains include the lysis of eukaryotic or bacterial cells and nucleic acid purification or concentration for subsequent analysis. (2) The second part involves the post processing of nucleic acids with process chains such as nucleic acid amplification, *e.g.*, mostly PCR and unit operations for the detection of the amplification result.

**3.1.1 Sample preparation for nucleic acid analysis.** The diversity of sample materials (including blood, saliva, urine, sputum, and culture media) and the respective preparation protocols for the extraction of high quality and inhibitory free DNA and RNA renders sample preparation labor intensive and complex. Thus, it can be regarded as the major bottleneck toward fully integrated microfluidic sample-to-answer solutions.<sup>89</sup> In this section, studies that used integrated lysis are first reviewed, followed by systems with integrated purification and then those with completely integrated extraction. The reviewed systems are listed in Table 5.

A process chain for mechanical lysis on a centrifugal microfluidic PDMS cartridge was first integrated by Kim *et al.* using the collision and friction of glass beads in a rimming flow. The rimming flow in a co-axially arranged microfluidic chamber was a result of alternating rotation, which depended on the bead density, solid volume fraction, acceleration rate, and angular velocity.<sup>167</sup> Another centrifugal microfluidic cartridge for mechanical lysis was presented by the same group. Lysis was supported by the collision of glass beads, agitated by an oscillating magnetic disk in a radially arranged microfluidic chamber. The cell debris was centrifuged radially outward, while the supernatant was transferred to a collection port *via* a capillary siphon. To induce the oscillation of the ferromagnetic disk, integrated permanent magnets were rotated above the non-rotating microfluidic cartridge on a second spin stand, which consequently required the manual transfer of the cartridge between the different processing devices.<sup>168</sup>

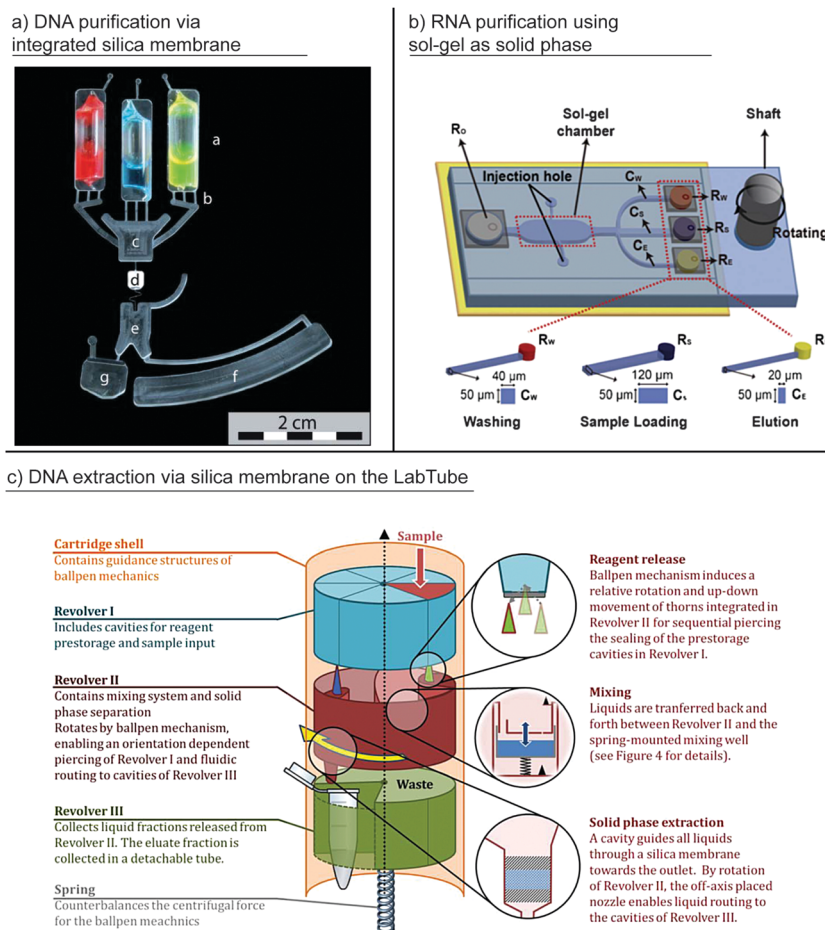
An improved version of the aforementioned work was presented by Siegrist *et al.*, in which the ferromagnetic disk in the microfluidic lysis chamber was actuated by the defined rotation of the centrifugal microfluidic polycarbonate cartridge over a set of external stationary magnets. In this approach, four lysis chambers were arranged isoradially, making it possible to process up to four samples in parallel. Centrifugo-pneumatic under-pressure valves were used to prevent sample flow into the clarification chamber during lysis. After centrifugation, the clear supernatant was transferred to a collection port *via* a capillary siphon. For the subsequent PCR analysis, heat inactivation of the inhibitors in the sample was required.<sup>76</sup>



Table 5 Comparison of centrifugal microfluidic process chains for lysis and DNA or RNA purification or extraction with respect to performance parameters and processing time<sup>a</sup>

Ref.	Lysis	Purif.	Lysis/purification method	Sample matrix and volume	Target	Performance parameters	Time	Notes
Kim J. <i>et al.</i> <sup>167</sup>	✓		ML: beads in rimming flow	Culture media	CHO-K1 cells, <i>E. coli</i> and <i>S. cerevisiae</i>	Lysis efficiency 65% vs. conventional lysis protocol	5–7 min	No connection to downstream fluidics demonstrated
Kido H. <i>et al.</i> <sup>168</sup>	✓		ML: magnetically assisted bead beating	70 $\mu$ L: (1) LB culture media (2) YPD culture media	(1) <i>E. coli</i> and (2) <i>S. cerevisiae</i>	Released DNA from (1) $\leq 40 \mu\text{g mL}^{-1}$ ; (2) $\leq 60 \mu\text{g mL}^{-1}$	30–480 s	Two processing stages required
Siegrist J. <i>et al.</i> <sup>76</sup>	✓		ML: magnetically assisted bead beating	4 $\times$ 90–95 $\mu$ L or 1 $\times$ 360–380 $\mu$ L; (1) DI water; (2) clinical nasopharyngeal aspirate (NPA)	(1) <i>B. subtilis</i> spores (2) human metapneumovirus or adenovirus	(1) Equivalent lysis vs. reference; (2) correct identification of all viruses	< 6 min	Lysis of spores demonstrated
Hoffmann J. <i>et al.</i> <sup>24</sup>	✓		SPE; silica matrix integrated into cartridge	32 $\mu$ L lysed whole blood	Human DNA	$\leq 77\%$ vs. off-chip reference	Not stated	Liquid reagent prestorage in glass ampoules
Müller M. <i>et al.</i> <sup>96</sup>	✓		SPE; silica matrix integrated into cartridge	32 $\mu$ L lysed blood	Human DNA	53 $\pm$ 8% vs. reference	66 min	Commercially available reagents prestored
Park B. H. <i>et al.</i> <sup>131</sup>	✓		SPE; silica sol-gel integrated into cartridge	Virus lysate (5 $\mu$ L)	RNA from influenza H1N1 virus	RNA capture yield 80%	5 min	Small reagent volumes
Jung J. H. <i>et al.</i> <sup>130</sup>	✓		SPE; integrated glass bead column	3.5 $\mu$ L RNA sample (0.5 $\mu$ L virus lysate, 1.25 $\mu$ L EtOH, 1.75 $\mu$ L 6M Gu-HCl) LB media (50 $\mu$ L)	RNA from influenza H3N2 virus	RNA capture yield $\sim 81\%$	440 s	Lysis process not included. Elution with RT-PCR cocktail demonstrated
Strohmeier O. <i>et al.</i> <sup>138</sup>	✓		SPE; magnetic silica beads	DNA from lysed <i>Listeria innocua</i> and lambda phage	DNA from lysed <i>Listeria innocua</i> and lambda phage	Up to 68% $\pm$ 24% for <i>L. innocua</i> and 43% $\pm$ 10% for lambda phage vs. manual reference	12.5 min	Novel handling concept for magnetic beads
Wadle S. <i>et al.</i> <sup>170</sup>	✓		SPE; magnetic silica beads	Human DNA	Human DNA	Extracted DNA: 4.6 $\pm$ 0.7 ng $\mu\text{L}^{-1}$ (disk) vs. 4.1 $\pm$ 0.4 ng $\mu\text{L}^{-1}$ (reference)	Not stated	Commercially available extraction reagents
Strohmeier O. <i>et al.</i> <sup>171</sup>	✓		SPE; magnetic silica beads	Human DNA, DNA from <i>B. subtilis</i> and <i>E. coli</i> and RNA from Rift Valley fever virus	Human DNA, DNA from <i>B. subtilis</i> and <i>E. coli</i> and RNA from Rift Valley fever virus	Up to 98.5% for <i>B. subtilis</i> , 102.1% for <i>E. coli</i> and 34.2% for Rift Valley fever	$\sim 30$ min	Measurement of PCR inhibitors included. Commercially available reagents
Cho Y. K. <i>et al.</i> <sup>89</sup>	✓		IMS with beads; TL by laser-induced heating	100 $\mu$ L whole blood	<i>E. coli</i> and <i>Hepatitis B virus</i> (HBV)	Comparable to bench top extractions	12 min	Blood plasma separation included
Kloke A. <i>et al.</i> <sup>36</sup>	✓		SPE; silica matrix integrated into cartridge	200 $\mu$ L whole blood	Human DNA	Equal to manual reference	50 min	Operated on standard laboratory centrifuge

<sup>a</sup> ML: mechanical lysis; TL: thermal lysis; SPE: solid phase extraction; IMS: immunomagnetic separation.



**Fig. 10** Centrifugal microfluidic process chains for nucleic acid purification and extraction. (a) DNA purification from lysed whole blood *via* integrated silica matrix “d” with onboard liquid reagent prestorage “a.” An integrated Coriolis switch “e” is used to direct purified DNA and waste to different microfluidic chambers “f” and “g”.<sup>24</sup> (Reproduced with permission from The Royal Society of Chemistry.) (b) RNA purification from virus lysates *via* sol-gel matrix.<sup>131</sup> (Reproduced with permission from The Royal Society of Chemistry), and (c) DNA extraction in LabTube *via* integrated silica matrix.<sup>36</sup> (Reproduced with permission from The Royal Society of Chemistry.)

For nucleic acid purification from lysed whole blood *via* a bind-wash-elute protocol, the so-called “Boom chemistry”,<sup>129</sup> a centrifugal microfluidic cyclic olefin copolymer cartridge with on-board liquid reagent prestorage was presented by Hoffmann *et al.* (Fig. 10a). As the solid phase for DNA purification, silica membranes from commercially available QIAGEN spin columns were integrated into the cartridge. During processing, the pre-lysed sample and binding buffer mixture first passed through the silica membranes to capture the DNA. This was followed by a washing buffer. Finally, an elution buffer was supplied to elute the purified DNA from the membrane. An integrated Coriolis switch<sup>92,169</sup> was used to separate the waste (lysed sample and washing buffers) and elution buffer containing the purified DNA.<sup>24</sup> A similar system was presented by Müller *et al.*, which was designed to be operated in a standard laboratory centrifuge.<sup>96</sup> In this work, the Coriolis switch was replaced by a switch for unidirectional rotation because the centrifuge only supports one direction of rotation. Neither approach integrated lysis of the blood.

A microscope slide-shaped microchip for RNA purification from low volumes (5 μL) of virus lysates *via* a bind-wash-elute

chemistry was reported by Park *et al.* A sol-gel matrix in a microfluidically patterned PDMS layer was used as a solid phase for the separation of RNA from the lysate (Fig. 10b). A lysed sample premixed with ethanol for binding, washing buffer, and elution buffer were added to microfluidic reservoirs prior to rotation and sequentially released using the differences in the flow resistances of the connecting channels.<sup>131</sup> In a later work, the sol-gel solid phase was replaced by a column of tetraethoxy orthosilicate (TEOS)-activated glass beads contained in a zig-zag-shaped microfluidic channel. Here, capillary valves between the washing buffer reservoirs and the zig-zag channel and a capillary siphon between the elution buffer reservoir and the zig-zag channel were exploited for the sequential release of the reagents to the glass bead bed.<sup>130</sup> In both approaches, lysis of the virus samples was conducted off chip. Although all the reagents could be added to the chips at the beginning, the waste (washing buffer and lysate) had to be removed manually from the capture chamber during processing.

The purification of DNA from lysate samples with silica-coated magnetic beads was demonstrated using integrated-gas-phase



transition magnetophoresis (GTM) on a microthermoformed foil cartridge. Bead transport was a result of the defined positioning of the foil cartridge in relation to an external stationary permanent magnet and did not require any human interaction. Initially, beads bound the DNA from the lysate in a first chamber. After binding, the beads were automatically transported through an air-gap into a second chamber containing washing buffer and finally into a third chamber with elution buffer.<sup>138</sup> The modular concatenation of multiple chambers with different volumes was then applied for bead-based DNA extraction from whole blood, including lysis.<sup>170</sup> In a later work, this process chain for nucleic acid extraction was extensively characterized for extractions from logarithmic dilutions of various target pathogens and sample matrices including Gram-positive *Bacillus subtilis*, Gram-negative *Escherichia coli*, Rift Valley fever RNA viruses from blood plasma and human genomic DNA from whole blood.<sup>171</sup>

Recently, the LabTube was introduced as a versatile centrifugal microfluidic platform for bind-wash-elute-based DNA extraction from blood and other samples.<sup>36</sup> Microfluidic and micromechanical elements are integrated in a centrifuge tube with the outer dimensions of a 50 mL centrifuge tube, as depicted in Fig. 10c. An integrated centrifugally actuated ball-pen mechanism enables reagent release and liquid routing. Unit operations for mixing and separation-based extraction are also integrated. Using LabTube, extractions of genomic DNA from whole blood were demonstrated with yields and purities equal to manual reference runs. Sample addition, the transfer of LabTube into the centrifuge, and the withdrawal of a standard reaction tube containing the eluate remained as the only manual steps.

A highly comprehensive approach for pathogen specific DNA extraction on a centrifugal microfluidic polycarbonate cartridge was presented by Cho *et al.*<sup>89</sup> In this work, target pathogens were separated from a sample by immunomagnetic separation using antibody-coated magnetic beads subsequent to disk-integrated blood plasma separation. Pathogens were thermally lysed by heating the beads with a laser. Multiple integrated ferrowax microvalves (LIFM) could be opened or closed by laser irradiation, thereby defining the fluidic routing.

**3.1.2 Nucleic acid amplification and detection.** The most common method for nucleic acid analysis is amplification and subsequent detection. Amplification can be divided into the standard method, the polymerase chain-reaction (PCR) that requires different temperatures, typically between 55 °C and 95 °C, and isothermal methods (such as loop mediated isothermal amplification (LAMP), recombinase polymerase amplification (RPA), rolling circle amplification (RCA), and helicase dependent amplification (HDA)). Monitoring the PCR in real-time allows for the highly sensitive quantification of DNA down to the single molecule level. Isothermal methods are significantly faster and achieve a similar sensitivity, but often have deficiencies in their quantification capability.

Detection can be achieved using fluorescently labeled probes, by intercalating fluorescent dyes, after PCR, *e.g.*, by the detection of the PCR product *via* gel- or capillary electrophoresis, or by hybridization to immobilized DNA capture probes (DNA microarrays). Although the application of centrifugal microfluidics for

automating process chains like nucleic acid amplification has advantages (*i.e.*, a reduced risk of cross contamination because of the closed systems, homogeneous temperature distribution, and recondensation of vapor), the interfaces required for thermocycling and optical readout remain technically challenging. In this context, the review of the amplification and detection methods is structured as follows. First, centrifugal microfluidic systems that only integrate the amplification process chain are reviewed. Then, systems with additionally integrated unit operations for detection are reviewed. These systems are compared by the degree of multiplexing (*i.e.*, the ability to simultaneously detect different target nucleic acids), sensitivity, and time to result (Table 6). At the end of the section, we review centrifugal microfluidic systems that were exploited for processing microarrays.

A centrifugal microfluidic cartridge for PCR-based amplification has been presented where contact heating and cooling using three thermoelectric modules was employed for thermocycling (1 module) and in parallel for freezing sub-volumes of the PCR buffer in the channel network (2 modules) to ice valves. These ice valves were integrated to block the connection channel between the PCR chamber and venting hole and thus prevent cross contamination through the vent because stationary thermocycling was conducted, without rotating the disk.<sup>90</sup> Jung *et al.* developed a PDMS/glass cartridge for the reverse transcriptase PCR detection of viral RNA. The microfluidic cartridge was serially rotated over three temperature blocks at different temperatures for denaturation, annealing, and extension.<sup>172</sup> In both approaches, the detection of the generated PCR product had to be conducted off-disk using gel electrophoresis<sup>90</sup> or microcapillary electrophoresis.<sup>172</sup>

Further applications have been demonstrated using centrifugal forces to force a bacterial sample through 24 zig-zag shaped channels integrated into a centrifugal microfluidic PDMS cartridge. Single bacterial cells from the sample were distributed into multiple 1.5 nL microchambers connected to each zig-zag channel. For the thermal lysis of the cells and PCR-based amplification, the cartridge was placed on a custom-made thermocycling system for contact heating. After PCR, the fluorescence intensity was measured by placing the cartridge into an image analyzer.<sup>173</sup>

Digital PCR on centrifugal microfluidic cartridges was presented by Sundberg *et al.* By spinning the disk, a PCR mixture that included plasmid DNA was forced through a spiral channel and aliquoted into one thousand 33 nL amplification wells (Fig. 11a). Afterward, the PCR mixture aliquots in the wells were separated by forcing mineral oil through the spiral channel. An air-mediated temperature setting for thermocycling allowed PCR cycle times of 33 seconds.<sup>101</sup> The proposed digital PCR platform has been commercialized and distributed by Espira Inc.<sup>174</sup>

Centrifugal microfluidic cartridges have been exploited for the real-time PCR-based genotyping of methicillin-resistant *Staphylococcus aureus* (MRSA).<sup>38</sup> Cartridges were fabricated from thin polymer foils using microthermoforming<sup>175</sup> to allow fast, air-mediated, heat transfer (Fig. 11b). An integrated unit operation for two-step aliquoting made it possible to divide and

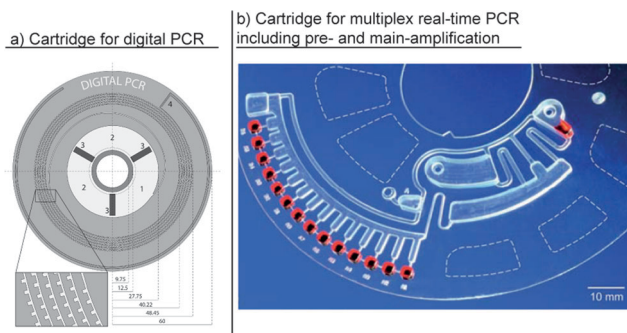




Table 6 Comparison of centrifugal microfluidic cartridges for nucleic acid amplification and detection

Ref.	Amplification	Target	Degree of geometric multiplexing	Sensitivity	Time (cycles)	Detection technology	Heating technology
Focke M. <i>et al.</i> <sup>38</sup>	PCR	Resistance genes in <i>S. aureus</i>	7 + 1 internal control	<10 DNA copies per well	110 min (50 cycles)	FAM-labeled hydrolysis probes; real-time fluorescence detection	Air mediated in commercially available PCR thermocycler
Lutz S. <i>et al.</i> <sup>26</sup>	RPA	mecA gene in <i>S. aureus</i>	Monoplex	<10 DNA copies per well	<15 min	Real-time fluorescence detection	Air mediated in commercially available PCR thermocycler
Focke M. <i>et al.</i> <sup>37</sup>	Multiplex-preamplification, nested PCR	Resistance genes in <i>S. aureus</i>	Up to 4	Down to 7 copies per sample	17 min (10 cycles) pre-amp, 52 min (50 cycles) main amplification <sup>a</sup>	FAM-labeled hydrolysis probes; real time fluorescence detection	Air mediated in commercially available PCR thermocycler
Strohmeier O. <i>et al.</i> <sup>39</sup>	Allele-specific PCR	KRAS point mutations on tumor cell DNA	8	Not stated	Not stated	FAM-labeled hydrolysis probes; real-time fluorescence detection	Air mediated in commercially available PCR thermocycler
Strohmeier O. <i>et al.</i> <sup>41</sup>	PCR	DNA from 6 different food borne pathogens	6	0.1 pg DNA per well for <i>Salmonella</i> and <i>Listeria</i>	~2 h (50 cycles)	FAM-labeled hydrolysis probes; real-time fluorescence detection	Air mediated in commercially available PCR thermocycler
Sundberg S. O. <i>et al.</i> <sup>101</sup>	Digital PCR	300 base pair plasmid DNA	Monoplex	Amplification in 58 out of 1000 wells (DNA concentr.: $6 \times 10^0$ copies $\mu\text{L}^{-1}$ )	~25 min (45 cycles); additional 25 min for loading, fluorescent imaging and image analysis	Intercalating dye; "accumulated" real-time fluorescence detection of hundreds of wells for melting curve analysis; post PCR image acquisition with CCD camera for digital well analysis	Air mediated
Furutani S. <i>et al.</i> <sup>173</sup>	PCR	<i>invA</i> gene in <i>Salmonella enterica</i>	Monoplex	PCR on isolated single cells	95 °C/2 min for thermal lysis; denat. 95 °C/5 s, anneal. 55 °C/10 s; elongate 72 °C/10 s optimum 40 cycles 53 min (35 cycles)	FAM-labeled hydrolysis probes; post-PCR fluorescence detection	Contact
Amasia M. <i>et al.</i> <sup>90</sup>	PCR	<i>Bacillus anthracis</i> ; <i>Bacillus cereus</i>	Monoplex	Not stated		Off-chip (analysis of PCR products by gel electrophoresis)	Contact; with thermo electric modules
Jung J. H. <i>et al.</i> <sup>172</sup>	RT-PCR	Influenza A subtypes: H3N2, H5N1, and H1N1	Monoplex and duplex	~2 RNA copies (demonstrated for H3N2)	25.5 min	Off-chip (microcapillary electrophoresis)	Contact; serially on thermal blocks

PCR: polymerase chain reaction; RT-PCR: reverse transcriptase polymerase chain reaction; RPA: recombinase polymerase amplification; *S. aureus*: *Staphylococcus aureus*. <sup>a</sup> Time for heating and cooling not included.



**Fig. 11** Centrifugal microfluidic cartridges for nucleic acid amplification: (a) cartridge for digital PCR using unit operation for one-step aliquoting to 1000 1 nL amplification wells.<sup>101</sup> (Reprinted with permission from the American Chemical Society.) and (b) Cartridge for pre amplification and subsequent multiplex real-time PCR-based main amplification, including integrated two-stage aliquoting into fourteen 10  $\mu$ L amplification wells.<sup>37</sup> (Reproduced with permission from The Royal Society of Chemistry.)

fluidically separate an initial volume of PCR mastermix into eight aliquots of 10  $\mu$ L each. The aliquots were then transferred into a separate amplification chamber harboring a set of dryly prestored primers and probes. Thereby, “geometric” multiplexing was achieved. Up to four separate DNA samples could be analyzed per cartridge.<sup>38</sup> To increase the sensitivity, an advanced version of the aforementioned cartridge was presented by the same group, which included pre-amplification prior to aliquoting and a downstream nested PCR. A translation of the integrated functionality into a schematic description highlighting the implemented process chains and unit operations is depicted in Fig. 12. As an advantage, the integration of the pre- and main amplification into the same cartridge circumvented the risk of cross contamination by sample handling after pre-amplification.<sup>37</sup>

A similar cartridge has been used for isothermal real-time amplification by recombinase polymerase amplification (RPA).

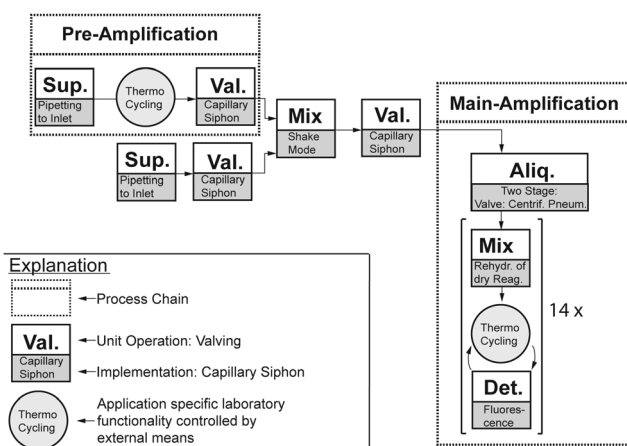


**Fig. 12** Schematic interpretation of integrated functionality of Focke *et al.*<sup>37</sup> Dashed boxes represent process chains, and solid boxes depict unit operations and the demonstrated implementation (Sup.: sample or reagent supply; Val.: valving; Mix: mixing; Aliq.: aliquoting; Det.: detection). Circles illustrate application specific laboratory functionalities that are controlled by external means.

In this work, a lyophilized polymerase pellet and liquid rehydration buffer were prestored on the cartridge. Thus, only a template DNA addition was required. The rehydration of the lyophilized polymerase pellet was achieved by integrated shake mode mixing before the RPA mastermix was transferred into an aliquoting structure *via* a capillary siphon valve. Up to six samples could be analyzed per cartridge.<sup>26</sup> For multiplex point mutation detection, an allele-specific PCR has been integrated into centrifugal microfluidic foil disk-segments to allow the independent processing of up to four samples per run. The automation comprises the aliquoting of a PCR mastermix into multiple fluidically separated amplification chambers with dryly prestored primers and probes, followed by an allele-specific PCR.<sup>39</sup> In another approach, Strohmeier *et al.* presented a cartridge for the detection of six common food borne pathogens. This cartridge included amplification chambers for integrated positive and negative controls and demonstrated the capability for quantitative real-time PCR by the parallel amplification of integrated DNA standards.<sup>41</sup> As an advantage, all the cartridges and disk segments could be processed in a modified, commercially available centrifugal real-time PCR thermocycler for fluidic processing, amplification, and fluorescence detection, and did not require additional equipment. Recently, Czilwik *et al.* presented a passive microfluidic vapor diffusion barrier to reduce pressure increase during thermocycling. The application of this unit operation was demonstrated for PCR amplification and subsequent transport of the amplification product for further analysis.<sup>176</sup>

Recently, Focus Diagnostics and 3M introduced the integrated cyclers, a real time PCR cycler, to the market. Up to 96 pre-extracted nucleic acid samples can be pipetted to a universal single-use disk. Each of the 96 radially inward inlet wells is directly connected to one of 96 amplification wells located at the outer rim of the cartridge. Contact heating is employed for thermocycling. Up to four fluorescence channels are available in the instrument for real-time detection. In 2012, Focus Diagnostics' Flu Test for use in combination with the 3M integrated cycler was approved by the FDA.<sup>177</sup> A list of the relevant patents for the disposable disk and device can be found on the website.<sup>178</sup>

In addition to the integration of process chains like those for nucleic acid amplification and detection, in the past, multiple centrifugal microfluidic cartridges have been presented for automating microarray processing.

Peng *et al.* presented a glass disk that was first attached to a PDMS disk with 96 radial channels. Using centrifugal forces, DNA probes were then pumped through the channels for “printing” radially DNA probe lines on the glass disk. The first PDMS disk was then peeled off and replaced by a second PDMS disk with 96 spiral channels that orthogonally intersected the 96 probe lines. Finally, DNA samples were forced through the spiral channels and hybridized to the probe lines. Successful hybridization was detected using a fluorescence scanner.<sup>132</sup> This centrifugal microfluidic cartridge for DNA hybridization with slightly increased channel dimensions was later used by the same group for the detection of PCR products from the





fungal pathogens *Botrytis cinerea* and *Didymella bryoniae*. The presented system was capable of detecting 3 ng PCR products after hybridization for 2 h at 45 °C.<sup>179</sup> By improving the flow control and channel design and adding an additional fluorescent dye, the detection of less than 0.2 ng of PCR products derived from three different fungal pathogens (*Didymella bryoniae*, *Botrytis cinerea*, and *Botrytis squamosa*) within 3 min at 23 °C<sup>180</sup> was presented.

Peytavi *et al.* developed a slide-shaped PDMS chip with integrated microfluidic channels for the discrimination of the single nucleotide polymorphisms of four clinically relevant *Staphylococcus* species. The serial release of samples (PCR products with incorporated Cy-labeled dUTPs), washing buffer, and rinsing buffer into the array chamber was controlled by the spin speed and integrated capillary valves. Afterward, the slide was dried during rotation at a high spin speed. For readout, the glass slide was transferred into an array scanner. A 10-fold increase in the hybridization signal was reported for the microfluidic flow-through approach compared to passive systems that solely rely on the diffusion of an analyte to the capture probe.<sup>134</sup> A similar microfluidic chip was later used for the hybridization of 25-mer DNA samples. Enzyme-labeled fluorescence technology was used to generate the signal for detection. A threefold increase in fluorescence intensity compared to passive assays was reported for similar hybridization times.<sup>133</sup>

**3.1.3 Sample-to-answer nucleic acid analysis.** The term “sample-to-answer analysis” of nucleic acids refers to an integrated analytical solution that comprises all the necessary process chains for sample preparation and subsequent detection. Because of the complexity of microfluidic integration and connecting the interfaces to external means (thermocycling, modules for optical detection, *etc.*), sample-to-answer analysis remains very challenging. Although all the required process chains have been separately demonstrated on centrifugal microfluidics, to the best of our knowledge, no completely integrated and automated system with sample-to-answer capability for nucleic acid analysis has so far been reported in a peer-reviewed journal. However, several conference proceedings are available and included in the review. Although they showed no full sample-to-answer capability, we included systems that have integrated combinations of process chains for both sample preparation and post processing in this chapter.

Hoehl *et al.* presented a LabTube<sup>36</sup> with an integrated process chain for solid-phase-based DNA purification from lysates of a verotoxin produced by *Escherichia coli* spiked in water, milk, and apple juice samples, combined with the subsequent isothermal LAMP amplification. In this work, a battery-driven heating system was integrated for the direct amplification in the tube. The positive LAMP amplification resulted in a visible color change for the LAMP reaction. A reduction in the manual labor time from 45 to 1 minute was reported, requiring only a single pipetting step to load the LabTube with the pre-lysed bacterial sample.<sup>181</sup>

Kim *et al.* presented a centrifugal microfluidic cartridge for the detection of *Salmonella* from PBS and milk samples that included process chains for laser-induced thermal lysis<sup>89</sup> and

isothermal amplification *via* RPA. For sequential fluid control, several ferrowax valves<sup>89</sup> were integrated. Read-out of the result was possible *via* visual detection on an integrated lateral flow strip. Detection limits of 10 CFU mL<sup>-1</sup> and 10<sup>2</sup> CFU mL<sup>-1</sup> were reported for the PBS and milk samples, respectively, with a time to result of 30 minutes. Not included in the microfluidically automated process was the process chain for immunomagnetic sample enrichment from the 1 mL milk and PBS samples. After capturing the pathogens, the capture beads were magnetically collected, washed twice, and resuspended in 5 µL of distilled water, which was then loaded onto the cartridge.<sup>146</sup>

Strohmeier *et al.* presented a centrifugal microfluidic polymer foil cartridge for the sample-to-answer analysis of bacterial targets from a blood plasma sample. The following process chains were combined on the cartridge in sequential order: chemical lysis, magnetic bead-based DNA purification, and isothermal amplification *via* RPA with real-time fluorescence detection relying on unit operations such as capillary siphons, gas-phase transition magnetophoresis for DNA separation,<sup>138</sup> and aliquoting.<sup>98</sup> The disk could be processed in a portable device, and successful sample-to-answer detection was demonstrated for 6 × 10<sup>4</sup> genome equivalents of *Bacillus anthracis* and 6 × 10<sup>6</sup> genome equivalents of *Francisella tularensis* spiked into blood plasma samples. A total processing time of 45 minutes was reported.<sup>43</sup> An updated version of the aforementioned work demonstrated real-time PCR-based detection of *Staphylococcus warneri*, *Streptococcus agalactiae*, *Escherichia coli* and *Haemophilus influenzae* from a 200 µL serum sample. Limits of detection were reported to be 3, 150, 5 and 18 colony forming units, respectively. In addition to the above-mentioned process chains, a stickpack for prestorage and on-demand release of rehydration buffer and a process chain for pre-amplification prior to target specific PCR was integrated to increase the sensitivity.<sup>29,182</sup> Pre-amplification required further unit operations for metering the eluate and pumping<sup>49</sup> the pre-amplified solution toward the center of the cartridge. Processing was conducted in a portable PCR device.<sup>182</sup>

Jung *et al.* presented a centrifugal microfluidic cartridge for the purification of viral RNA from H3N2 influenza combined with the subsequent amplification and detection. No process chain for sample lysis was included. RNA separation from the lysate and purification were conducted using a microglass bead solid phase, while an RT-PCR cocktail was used to elute the purified RNA from the bead bed. The sample, washing buffers, and RT-PCR mix were sequentially released from their inlet chambers by differences in the flow resistance values of the respective channels or by capillary siphons.<sup>183</sup>

3M recently commercialized the “direct amplification disc”<sup>184</sup> for the sample-to-answer analysis of influenza virus A/B and respiratory syncytial virus (RSV). The “direct amplification disc” can be operated in the 3M integrated cyclor. The disk allows the real-time amplification of up to eight unprocessed clinical samples by making use of direct amplification chemistries<sup>185</sup> that can perform nucleic acid extraction and amplification in one protocol. For processing, a 50 µL patient sample and 50 µL reaction mix have to be pipetted to the direct amplification disc prior to



processing. The microfluidic layout has not been published, although several patents might disclose the functionalities of single unit operations such as metering<sup>186</sup> and valving.<sup>187</sup> Up to four fluorescence channels are available for detection.

The Canadian company GenePOC Inc. is approaching the market with a centrifugal microfluidic disk segment with sample-to-answer capability, which includes process chains for mechanical lysis and subsequent amplification and detection. Up to eight disk segments can be processed in parallel, allowing the independent analyses of up to eight samples with volumes of 100–200  $\mu\text{L}$  in parallel. According to the corresponding patent application,<sup>188</sup> the system features mechanical lysis using glass beads that are actuated by an additional magnetizable element in the microfluidic chamber similar to the system presented by Kido *et al.*<sup>168</sup> Afterwards, a portion of the lysate is diluted with a dilution buffer, heated up, and aliquoted into three separate amplification chambers that contain specific PCR reagents. By using four different dyes, up to 12 targets should be detectable from one sample in less than 1 hour with less than 1 minute of hands-on time.<sup>189</sup>

Although showing full sample-to-answer capability, neither commercial system has an integrated process chain for nucleic acid purification after lysis. On the one hand, this makes microfluidic integration easy because of the reduced complexity. On the other hand, the approach might only be suitable for certain sample materials with low amounts of inhibitors and sufficient pathogen-loads because no DNA/RNA concentration step is included.

### 3.1.4 Trends and perspectives in nucleic acid analysis.

Platforms based on centrifugal microfluidics have proven to be suitable for the automation of nucleic acid analysis. Because no connection to external pressure sources is required, the risk of cross contamination is reduced, which might be of particular relevance if bio-hazardous material is processed or the release of post-amplification products has to be avoided. All the relevant process chains, including lysis, purification, and amplification, have successfully been demonstrated on centrifugal microfluidic platforms. However, the combination of all these process chains for integrated sample-to-answer analysis has not yet been presented in a peer-reviewed journal publication. A possible reason might be the limited available space in the radial direction, which would require the implementation of unit operations for pumping liquid back toward the center of a disk. Still, many systems require manual interaction during processing;<sup>130–132,173</sup> lack suitable prestorage concepts, particularly for liquid reagents;<sup>43,130,131,170,182</sup> or use fabrication technologies that are not compatible with mass production.<sup>131,132,134</sup> In the future, isothermal amplification techniques<sup>190</sup> such as HDA, LAMP, and RPA might boost the development of fully integrated sample-to-answer solutions because no complicated thermocycling is required, while the implementation of recently presented unit operations for liquid transport by pneumatic pumping and reagent prestorage might be suitable to solve the remaining system integration challenges.

To circumvent the need for additional equipment, the processing of centrifugal microfluidic cartridges for sample preparation<sup>36</sup> or amplification and detection<sup>26,37–39,41,181</sup> in

commercially available equipment has been demonstrated. These microfluidic chips, which extend the functionality of an existing processing device, have been called “microfluidic apps”.<sup>191</sup> Other cartridges could be processed in small and portable devices, making them suitable for single sample testing and application at the point-of-care.<sup>43,170,182</sup> In addition to single sample and point-of-care testing, first applications have been demonstrated for highly parallel applications such as digital PCR.<sup>101</sup>

The application of centrifugal microfluidics for automation of nucleic acid analysis provides unique advantages for assay automation as multiple standard laboratory process chains already exploit centrifugal forces when conducted manually. The advantages include the possibility to perform density based separations during sample preparation such as the separation of blood plasma from whole blood or the concentration of bacterial pathogens by sedimentation. Furthermore, nucleic acid extraction on the bench commonly uses so called “*spin columns*” where the sample and liquid reagents are serially forced through solid phase membranes by centrifugation. With respect to PCR based nucleic acid amplification, centrifugal microfluidic cartridges may benefit from the straight forward approach to remove bubbles (due to buoyancy in the centrifugal gravity field) at elevated temperatures.

### 3.2 Immunoassays

Immunoassays (IA) are widely established in (bio-) medical diagnostics, biological and biochemical studies, drug development, environmental analyses, and food safety.<sup>59,156,192</sup> Immunoassays are based on the highly specific affinity of antibodies (Ab) to antigens (Ag), allowing for the detection of bioanalytes that provide appropriate binding sites (epitopes). Either the antigen or antibody can be the target bioanalyte. In heterogeneous immunoassays, the capture antibody is immobilized either on macroscopic solid supports or on microscopic beads suspended in the solution. The analyte is present in the liquid phase. After a certain incubation period, the bound analyte is measured directly on the surface using a suitable transducer or biosensor system, or using a secondary antibody in solution conjugated with a suitable tracer. In the latter case, an active bound/free separation step, *e.g.*, by washing, is required. Alternatively, homogeneous immunoassays do not require a bound/free separation step. In this case, a signal is generated by the binding of the appropriate tracer or tracer combination to the analyte.

A wide variety of immunoassay formats are in place, and two main categories can be considered. An immunometric assay employs an antibody labeled with a tracer, which is advantageous if the target analyte exposes multiple binding sites or epitopes. In this case, for example, the primary or capture antibody binds the analyte to the solid phase, and the secondary labeled antibody builds up a sandwich-type structure with the analyte. After the bound/free separation, the tracer bound *via* the sandwich to the solid phase can be quantified. Competitive assay formats are often used for small analytes, which expose only one binding site or epitope. In this case, an analyte



analogon conjugated with a tracer competes with the analyte in the sample. The analyte analogon is applied in a defined, limited concentration to enable balanced competition with the analyte for the binding antibody.

The integration and automation of immunoassays on centrifugal microfluidic platforms are especially regarded as attractive because conventional assay protocols are labor intensive and consist of a large number of manual processing steps.<sup>59</sup> As most of the steps are similar for a broad variety of assays, platform-based automation offers unique advantages to reduce costs and ensure consistent results.<sup>60,135,193</sup> Yet, the most commonly employed platform for immunoassays are microtiter plates having, for example, 96 wells in a well-defined pitch,<sup>194</sup> where liquid handling can be automated by pipetting robots. In contrast, the microfluidic automation of immunoassays offers some unique advantages such as reduced reaction times due to reduced diffusion distances, as well as reductions in the reagent and sample volumes.<sup>59,156</sup>

As the accuracy of diagnostic findings can be enhanced by simultaneous analyses of multiple biomarkers, the degree of multiplexing of one sample within an IA automation is an additional important characteristic.<sup>194</sup> Similar to nucleic acid analysis, multiplexing is typically achieved by differentiation in the spatiotemporal or spectroscopic domain.<sup>194</sup> In this context, we propose an evaluation of centrifugal microfluidic cartridges for immunoassays based on the following criteria: the analytical sensitivity (limit of detection, LOD) and reproducibility/precision (coefficient of variation, CV) achieved for the specific analyte. Further, if the performance criteria for a specific analyte can be met, the time to result and degree of automation, integration, parallelization, and multiplexing should be evaluated. Table 7 summarizes important key characteristics of the reviewed systems. The review section is split into two subchapters, centrifugal microfluidic systems for ELISA followed by a section on other immunoassay formats.

**3.2.1 Centrifugal microfluidic systems for ELISA.** A very prominent format for immunoassays is the enzyme-linked immunosorbent assay “ELISA,” where an enzyme is used as a tracer in an immunometric assay, and the signal generation is a result of a substrate reaction. Different ELISA formats can be realized, such as the sandwich and competitive formats mentioned above.

The majority of the steps in the laboratory workflow for a typical heterogeneous sandwich ELISA can be automated by utilizing the immunocapture process chain: (1) the immobilization of the primary/capture Ab or Ag on a solid phase, (2) binding of the target Ag or Ab in the sample to the primary Ab or Ag on the solid phase, and (3) binding of the enzyme-labeled secondary/detection Ab to the target Ag or Ab. The blocking process chain is thereby applied between the first and second steps to prevent unspecific binding, whereas all the steps are separated by multiple washing process chains to rinse away the unbound material. The remaining steps for signal generation and detection involve unit operations for (4) supplying the substrate solution for the enzymatic reaction, (5) the eventual termination of the enzymatic reaction by supplying a stopping

solution, and (6) the quantification of the enzymatic reaction product. An early centrifugal microfluidic cartridge for ELISA-based immunoassays was reported by Lai *et al.* Integrated capillary valves allow for the sequential release of pre-loaded reagents into a microchannel with immobilized primary antibodies. Each liquid solution displaces the aforementioned into a waste chamber. A singleplex analysis of rat IgG from a hybridoma culture proved advantageous with respect to reagent consumption and assay time.<sup>59</sup> Later, a similar system was used for the detection of cytokine interferon-gamma.<sup>192</sup>

A later approach for direct ELISA was presented by Riegger *et al.* Up to eight separate immunoassays could be processed per cartridge in parallel for the detection of the relevant biomarkers for acute myocardial infarction. High-speed chemiluminescence detection with a photo-multiplier was performed under rotation in less than 1 second.<sup>195</sup>

An increase in parallelization to 18 immunoassays per cartridge was presented by Nagai *et al.* A single bead served as the solid phase for the competitive, indirect ELISA targeting a mental stress biomarker. Prior to the on-cartridge automation, time-consuming off-chip steps had to be performed.<sup>136</sup> An injection-molded cartridge featuring 24 parallel immunoassays was reported by Welte *et al.* A multiplicity of unit operations, including capillary siphon and hydrophobic valves were integrated to route the reagents. All the reagents had to be loaded step-by-step during the protocol.<sup>196</sup>

A totally integrated ELISA for detecting the antigens and antibodies of the hepatitis B virus was presented by B. S. Lee *et al.* An integrated process chain for blood-plasma separation allowed the use of a whole-blood sample. The routing of the sample and reagents was controlled by integrated active laser irradiated ferrowax microvalves. Shake-mode mixing was implemented to mix beads (solid phase) with the plasma, detection probe, washing buffers, or tetramethyl benzidine (TMB) solution. The parallelization of three separate immunoassays allowed tests to be performed for the antigen and antibody of the hepatitis B virus, HBsAg and anti-HBs, and a control, in parallel on a single cartridge. The assay time increased by 2/3 compared to processing a single IA. All the required assay components were pre-loaded onto the disk.<sup>135</sup> Later, an advanced version of the aforementioned injection-molded cartridge, combining the demonstrated IA principle and a biochemical analysis applying a lipid test panel (see Section 3.3) was presented. These tests were performed simultaneously from one whole-blood sample, aiming at the detection of CK-MB (muscle and brain fraction of creatine kinase) as a biomarker for recent heart attacks.<sup>137</sup>

The combination of a high degree of integration with multiplexing ability was reported by Park *et al.* The cartridge featured two ELISAs in parallel (Fig. 14a), each capable of testing a sample for three targets or controls, respectively. Reagents were pre-loaded onto the cartridge prior to the test. An analysis of cardiovascular disease biomarkers in whole saliva or blood was performed. The reaction chambers were first flushed with common liquids simultaneously. Later, the fluidic pathways were isolated from each other by active laser-actuated





**Table 7** Centrifugal microfluidic systems for immunoassay automation compared by demonstrated degree of multiplexing (defined as number of tested analytes per sample), parallelization (defined as number of tested samples per run), and limit of detection (LOD)

Ref.	Assay format/solid phase/detection	Sample matrix	Multiplexing	Parallelization	Reagent pre-loading/storage	Total time [min]	Target analyte/LOD
Lai <i>et al.</i> <sup>59</sup>	ELISA/channel/fluorescence	Cell culture	1	Up to 24	Yes	> 60	rat IgG/31 nM
Honda <i>et al.</i> <sup>71</sup>	FIA/beads/fluorescence	PBS with BSA	1	104	Yes <sup>a</sup>	50	$\alpha$ -Fetoprotein/0.15; interleukin 6/1.25; carcinoembryonic Ag/1.31 pmol L <sup>-1</sup>
Inganäs <i>et al.</i> <sup>15</sup>	FIA/beads/fluorescence	Whole blood	1	104	Yes <sup>a</sup>	50	Human interleukin 2; human interleukin 1 $\beta$ ; myoglobin/all subpicomolar
Cho <i>et al.</i> <sup>199</sup>	If IA/cantilever/resonance frequency	Buffer solution	1	5	Yes	N/A	Prostate specific Ag/picomolar
Riegger <i>et al.</i> <sup>151</sup>	FIA/beads/fluorescence	Serum	15	4	No	N/A	Tetanus Ab/158; hepatitis A Ab/215 mIU mL <sup>-1</sup>
Riegger <i>et al.</i> <sup>195</sup>	ELISA/beads/chemiluminescence	Plasma	1	8	No	N/A	Myoglobin/12.2 ng mL <sup>-1</sup>
Nagai <i>et al.</i> <sup>136</sup>	ELISA/beads/fluorescence	Mixture of secretory IgA and HRP-labeled anti-IgA antibodies	1	18	Yes <sup>c</sup>	30 <sup>b</sup>	Secretory IgA/6.4 nM
B. S. Lee <i>et al.</i> <sup>135</sup>	ELISA/beads/absorbance	Whole blood	1	3	Yes	30–50	Hepatitis B Ag/0.51 ng mL <sup>-1</sup> ; anti-hepatitis B Ab/8.6 mIU mL <sup>-1</sup>
Koh <i>et al.</i> <sup>198</sup>	FIA/beads/fluorescence	Serum	N/A	N/A	Yes <sup>c</sup>	< 20	Shiga-like toxin 1/0.8; ricin/1; anthrax/1.9 pM
B. S. Lee <i>et al.</i> <sup>137</sup>	ELISA/beads/absorbance	Whole blood	1	1	Yes	22	Creatine-kinase MB/0.92 ng mL <sup>-1</sup>
Noroosi <i>et al.</i> <sup>106</sup>	ELISPOT/membrane/colorimetric	Serum	25	8	No	N/A	Burkholderia Ag/N/A
Schaff and Sommer <sup>88</sup>	FIA/beads/fluorescence	Plasma/whole blood	> 15	20	Yes	15	Interleukin 6/63; C-reactive protein/92 pmol L <sup>-1</sup>
Park <i>et al.</i> <sup>194</sup>	ELISA/beads/absorbance	Whole blood*/saliva**	3	2	Yes	20	High sens. C-reactive protein/0.27*, 0.30**;
Burger <i>et al.</i> <sup>122</sup>	FIA/beads/fluorescence	PBS with BSA	3	4	No	N/A	B type natriuretic peptide/0.32*, 0.24** ng mL <sup>-1</sup>
W. Lee <i>et al.</i> <sup>162</sup>	AuNP IA/SAW sensor/mass enhancement	Plasma/whole blood	1	N/A	Yes	20	Cardiac troponin I/6.7 pg mL <sup>-1</sup>
Kim <i>et al.</i> <sup>34</sup>	ELISA/beads/electrochemical	PBS	1	3	Yes	< 20	C-reactive protein/4.9 pg mL <sup>-1</sup>
Nwankire <i>et al.</i> <sup>150</sup>	FIA/SAF chip/fluorescence	Bioprocess sample	1	N/A	No	< 30	Human IgG/N/A
Welte <i>et al.</i> <sup>196</sup>	CLIA/chamber/chemiluminescence	Standard solution	1	24	No	45	Estradiol/60 pg mL <sup>-1</sup>
Otsuka <i>et al.</i> <sup>154</sup>	If IA/SPR sensor/optical	Buffer solution	1	8	Yes	N/A	Human IgA/N/A

LOD = limit of detection, ELISA = enzyme-linked immunosorbent assay, IgG = immunoglobulin G, FIA = fluorescence based immunoassays, CLIA = chemiluminescent IA, Ag = antigen, PBS = phosphate buffered saline, BSA = bovine serum albumin, If = label-free, Ab = antibody, IgA = immunoglobulin A, HRP = horseradish peroxidase, MB = muscle-brain type, ELISPOT = enzyme-linked ImmunoSpot assay, AuNP = gold nanoparticle, SAW = surface acoustic wave, SPR = surface plasmon resonance, SAF = supercritical angle fluorescence. <sup>a</sup> Reagents are automatically dispensed by a robotic loading system. <sup>b</sup> Off-chip sample and detection Ab incubation requires 90 min. <sup>c</sup> Essential assay steps take place off-chip.

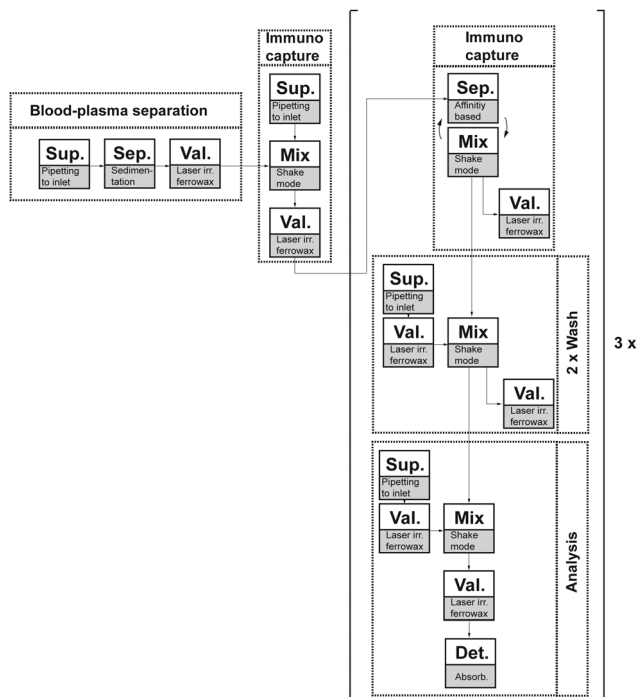


Fig. 13 Schematic representation of integrated process chains (dashed boxes: blood-plasma separation, immunocapture, washing, and analysis) and corresponding sequence of unit operations (solid boxes: Sup.: supply of reagents or sample; Sep.: separation; Val.: valving; Det.: detection).<sup>194</sup>

microvalves for individual substrate and stop solution supply, as well as for detection.<sup>194</sup> A schematic representation of the integrated application highlighting the implemented process chains and unit operations is depicted in Fig. 13.

Recently, new readout concepts were the subject of intensified research. A cartridge featuring flow-enhanced electrochemical detection under rotation was shown by Kim *et al.* This measuring method featured an adjustable sensitivity (LOD values of 21.3, 4.9, and 84.5 pg mL<sup>-1</sup> for stagnant, flow, and reference, respectively) due to its demonstrated dependency on the flow rate. Flow control was realized by integrated active ferrowax microvalves. The target biomarkers for cardiovascular disease (CVD) were indirectly detected by measuring an electroactive substrate catalyzed by an enzyme conjugated with the detection Ab. Liquid reagents were pre-stored on the cartridge prior to sealing.<sup>34</sup>

**3.2.2 Centrifugal microfluidic systems for other immunoassay formats.** The Gyrolab Bioaffy™ cartridge reported the massive parallel integration of fluorescence-based immunoassays (FIA). Up to 104 immunoassays can be run in parallel on one cartridge. The principle was presented by Honda *et al.*<sup>71</sup> and commercialized by Gyros AB.<sup>197</sup> The parallelization degree was realized by omitting the integration of reagent reservoirs on the cartridge, while non-contact reagent addition was realized by utilizing the Gyrolab Workstation™. Pre-packed bead-microcolumns acting as a solid phase are microfluidically connected to individual and mutual inlets, the latter serving eight FIA structures with common fluids to reduce processing time. Coating-enhanced capillary filling and hydrophobic valves

allow for sample volumes down to 200 nL. The injection-molded cartridge was further characterized with respect to the recovery, precision, and integration of blood plasma separation. The detection of recombinant human interleukin-1β (hIL-1β), hIL-2, and myoglobin for the purpose of determining the performance characteristics was presented by Inganäs *et al.*<sup>15</sup> Up to five cartridges can be processed on the Gyrolab Workstation™ in parallel.

Multiplexed FIA for centrifugal microfluidics applying colored beads as the solid phase was shown earlier by Riegger *et al.* Here, the beads were color-encoded with dyes or quantum dots with theoretical degrees of multiplexing of fifteen and five, respectively. Prior to fluorescence readout of the detection Ab, dye and quantum dot beads were identified with >90% and >80% reliabilities, respectively. The detection was realized within 15 seconds using a color CCD-camera and software algorithm.<sup>151</sup> Noroozi *et al.* demonstrated a cartridge with decreased assay time due to enhanced Ag-Ab interaction employing micro-mixing by flow reciprocation. Multiplexing was achieved by spotting an array of antigens on the surface of the detection chamber.<sup>106</sup> In both setups, reagents had to be loaded step-by-step onto the cartridge. Later, the combination of color-coded multiplexing with beads, captured in V-shaped cups, was presented by Burger *et al.*, where reagents had to be introduced to the cartridge step-by-step.<sup>122</sup>

A cartridge replacing the conventional washing steps by the centrifugation of beads through a density medium was presented by Schaff and Sommer. Sedimentation allowed the multiplexing of two inflammation biomarkers (interleukin 6 (IL-6)/C-reactive protein (CRP)) inside a single channel by separating beads of different sizes and densities. A theoretical multiplexing degree of >15 was reported. A whole-blood sample (IL-6) could be processed without the need of plasma separation. Wax valves employing phase change paraffin were integrated into the cartridge for fluidic routing.<sup>88</sup> The presented work was extended by Koh *et al.*, who showed the detection of three high priority potential bioterrorism agents (Fig. 14b).<sup>198</sup>

An early demonstration of label-free IA on a centrifugal cartridge was presented by Cho *et al.*<sup>199</sup> Resonant frequency changes in electromechanical cantilever sensors were used for the IA readout. The cantilever required drying *via* centrifugation prior to readout. Reagents were pre-loaded prior to testing. Later, a cartridge applying a surface plasmon resonance (SPR) sensor for label-free detection was reported by Otsuka *et al.* The SPR allowed for the real-time measurement of biomolecular interactions.<sup>154</sup> In this work, the serial fluid transport of all the required reagents was realized, similar to Lai *et al.*,<sup>59</sup> by the integration of cascades of capillary valves.

A cartridge applying an injection-molded COC surface-confined supercritical angle fluorescence (SAF)-chip in a hybrid assembly for readout was demonstrated by Nwankire *et al.* The readout concept allowed simple and cost-efficient hardware components. Hybrid assembly *via* the stacking of different layers enabled “3D fluidic flow.” Serial capillary siphon valving allowed the sequential release of pre-loaded reagents. All the reagents had to be adjusted for siphon-priming using Tween® 20.<sup>150</sup>



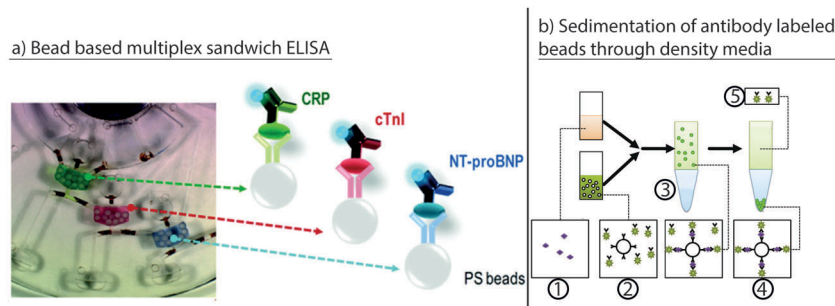


**Fig. 14** Various implementations of immunoassays on the centrifugal microfluidic platform. (a) Bead-based multiplex sandwich ELISA.<sup>194</sup> Depicted are three reaction cavities with differently labeled solid phases and individual substrate solutions (green, red, blue). Shadows were caused by the image acquisition. (Reprinted with permission from the American Chemical Society.) (b) Immunoassay based on the sedimentation of antibody-labeled beads through a density medium according to:<sup>198</sup> (1) sample with analyte and (2) detector suspension with beads and labeled antibodies are mixed, forming a layer on (3) a density medium for incubation. Upon rotation, (4) a pellet is formed in the density medium with (5) the sample with unbound label remaining above. (Reprinted with permission from The Chemical and Biological Microsystems Society.)

A rectangular injection-molded cartridge, which could be inserted into a centrifugal processing device, was demonstrated by W. Lee *et al.* The cartridge incorporated a dual-type architecture with two surface acoustic wave (SAW) immunosensors for readout. The liquid flow was controlled by active laser-irradiated ferrowax microvalves, allowing for the preloading of reagents and their release on demand. The sensitivity of the sensor was increased by mass enhancement using gold staining with gold nanoparticle conjugates, along with the detection of Ab targeting biomarkers for acute myocardial infarction. A comparison with a standard laboratory instrument was conducted with 44 patient samples, yielding a correlation coefficient of 0.998.<sup>162</sup>

**3.2.3 Trends and perspectives for immunoassay integration.** Besides nucleic acid analyses, immunoassays seem to be the most attractive application for automation on centrifugal microfluidic platforms. Centrifugal microfluidics thereby bring the unique advantages of reduced assay time and costs, and increased sensitivity to immunoassays, by minimizing the diffusion lengths and reagent consumption, and optimizing the read-out concepts. Generally, the automation of an immunoassay on a centrifugal microfluidic platform proves beneficial for two major operation sites. Either development is focused on the maximization of the degree of parallelization<sup>71,136,196</sup> or on the level of integration,<sup>135,137</sup> with the ability of point-of-care testing (POCT). Recently, the latter has evolved to mature cartridges comprising the pre-storage of all the required reagents and their processing in sophisticated devices.<sup>137,162</sup> As parallelization decreases with the increase in integration due to the space-consumption of reagent reservoirs and valving concepts, the corresponding systems aim at small-to medium-throughput laboratories, doctors' offices, patient self-testing sites, or remote areas.<sup>88,135</sup>

Conversely, the required handling steps for cartridges featuring a high degree of parallelization may be conventionally automated off-chip by robotic dispensing, as demonstrated in the Gyrolab Workstation™.<sup>197</sup> The corresponding systems must thus be operated at (already automated) laboratories, with the benefit of bringing the aforementioned improvements in centrifugal microfluidics to them.

Independent of the operational site, centrifugal microfluidic systems feature mature process chains for the automation of immunoassays. Unique unit operations that are available solely on centrifugal microfluidic platforms, are the density difference based separation of plasma from blood cells as sample preparation and the excellent performance of bound/free separation by scalable volume forces. The latter enabled the miniaturization of immunoassays to the nanoliter volume while maintaining sufficient sensitivity and specificity, as demonstrated by the Gyrolab Bioaffy LabCD series.<sup>200</sup>

Future research is expected to further improve automation of immunoassays with respect to point-of-care applications. An emphasis could lie on read-out concepts to increase the parallelization, sensitivity, and multiplexing, or to improve specificity of label-free detection. Another emphasis could lie on the reduction of turnaround times.

### 3.3 Clinical chemistry

If clinical chemistry parameters can be measured at the point-of-care, patients can be diagnosed faster, and treatment can start immediately. A reduced turnaround time for laboratory tests offers the opportunity to better monitor a patient's health, reduce unnecessary treatments, and reduce hospital costs.<sup>201</sup> Examples of parameters that especially benefit from short turnaround times are glucose and electrolytes (*e.g.*, sodium or potassium).<sup>201</sup> Centrifugal microfluidics makes it possible to analyze such parameters in a portable device directly from whole blood, by combining centrifuge-based plasma separation with subsequent automated assays.<sup>80</sup>

This has made blood-based clinical chemistry analyzers the most commercially successful field of centrifugal microfluidics. Among the centrifugal microfluidic systems available are the Piccolo Xpress (Abaxis), and the Cobas b 101 (Roche). With a total of 1.5 million cartridges sold in 2011, the Abaxis Piccolo Xpress is currently the most-used system.<sup>7</sup>

By nature, most commercial systems do not reveal the detailed fluidics. Nonetheless, to discuss blood separation methods as a preparation step for clinical chemistry, this section starts with a review of the blood separation techniques



presented in scientific journals. Subsequently, we highlight the major advances in both commercially available and scientific applications of clinical chemistry on centrifugal microfluidic platforms.

**3.3.1 Blood separation techniques.** Blood is one of the biological samples with the most information about a patient's health condition. For this reason, it is commonly used in diagnostics. The analysis of blood samples requires either whole blood, purified plasma, white blood cells, or rare cells. One of the most prominent and best-researched process chains in blood analysis on centrifugal platforms is the separation of plasma from whole blood (Table 8). It includes two steps, namely the sedimentation of blood cells by centrifugation and the decantation of the purified plasma. These steps can be performed continuously or batchwise. Blood plasma is required for determining the concentrations of glucose, lipids, electrolytes, proteins, and other substances such as alcohol in human blood. Assays based on colorimetric detection require high-purity plasma, *i.e.*, a low concentration of red blood cells. The purity is commonly defined as 1-HCT, where HCT is the hematocrit and denotes the volume fraction of red blood cells in a whole blood sample. Other relevant characteristics for blood plasma separation are the process duration, maximum hematocrit for operation, and plasma yield, which is defined as the fraction of extracted plasma in reference to the total plasma volume.

Continuous plasma separation has been demonstrated employing a quasi-isoradial channel, in which the blood cells sediment at the outer perimeter and eventually slide into a waste chamber.<sup>127</sup> During this process, the blood plasma also flows into the waste chamber, but remains at a radially inner position due to its lower density. As the waste chamber becomes full, the purified plasma decants into a collection chamber and is available for further downstream processing. The process of cell sedimentation can be amplified by the Coriolis force and the inertial force that pushes the cells toward the outer rims of bent channels.<sup>128,202</sup>

In batch plasma separation, for the decantation of supernatant plasma after cell sedimentation, a siphon is used in combination with a sedimentation chamber, where the cells are concentrated by centrifugation. Dynamics of cell sedimentation are described by the equilibrium of centrifugal force and drag force (eqn (1) vs. eqn (10)). The inlet position of the siphon is chosen such that it is located radially inward of the shock interface, *i.e.*, the interface between the concentrated cells and

purified plasma. Subsequent siphon priming can be accomplished either by capillary action at a greatly reduced spin speed<sup>203</sup> or by pneumatic action.<sup>84,126</sup> The latter does not require any surface treatment because the pneumatic action is independent of the surface properties. In addition, it enables plasma extraction at a relatively high spin speed, which allows the cell resuspension by Euler forces to be suppressed. Apart from resuspension, the diffusion of cells back into the purified plasma should also be minimized, which can be achieved by creating a small interface between the two chamber compartments for cells and purified plasma.<sup>204</sup>

An alternative method for batchwise plasma separation without siphon valving has been presented for bead-based immunoassay<sup>135</sup> and ELISA.<sup>194</sup> After loading the blood sample into the microfluidic disk and the sedimentation of cells by centrifugation, valving of the supernatant plasma was performed by opening a ferro-wax valve. The normally closed valve opened upon laser irradiation with response times of less than 1 s when the disk was at rest.

**3.3.2 Centrifugal microfluidic systems for clinical chemistry.** One of the roots of centrifugal microfluidics is the centrifugal analyzer. This system was used with numerous rotors and applications for several clinical chemistry assays, *e.g.*, ions and glucose.<sup>205</sup> The rotor was filled with liquid dispensers. The samples and reagents were mixed in end cavities by the centrifugation of the rotor. Read-out was performed *via* a spectrophotometer.

Nwankire *et al.* presented a system for point-of-care liver function screening. The analyzer consisted of a small portable disk player and centrifugal microfluidic cartridge. The cartridge included automated blood plasma separation from finger-prick samples. After separation, the purified blood plasma was aliquoted into five reaction chambers *via* centrifugo-pneumatic aliquoting based on dissolvable films. The reactions were quantified *via* colorimetric measurements. A translation of the integrated functionality into a schematic description highlighting the combination of process chains and unit operations is depicted in Fig. 15. The authors successfully tested the system in a centralized lab in Nigeria, with a time to result for the complete assay panel of 20 min.<sup>206</sup>

Lin *et al.* demonstrated a centrifugal disk for blood coagulation. The disk detects both, partial thromboplastin time and activated partial thromboplastin time. After aliquoting of blood, the blood plasma is separated.<sup>207</sup> The separated plasma aliquots are then combined with either a first reagent for

**Table 8** List of methods for blood plasma separation on centrifugal microfluidic platforms

Ref.	Separation principle	Sample volume [ $\mu\text{L}$ ]	Duration [s]	Yield <sup>a</sup> [%]	Purity	Maximum hematocrit (HCT) [%]
Burger R. <i>et al.</i> <sup>125</sup>	Centrifugo-pneumatic gating	5	120	80	20 cells $\mu\text{L}^{-1}$	N/A
Zehnle S. <i>et al.</i> <sup>126</sup>	Centrifugo-pneumatic valving	40	43	88	99.8%	60
Amasia M. <i>et al.</i> <sup>203</sup>	Capillary siphon	2000	320	77	>99.99%	49
Zhang J. <i>et al.</i> <sup>202</sup>	Multi-force separation	0.5	1–2	22	99%	6
Haerberle S. <i>et al.</i> <sup>127</sup>	Separation by decanting	5	20	N/A	>99.89%	N/A

<sup>a</sup> Yield is defined as the portion of plasma volume extracted from the total plasma volume.



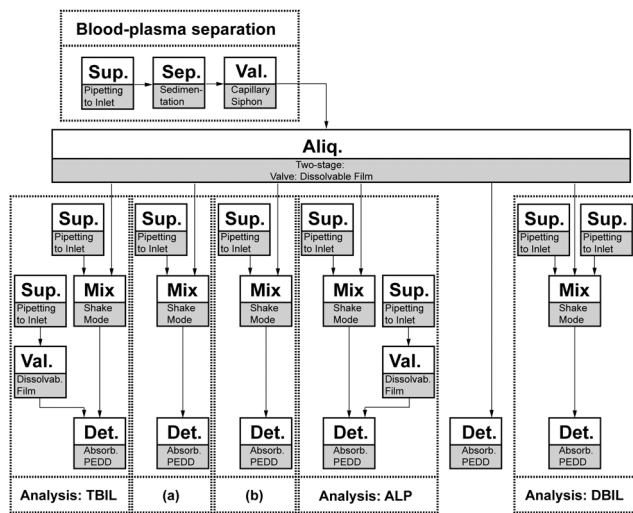


Fig. 15 Schematic representation of microfluidic process, including implemented process chains (dashed boxes; TBIL: total bilirubin; (a) albumin; (b)  $\gamma$ -glutamyltransferase; ALP: alkaline phosphatase; DBIL: direct bilirubin) and unit operations (solid boxes; Sup.: supply of reagents or sample; Sep.: separation; Aliq.: aliquoting; Val.: valve; Det.: detection; Mix.: mixing).<sup>206</sup>

quantification of partial thromboplastin time or with a first and second reagent for quantification of the activated partial thromboplastin time.<sup>208</sup> Both parameters were quantified *via* colorimetric measurements in a microfluidic disk analyser.<sup>209</sup>

Typically, clinical chemistry testing involves absorbance-based measurements such as those applied to determine the concentrations of glucose<sup>149</sup> and alcohol<sup>100,203</sup> in whole blood.

Recently, an electrochemical lab-on-a-CD system for whole blood analysis was introduced.<sup>161</sup> This system incorporates nanoporous electrodes coated with an enzyme layer that triggers the production of  $\text{H}_2\text{O}_2$  in the presence of a specific analyte. By applying a potential, the concentration of  $\text{H}_2\text{O}_2$  can then be detected electrochemically. The system performance was comparable to colorimetric methods for the tested analytes (glucose, lactate, and uric acid) and could easily be extended to other enzymatic reactions producing  $\text{H}_2\text{O}_2$ .

Most of the centrifugal microfluidics systems for clinical chemistry reported so far have focused on blood samples. However, a notable exception is a recently presented cartridge featuring an assay for the determination of *N*-acetyl- $\beta$ -D-glucosaminidase activity from urine.<sup>210</sup> From 15  $\mu\text{L}$  of artificial urine, 330 nL was metered using two-stage metering with capillary valves and mixed with 5  $\mu\text{L}$  of a substrate solution. After 20 min of enzyme reaction, the incubated mixture was transferred *via* a second capillary valve to the read-out cavity, where it was mixed with a stop solution, and readout was performed using fluorescence detection.

The Abaxis Piccolo Xpress offers a range of cartridges with different lyophilized reagents for a wide variety of whole-blood and blood-plasma tests, including a lipid panel and an electrolyte panel for veterinary and medical diagnostics. All the cartridges are based on the same microfluidic operations, making it a perfect example of a platform-based approach.<sup>8</sup>

Blood plasma is separated from 100  $\mu\text{L}$  of the patient's blood. At the same time, a pre-stored diluent is released from a central container. A defined volume of diluent and blood plasma are then combined *via* capillary siphons and mixed using shake-mode mixing. The mixture is subsequently aliquoted into 21 test cavities *via* one-stage aliquoting. Up to 12 test reactions can be monitored on one cartridge using nine different wavelengths. For online quality control, multiple cuvettes are used to ensure that the sample is introduced and the diluent is released properly.<sup>80,211</sup>

The Samsung LABGEO A20A system is based on a previously reported combined immunoassay (see Section 3.2) and biochemical analysis of whole blood.<sup>137,212</sup> The system reported by B. S. Lee *et al.* uses up to 350  $\mu\text{L}$  of a patient's blood for both the immunoassay and biochemical analysis. Plasma separation, valving, incubation, washing, mixing, and aliquoting are controlled on the disk using ferrowax valves. In contrast to earlier published methods, the system generates two different dilutions of blood plasma. According to the authors, this allows for the integration of a wider range of assays. Read-out is done by the absorbance at 10 different wavelengths.<sup>137</sup> The total reported analysis time for all the liquid operations was 22 min.

The Roche Cobas b 101 currently offers disks for HbA1c and a complete lipid profile. The required blood volumes are 2  $\mu\text{L}$  for the HbA1c test and 19  $\mu\text{L}$  for the lipid profile. The analysis time for each disk is about 6 minutes. A unique feature of the disks is a sideways lid within the disk plane. This lid covers the inlet, which can be used to aspirate a patient's blood directly from a finger stick onto the disk, thereby eliminating the need for pipettes or capillaries.

**3.3.3 Trends and perspectives in clinical chemistry.** With multiple commercial systems already on the market, centrifugal microfluidics for clinical chemistry analysis is a comparatively mature technology. A major advantage of centrifugal microfluidics for clinical chemistry is the straight forward automation of blood plasma separations. To date, plasma separation from whole blood is a well-studied process chain and is ready to be integrated in fluidic networks with higher complexity. The recent developments confirm the trends observed in the development of unit operations, namely the obviation of surface pre-treatment. The functional extension of plasma separation to the separation of white blood cells (WBCs) and circulating tumor cells (CTCs) has already been realized, and might be of increasing importance in the future. Regarding other applications in clinical chemistry, recent trends show potential for future developments in alternate sample materials (urine,<sup>210</sup> stool) and in the integration of novel read-out methods like electrochemical read-out.<sup>161</sup>

### 3.4 Cell handling, separation, and analysis

In the last few years, a growing interest in cell handling on centrifugal microfluidic platforms could be observed.<sup>213</sup> Starting from cell suspensions with concentrations generally in the range of  $10$ – $10^3$  cells per microliter, researchers have developed methods to isolate, count, and separate different cell types. To date, these methods can be categorized into three





different types: geometric, magnetophoretic, and dielectrophoretic approaches.

Geometric cell isolation employs centrifugation to pump a suspension of cells along micro-cavities in a centrifugal disk. These cavities are arranged to capture and trap mammalian cells or bacteria, where they can be used to perform an assay.<sup>173,214,215</sup> Cell isolation enables studies and analyses of single cells in a defined environment. As an example, the cytotoxicity of paraformaldehyde has been tested using isolated HEK293 cells, and apoptosis tests have successfully been performed with isolated Jurkat cells after UV exposure.<sup>214</sup> In order to test the applicability of such isolation methods, cell isolation has been combined with cell viability tests based on cell staining and fluorescence microscopy. In this way, the isolation performance can also be determined by testing the cell occupancy of the cavities on-disk. After cell isolation, single cell PCR makes it possible to determine the cell type, as demonstrated with *Salmonella enterica*. The bacteria were lysed thermally within the disk, and a specific *Salmonella* gene was amplified. In this work, the disk consisted of a micro-structured silicon wafer bonded to glass.<sup>173</sup> Burger *et al.* extended their V-cup array for geometrical cell capture under stopped flow (*cf.* Section 2.6.1) by an optical setup comprising optical tweezers and a fluorescence microscope. In that, cells from different cell lines could be discriminated by fluorescence imaging. As a preparative step for single cell assaying, a single target cell of the HL-60 line could be selected and moved to a defined location within the PDMS disk using the optical tweezers.<sup>216</sup>

While geometrical cell isolation aims at all cell types within a certain size range, magnetophoresis can be employed to extract specific cells that are tagged to magnetic beads. In this process chain, magnets are used on-disk or off-disk to attract magnetically labeled target cells (positive selection) or non-target cells (negative selection). The magnetically labeled cells can be either deflected or immobilized using the interplay of centrifugal and magnetic forces, and can thus be separated from the non-labeled cells. In positive selection approaches, rare MCF-7 cancer cells have been separated from background Jurkat cells<sup>217</sup> or whole blood<sup>218</sup> using on-disk magnets. In a negative selection approach, non-target cells labeled with magnetic beads were separated from target MCF-7 cells with rarities down to  $10^{-6}$ . While the labeled non-target cells were kept at a radially inner position, the target cells were centrifuged and concentrated radially outward.<sup>164</sup>

A further cell-handling possibility was shown using electrically contacting centrifugal microfluidic cartridges.<sup>120,219</sup> These made it possible to combine centrifugation with dielectrophoresis. In a hybrid setup, platinum coated glass slides that formed a microfluidic channel were mounted onto a centrifugal disk, together with two 9 V batteries for the power supply and a signal generator. At a spin frequency of 25 Hz, U-937 lymphocytes were separated from erythrocytes in diluted human whole blood.<sup>219</sup>

Apart from the isolation and purification of cells, the cell count is a central parameter to obtain quantitative diagnostic results. In particular, the hematocrit is a significant indicator

for the physiological condition of a patient. With the use of a single dead-end channel in a microfluidic disk, cell sedimentation has been demonstrated in a standard CD drive. After processing, the hematocrit was determined visually from a scale bar on the disk.<sup>148</sup>

A similar method has been employed to assess the count of bovine somatic cells in milk, as well as the fat content of milk.<sup>220</sup> For a case where discrimination between different cell types is not required, a standard CD drive was used to run a modified data CD that incorporated a microfluidic PDMS layer. Once a cell suspension was injected into the microfluidic layer, the CD was run to check the data error rate arising from defects (or biological cells) on the CD. It was shown that the error rate was proportional to the concentration of cells.<sup>221</sup>

The increasing demand for mobile diagnostic platforms also includes the ability to isolate, count, and discriminate between different white blood cells (WBCs). The first publications in this field had the goal of centrifugation using gradient density media. Such methods take advantage of the fact that different cells have different mass densities. Blood constituents are concentrated by centrifuging the blood, together with one or more gradient density media (DGM) with densities ranging between those of the blood constituents. In this way, concentrated layers of the desired species can be formed, made visible, and quantified by specific fluorescent labeling, and even isolated by siphon valving the different layers.<sup>222,223</sup> Park *et al.* presented a way to use anti-EpCAM to selectively bind rare circulating tumor cells (CTCs) to magnetic beads which were centrifuged and collected separately from a 5 mL blood sample. The high density of the magnetic beads made it possible to centrifuge the bead-bound CTCs through a density gradient medium (DGM) that had a lower density than the beads, but a higher density than the blood sample. In this process chain, the fluidic routing was realized using laser-triggered ferro-wax valves. The procedure included an incubation time of 1 hour to bind the CTCs (100 HCC827 lung cancer cells per 5 mL) to the beads, while a recovery rate of over 95%, cell viability of around 90%, and purity of approximately 12 remaining leukocytes per milliliter could be achieved.<sup>224</sup> The implemented sequence of process chains and unit operations for this work is depicted in Fig. 16. Recently, Lee *et al.* isolated CTCs from whole blood samples circumventing the need for functionalized beads. Instead, a thin membrane with a pore size of 8  $\mu\text{m}$  was implemented in a leak-proof fashion in the centrifugal disk. In this way, more than 50% of MCF-7 cells could be captured from whole blood samples with different concentrations of spiked MCF-7 cells. While red blood cells could be discarded completely, the number of captured white blood cells could be reduced by a factor of 20, compared to the ScreenCell system that was used for reference.<sup>119</sup>

**3.4.1 Trends and perspectives in cell handling.** The process chains for cell handling and analysis are rather new in the field of centrifugal microfluidics, with specific unit operations consisting of geometric, density, or affinity-based separation. However, based on the knowledge that has been accumulated in this field, the processing of cell suspensions could become more



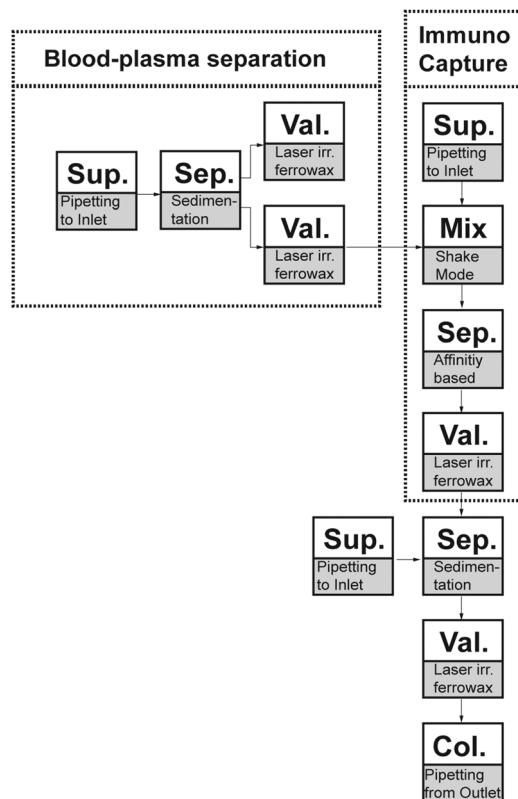


Fig. 16 Schematic representation of implemented sequence of process chains (dashed boxes) and unit operations for separation of CTC by immunocapture (solid boxes; Sup.: supply of reagents or samples; Sep.: separation; Val.: valving; Col.: collection of product).<sup>224</sup>

comprehensive. Such processing could include cell differentiation between white blood cells, epithelial cells, and rare cells, as well as cell counting and multidimensional cell processing. Due to the generation of artificial gravity, centrifugal platforms offer unique possibilities for cell collection, similar to blood plasma separation techniques. The use of density gradient medium enables the concentration of target cells inbetween fluid layers of specific density. On-chip magnetophoresis might be one promising approach for multidimensional cell separation, while dielectrophoresis could be employed for cell sorting. Together with appropriate analysis techniques, integrated in processing devices, cell-based sample-to-answer systems could potentially be realized.

### 3.5 Water, food, and soil analyses

Currently, complex environmental and food quality analyses mostly depend on manual sample collection and analyses with standard laboratory procedures such as autosamplers.<sup>225</sup> However, in many cases, these methods are too labor- and cost-intensive for continuous sampling at point-of-care. A possible solution would be a portable bio-sensor, capable of sampling environmental or food samples directly on-site with minimal sample preparation. For this purpose, centrifugal microfluidics is a promising approach. In the following, we describe the

available centrifugal microfluidic cartridges for water, food, and soil analyses.

**3.5.1 Water analysis.** In water analysis, the most common parameters of interest are ions, pH, turbidity, organic contaminants, and waterborne pathogens.

Spa and pool water is one of the largest markets for on-site water analysis.<sup>226</sup> One commercially available system is the LaMotte Water Spin for pH and ion sensing. Water is inserted into the cartridge *via* a syringe and split into 10 receiving cavities, containing pre-stored reagents, using one-stage aliquoting. Two different test panels with up to ten different parameters are available for the system: a chlorine disk and biguanide disk.<sup>227</sup> These disks are processed, and reactions are read out on a portable instrument using spectrophotometry. According to LaMotte, the system achieves “[...] greater precision than current water labs without time consuming procedures or sacrificing accuracy by using test strip scanners”.<sup>14</sup>

Other fields for water analysis are waste, river, lake, and sea water. Czugala *et al.* introduced a cartridge used for turbidity measurement and colorimetric pH analysis. The turbidity is measured from particles at a filter structure integrated directly after the sample inlet. Different pH levels can be measured *via* the absorbance of prestored ion-gels. Up to seven samples can be processed on one disk (Fig. 17a). The capability of the system was first demonstrated using water samples from the Tolka River (Dublin, Ireland).<sup>117</sup>

Hwang *et al.* showed a disk for the colorimetric detection of nutrients in water. The disk was loaded with up to four samples (Fig. 17b). After the on-disk filtration of particulates, each sample was aliquoted, and the concentrations of five different targets, ammonium, nitrite, nitrate, silicate, and orthophosphate, could be measured in parallel. The integration of the high number of independent tests per sample was made possible *via* the use of ferrowax-based microvalves for both liquid routing and reagent pre-storage. The first demonstrations of the cartridge were performed using seawater from Chunsu Bay, Korea.<sup>30</sup> The integrated process, highlighting the implemented process chains and unit operations, is shown in a schematic representation in Fig. 18.

Watts *et al.* employed four specific ion sensing optodes for the detection of potassium, sodium, calcium, and chloride from aquarium water samples. The presented cartridge incorporated six liquids that were sequentially released using capillary valves of different dimensions. First, a three-point calibration was performed by washing the optodes with three specifically designed calibration solutions. Subsequently, three replicates of the sample solution were measured. The results of the first test using aquarium water samples were in agreement with those of standard laboratory methods, but did not yet reach the same sensitivity.<sup>153</sup>

LaCroix-Fralish *et al.* presented a minimalistic single-step centrifugal microfluidic disk for the determination of nitrite and hexavalent chromium in natural water and wastewater. The disk consisted of 24 chambers loaded with dry reagents. In each cavity, an individual sample could be loaded, mixed, and measured using spectrophotometric detection.<sup>42</sup> The platform



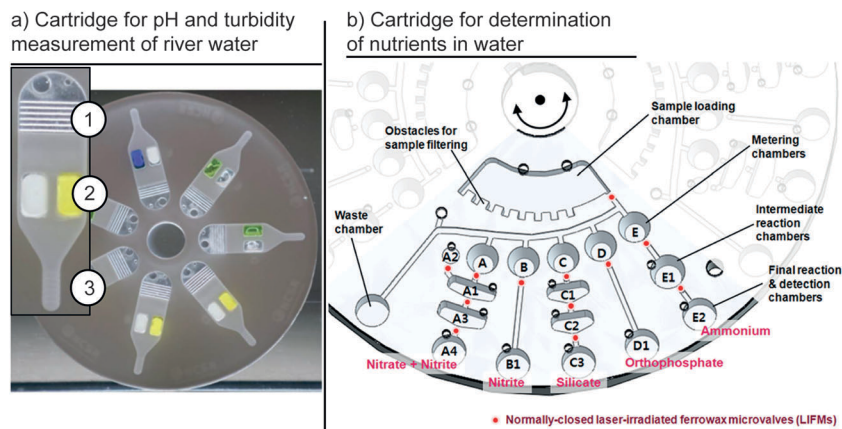


Fig. 17 Embodiments of centrifugal microfluidic cartridges for water analysis. (a) Cartridge for turbidity and pH measurement reported to Czugała *et al.* This cartridge includes a filter region for the removal of solid contaminants larger than  $86\ \mu\text{m}$  (1), along with a sensing area (2) and sedimentation region for solid contaminants smaller than  $86\ \mu\text{m}$ .<sup>117</sup> (Reproduced with permission from The Royal Society of Chemistry.) (b) Cartridge for measurement of nutrients in water.<sup>30</sup> Five different reactions can be performed in parallel using a single sample. (Reproduced with permission of the American Chemical Society.)

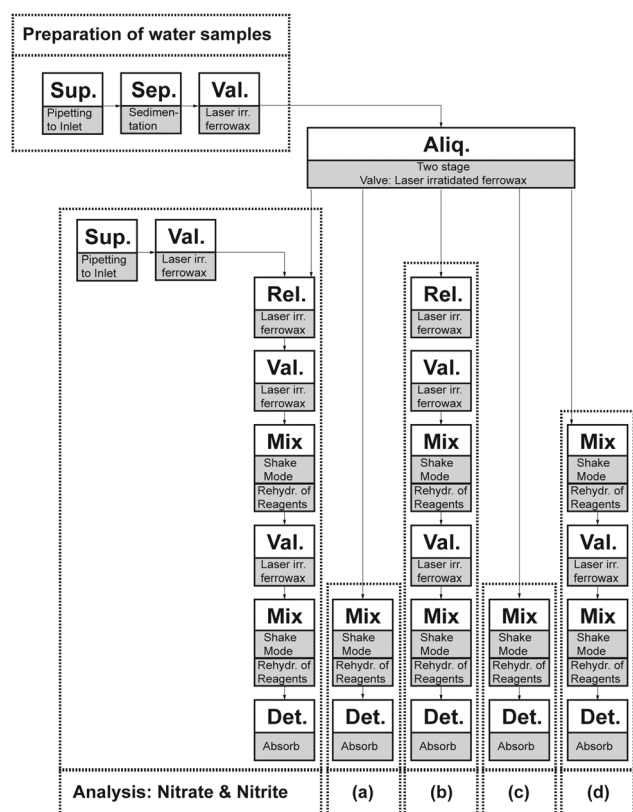


Fig. 18 Schematic of integrated functionality reported by Hwang *et al.*<sup>30</sup> The dashed boxes represent the process chains: (a) analysis of nitrite, (b) analysis of silicate, (c) analysis of orthophosphate, and (d) analysis of ammonium. The solid boxes depict the unit operation and demonstrated implementation (Sup.: sample or reagent supply; Val.: valving; Mix: mixing; Aliq.: aliquoting; Det.: detection; Sep.: separation; Rel.: reagent release).

was later extended to two-step reactions using a single capillary valve between two chambers. This cartridge was then used for simultaneous nitrate and nitrite analyses of up to twelve

samples each.<sup>228</sup> To further extend the dynamic range of the system, Kong *et al.* included a serial dilution step in the cartridge. After the first measurement in the first cavity, the sample is pumped inward using an external pneumatic source. Part of the sample is metered and mixed with a diluent in a second measurement cavity. The system can be used for the simultaneous determination of aqueous sulfide in up to three samples. The included three-fold dilution allowed for an increase in the dynamic range from  $0.4\text{--}2.0\ \text{mg L}^{-1}$  to  $0.4\text{--}6.0\ \text{mg L}^{-1}$ .<sup>229</sup>

To detect trace metals and organic contaminants in drinking water, the pre-concentration of the contaminants is often required.<sup>230</sup> Lafleur *et al.* proposed a cartridge for on-site pre-concentration using solid-phase extraction. This cartridge consisted of an inlet, a silica gel column, and an overflow reservoir. The capability of the cartridge was demonstrated for the quantification of trace metals *via* inductively coupled plasma mass spectrometry<sup>231</sup> and for organic contaminations *via* fluorescent excitation using an external LED.<sup>232</sup> The system could be used for the easy handling of sample material at the point of interest and the later analysis of the cartridge in a laboratory environment.<sup>232</sup>

**3.5.2 Soil & food analyses.** One of the strengths of the platforms based on centrifugal microfluidics is their ability to process comparatively complex sample materials. Examples of such applications are food quality analysis and the analysis of soil for contaminants.

A cartridge for the liquid–solid extraction of pyrene, an organic pollutant from soil was presented by Duford *et al.*<sup>233</sup> In this cartridge, three cavities are radially connected *via* capillary valves. In the first cavity, soil samples are mixed by an inserted magnet and external magnetic fields. The extraction is then transferred to the second chamber, where solid particulates are filtered out *via* sedimentation. Subsequently, the liquid is transferred to the third chamber, where the target analyte can be quantified *via* UV-absorbance. The same cartridge concept was later used for the inhibition-based determination of pesticide residues of carbofuran in both soil and vegetable samples.<sup>232</sup>



A major risk to the integrity of foodstuff and the food supply chain are bio-terroristic attacks. One potential candidate for such attacks is botulinum neurotoxin. A large number of individuals could be affected if this neurotoxin was used to contaminate the environment or food chain. Currently, botulinum neurotoxin is mainly tested in mouse models, which takes several days. Alternative *in vitro* tests such as ELISA are not sensitive to a wide range of toxin forms and types. Thus, Van Oordt *et al.* developed a centrifugal microfluidic cartridge for the bioluminescence-based detection of botulinum neurotoxin in water, milk, and other food samples. First, the cartridge is filled with a sample and luciferase-coated bead mixture. The luciferase is linked to the beads *via* a peptide linker, which is cleaved specifically by enzymatically active botulinum toxin. After the incubation of the beads in the sample, the sample is separated by a siphon structure and combined with a luciferin substrate. The concentration of active botulinum toxin is determined by the intensity of the bioluminescence signal as a result of the luciferase reporter assay.<sup>234</sup>

Garcia-Cordero *et al.* developed a centrifugal microfluidic cytometer for milk quality analysis. A milk sample (150  $\mu\text{L}$ ) is pipetted into the cartridge. Under artificial gravity during centrifugation, denser cells are pelleted in a dead-end funnel structure. The less-dense fat rises to the top, forming a cream band. By reading out the cell pellets *via* a microscope, the system can determine cell numbers between 50 000 to 3 000 000 to diagnose bovine mastitis. The fat content of the milk is measured from the cream band in order to additionally estimate the health and nutritional status of the cow.<sup>220</sup>

**3.5.3 Trends and perspectives in water, food, and soil analyses.** In future work, we expect smaller-footprint devices that can be operated on-site, like the one presented by Czugała *et al.* and LaMotte.<sup>227</sup> In order to get closer to the throughput of the currently used autosamplers, more samples might be integrated per disk,<sup>30</sup> or automatic disk changers could be integrated into the disk processing devices. The first systems toward the nucleic acid-based detection of pathogenic microorganisms in water and food are already in the research phase<sup>18</sup> and might enter the industrial validation and product development stage in the future.<sup>7</sup> A specific advantage of centrifugal microfluidics in the field of water, food and soil analysis is the ability to integrate density driven separations of emulsions and suspensions.

### 3.6 Analysis of protein structure and function

Proteins are one of the essential building blocks of life. Consequently, an analysis of the structure and function of protein is important for a variety of applications, from basic research to pharmaceutical studies. In the following, we present a selection of the contributions to protein structure analysis using a centrifugal microfluidic platform.

Protein structures analyzed by X-ray crystallography still constitute the majority of proteins in the Protein Data Bank. Protein crystallography could benefit significantly from the reduced volumes and increased parallelization offered by microfluidics, because of the large number of different screening conditions

needed for generating high-quality protein crystals and the limited amount of purified protein solutions available.<sup>102,235</sup>

A centrifugal microfluidic cartridge for protein crystallization was presented by Li *et al.* It automated the metering of 24 different precipitants and the two-stage aliquoting of the protein solution into the respective mixing wells. All the aliquoting and metering was controlled *via* the capillary filling of inverted V-shaped structures, with the valving controlled by capillary valves. The cartridge was used to demonstrate the on-disk crystallization and analysis of cyan fluorescent protein and lysozyme.<sup>102</sup>

Steinert *et al.* presented a cartridge for the protein crystallization screening of up to 100 different precipitants on one disk *via* free interface diffusion. The disks could be filled with protein volumes down to 1 nL using PipeJet dispensers.<sup>163</sup> Protein crystals of lysozyme, proteinase K, insulin, and catalase were successfully grown and could be measured on-chip at a synchrotron beamline.<sup>163</sup>

### 3.7 Other applications of centrifugal microfluidics

Apart from the studies covered in the previous chapters, there are numerous creative solutions that do not fit into the previously discussed categories, but deserve to be covered in this review.

Gubala *et al.* introduced a simple cartridge to study biomolecule adsorption in microfluidic channels. A 40  $\mu\text{L}$  sample was introduced on one side of the chip. It was then transported through a microfluidic channel by spinning on a standard spin coater. Part of the volume was extracted, and the concentration of the Cy5 tagged biomolecules was quantified *via* a fluorescence measurement. The amount of molecules adsorbed could be calculated from the difference in the concentrations before and after processing.<sup>236</sup>

Bruchet *et al.* investigated the use of a centrifugal microfluidic platform for the analysis of nuclear spent fuels. In a typical setting, nuclear spent fuels are dissolved in nitric acid and analyzed in a specially shielded hot cell. The authors showed a 1000-fold reduction in the required volume using centrifugal microfluidics, which allowed the analysis to be performed in a glove box. In a first proof of concept, Bruchet *et al.* showed that a centrifugal microfluidic cartridge with an integrated monolithic anion exchange stationary phase was capable of extracting europium at a yield of  $\sim 97\%$ .<sup>237</sup>

S.-K. Lee *et al.* presented a cartridge for the generation of photonic crystals. The cartridge was used to centrifuge suspensions of monodisperse silica or polystyrene latex spheres into dead-end channels, where the nanoparticles formed closely packed columns with predefined shapes. By subsequently spinning different bead solutions, the authors were able to fabricate hybrid colloidal crystals.<sup>238</sup>

Glass *et al.* reported on a miniaturized centrifugal microfluidic cartridge for potential use in handheld devices (mini-LOAD). The 10 mm disk could be rotated by acoustic actuation, eliminating the need for moving parts. The authors presented valving and mixing as the first simple unit operations on this platform.<sup>239</sup>



## 4. Embodiments of centrifugal microfluidic platforms

Many different embodiments (platforms) employing centrifugal microfluidics for a wide range of applications have been demonstrated in the quite short history of the field. Table 9 lists the systems that are either currently commercially available or are in a pre-commercial state. Additionally, we also want to give a brief overview of the history and mention companies that discontinued their developments, but still might be considered, *e.g.*, for patent search.

The history of centrifugal microfluidics dates back to the 1960s, to Oak Ridge National Laboratories' (ORNL) *centrifugal analyzer* for clinical chemistry.<sup>11</sup> At that time, the possibility of increasing the throughput for enzymatic assays compared to conventional flow-through systems led to the first commercialized centrifugal analyzer systems only a few years after the presentation of the original idea, the Electro-Nucleonics Inc. *GEMSAEC* system, in 1970.<sup>250</sup> Centrifugal analyzers exploited centrifugal forces to pump liquid from one point to another, but did not make use of unit operations, *e.g.*, valving to control the fluidic process.<sup>251</sup> Following these early days, multiple companies developed and/or commercialized centrifugal analyzers (Centri Union Carbide's "*CentrifChem*", American Instruments' "*Rotochem*", Instrumentation Laboratories Inc.'s "*Multistat*", and Roche's "*Cobas Bio*"<sup>11</sup>). For a more detailed overview of the history, we refer the reader to "Landmark Papers in Clinical Chemistry"<sup>252</sup> and Gorkin *et al.*<sup>11</sup>

The field gained momentum again with the introduction of the Abaxis Piccolo Xpress for the panel analysis of different blood parameters in 1995, a still successful product (Table 9). Besides the success story of the Piccolo Xpress, many well-known companies in the field of centrifugal microfluidics discontinued their development for different reasons. The US start-up Gamera developed a "*LabCD*" system for drug development assays.

Gamera was acquired by Tecan in 2000, and Tecan discontinued the development program for "*LabCD*" in 2005, giving difficulties in the development and delays in the commercialization as the reasons (Tecan press release, July 14, 2005). Spin-X, which used a proprietary virtual laser valve technology for "on-the-fly" valve generation and generic cartridges, discontinued their developments in 2011. Other embodiments of centrifugal microfluidics that have generated IPs include "*BCD*" by Burstein Technologies; "*BioCD*" by Quadraspec, which later became Perfinity Biosciences Inc.; Advanced Array Technologies, which later (from 2002 on) became Eppendorf Array Technologies, and Lingvitae.

Furthermore, it is worth naming prominent research groups from academia that made great contributions to progress in the field. Based on the number of publications, the most prominent groups are UC Irvine (Prof. Marc Madou), UNIST (Prof. Yoon-Kyoung Cho), the joint group at IMTEK and Hahn-Schickard (Prof. Roland Zengerle), and BDI (Prof. Jens Ducrée), while many other groups are entering the field and moving forward the state of the art of centrifugal microfluidics at a high pace.

## 5. General conclusions and outlook

This review aimed to provide a comprehensive description of centrifugal microfluidics, together with its various embodiments (platforms). It also aimed to provide an up-to-date overview of the available set of unit operations (providing basic fluidic functionalities) and how they can be concatenated for the automation of complex laboratory workflows. Additionally, we outlined how recent advances in unit operation development might significantly contribute to the development of centrifugal microfluidics as an enabling technology in the future. We introduced the category "*process chain*" as an assembly of unit operations representing workflows on a higher level of integration. Process chains can be used as stand-alone solutions for the

**Table 9** Embodiments of centrifugal microfluidic platforms that are either currently commercially available, in precommercial phase announcing release date in near future, or show promising developments

Ref.	Provider (developer)	Identifier cartridge/ name of system	Applications	Commercialization status
13	Abaxis	Piccolo Xpress	Blood parameter analysis	Commercially available
240	Samsung	LABGEO IB10	Immunoassays	Commercially available
241	Focus Diagnostics (3M)	Universal Disc & Direct Amplification Disk/Integrated Cyclor	Nucleic acid analysis	Commercially available
242	Roche (Panasonic)	Cobas 101b	Blood parameter analysis (HbA1c and lipid panel)	Commercially available
243	Capital Bio	RTisochip	Nucleic acid analysis (respiratory tract infections)	Commercially available
197	Gyros AB	Gyrolab Bioaffy CD	Immunoassays	Commercially available
14	LaMotte	Water Link Spin Lab	Water analysis	Commercially available
244	Skyla	VB 1 Veterinary Clinical Chemistry Analyzer	Blood chemistry testing for veterinary applications	Commercially available
245	Biosurfit	SpinIt	Immunoassays/blood parameter analysis	Commercially available
246	Radisens Diagnostics	Unknown	Immunoassay, clinical chemistry, and hematology assays	Precom (planned 2015)
247	GenePOC-Diagnostics	Unknown	Nucleic acid	Precom (planned 2016)
248	Spin Chip Diagnostics	Unknown	Blood analysis	Development
174	Espira Inc.	Unknown	Nucleic acid analysis	Development
36	Hahn-Schickard	LabTube	Various applications	Development
249	Sandia National Labs	Spin DX	Various applications	Development



automation of a particular laboratory process step, or multiple process chains can be combined to realize more complex (biomedical) applications. *Vice versa*, we demonstrated how some of the recently published applications using centrifugal microfluidics for automation are already based on the provided set of unit operations.

When aiming at the automation of laboratory workflows, the suitability of using centrifugal microfluidics for the desired application must first be evaluated. The decision about the suitability depends (1) on rather general aspects like the overall feasibility of miniaturization, integration, and parallelization, but also (2) on assay-specific details like the available volumes and required assay sensitivity, specificity, yield/efficiency, and reproducibility. The manufacturing technologies for cartridges, which typically need to be disposable, the hybrid integration, and the need for surface treatments will have large influences on the price-per-part and need to be cross checked with the requirements and reimbursement. Equally important are the specifications of the processing device and required auxiliary means. Finally, all the involved processing steps must cope with the application-specific regulations and certifications. The platform approach, with its well-defined unit operations (*e.g.*, known max/min volume, tolerances, and reproducibility) and process chains (*e.g.*, known yield, sensitivity, and specificity) of prior knowledge and art, plays a key role in a cost- and time-efficient layout and design.

The above outlined features are valid for all microfluidic platforms. Nonetheless, we conclude that the specific advantages of centrifugal microfluidics are evident. The single propulsion mechanism of the rotating frame enables the standardization of unit operations with minimum waste of sample and reagent volumes. Volume forces can be adjusted by rotation which enables the efficient removal of any disturbing bubbles and the separation of residual volumes from channels, chambers and sensor matrixes. For sample preparation, the density based separation is inherently available, for example for blood plasma separation. Sample supply is particularly simple: the sample is applied to an inlet cavity and transported further by centrifugation. Hence, the known cross-contamination from systems that need to be connected by a pump is avoided.

Until today, high throughput analysis systems based on centrifugal microfluidics have been realized for clinical chemistry and immunoassays. Gyros, for example, demonstrated the generation of 112 immunoassay data points per cartridge in less than one hour.<sup>197</sup> Different Gyrolab CDs comprise the same or very similar centrifugal microfluidic operations such as hydrophobic patch valves, overflow metering and the integration of same sized affinity columns, supporting the idea of using validated unit operations and process chains for efficient product development. For nucleic acid analysis, however, a remaining challenge is the limited number of individual samples that are processed in a given timeframe and a high-throughput nucleic acid analysis system for centrifugal microfluidics has not yet been presented, but might be addressed in future work.

Lately, the storage of pneumatic energy for liquid routing has enabled the monolithic integration of increasingly complex assays, which is a clear trend in centrifugal microfluidics. In this context, the overall system integration, including all aspects of the automation of laboratory workflows, still requires research. For immunoassays and clinical chemistry applications for example, Roche (cobas 101b) and Abaxis (Picolo Xpress) presented fully integrated concepts for the automated pre-storage and release of reagents. For nucleic acid applications however, the cost-efficient mass production of the disposables, including the onboard long-term storage and automated release of reagents, is still a major problem to be solved. Special care must be taken in relation to the properties of the different polymers used. The vapor permeability of the substrate material may cause liquid loss during storage, and the undesired adsorption of target molecules may occur during processing.

These are just a few examples where further research and development is needed. As a consequence, we foresee major research activity in the field of overall system integration, manufacturing, packaging, and parallelization.

Another approach, aiming at a lower market entry barrier, is the concept of using microfluidics as an “App”,<sup>191</sup> *i.e.*, using already existing laboratory instruments for processing, and thus minimizing the need for high initial investments for processing devices. Microfluidic Apps have successfully been demonstrated for sample preparation in nucleic acid analysis<sup>36,181</sup> and for the automated generation of dilution series.<sup>253</sup> Both Apps are operated on standard laboratory centrifuges. Other examples have demonstrated multiplexed PCR on different targets on a centrifugal microfluidic cartridge that can be operated in a commercially available PCR thermocycler.<sup>254</sup>

## References

- 1 H. Becker, *Lab Chip*, 2010, **10**, 271.
- 2 N. Blow, *Nat. Methods*, 2009, **6**, 683–686.
- 3 J. Ducrée, S. Haeberle, S. Lutz, S. Pausch, F. von Stetten and R. Zengerle, *J. Micromech. Microeng.*, 2007, **17**, S103.
- 4 S. Haeberle and R. Zengerle, *Lab Chip*, 2007, **7**, 1094.
- 5 Cepheid - GeneXpert, *Cepheid - GeneXpert*, available at: <http://www.cepheid.com/us/cepheid-solutions/systems/genexpert-systems/genexpert-iv>, accessed 29 October 2014.
- 6 Abbott Point of Care - i-STAT system, *i-STAT<sup>®</sup> System - Point-of-Care Testing - Handheld Blood Analyzer*, available at: <http://www.abbottpointofcare.com/>, accessed 29 October 2014.
- 7 Yole Développement SA: POC 2014 Point of Care Testing: Applications of Microfluidic Technologies, 2014.
- 8 D. Mark, S. Haeberle, G. Roth, F. von Stetten and R. Zengerle, *Chem. Soc. Rev.*, 2010, **39**, 1153.
- 9 M. L. Sin, J. Gao, J. C. Liao and P. K. Wong, *J. Biol. Eng.*, 2011, **5**, 6.
- 10 M. Madou, J. Zoval, G. Jia, H. Kido, J. Kim and N. Kim, *Annu. Rev. Biomed. Eng.*, 2006, **8**, 601–628.



- 11 R. Gorkin, J. Park, J. Siegrist, M. Amasia, B. S. Lee, J.-M. Park, J. Kim, H. Kim, M. Madou and Y.-K. Cho, *Lab Chip*, 2010, **10**, 1758.
- 12 M. C. R. Kong and E. D. Salin, *Anal. Chem.*, 2010, **82**, 8039–8041.
- 13 Abaxis, *Abaxis: Piccolo Xpress*, available at: <http://www.piccoloxpress.com/>, accessed 8 May 2014.
- 14 LaMotte, *LaMotte: WaterLink Spin Lab*, available at: <http://www.lamotte.com/en/pool-spa/labs/3576.html>, accessed 8 May 2014.
- 15 M. Inganäs, H. Dérand, A. Eckersten, G. Ekstrand, A.-K. Honerud, G. Jesson, G. Thorsén, T. Söderman and P. Andersson, *Clin. Chem.*, 2005, **51**, 1985–1987.
- 16 S. Haeberle, T. Brenner, H.-P. Schlosser, R. Zengerle and J. Ducleé, *Chem. Eng. Technol.*, 2005, **28**, 613–616.
- 17 A. P. Bouchard, D. A. Duford and E. D. Salin, *Anal. Chem.*, 2010, **82**, 8386–8389.
- 18 M. Karle, J. Wöhrle, F. von Stetten, R. Zengerle, D. Mark, *Proceedings of Transducers*, 2013, pp. 1235–1238.
- 19 M. Rombach, S. Lutz, D. Mark, G. Roth, R. Zengerle, C. Dumschat, A. Witt, S. Hensel, S. Frenzel, F. Aßmann, F. Gehring, T. Reiner, H. Drechsel, P. Szallies and F. von Stetten, *Proc. of  $\mu$ TAS*, 2012, pp. 782–784.
- 20 Roche, *cobas b 101 POC System*, available at: <https://www.roche-diagnostics.ch/de/ProductsRDS/Seiten/cobas-b-101.aspx>.
- 21 M. Hitzbleck and E. Delamarche, *Chem. Soc. Rev.*, 2013, **42**, 8494–8516.
- 22 J. Hoffmann, S. Hin, F. von Stetten, R. Zengerle and G. Roth, *RSC Adv.*, 2012, **2**, 3885.
- 23 S. K. Vashist, E. Lam, S. Hrapovic, K. B. Male and J. H. T. Luong, *Chem. Rev.*, 2014, **114**, 11083–11130.
- 24 J. Hoffmann, D. Mark, S. Lutz, R. Zengerle and F. von Stetten, *Lab Chip*, 2010, **10**, 1480.
- 25 Abaxis, *Piccolo Xpress*, available at: <http://www.piccoloxpress.com/products/piccolo/overview/>.
- 26 S. Lutz, P. Weber, M. Focke, B. Faltin, J. Hoffmann, C. Müller, D. Mark, G. Roth, P. Munday, N. Armes, O. Piepenburg, R. Zengerle and F. von Stetten, *Lab Chip*, 2010, **10**, 887.
- 27 T. van Oordt, Y. Barb, R. Zengerle and F. von Stetten, *J. Appl. Polym. Sci.*, 2014, **131**, 40291.
- 28 T. van Oordt, Y. Barb, J. Smetana, R. Zengerle and F. von Stetten, *Lab Chip*, 2013, **13**, 2888–2892.
- 29 G. Czilwik, T. Messinger, O. Strohmeier, F. von Stetten, R. Zengerle, P. Saarinen, J. Niittymäki, K. McAllister, O. Sheils, J. Drexler and D. Mark, *Proc. of  $\mu$ TAS*, 2014, pp. 2528–2529.
- 30 H. Hwang, Y. Kim, J. Cho, J.-y. Lee, M.-S. Choi and Y.-K. Cho, *Anal. Chem.*, 2013, **85**, 2954–2960.
- 31 T. Kawai, N. Naruishi, H. Nagai, Y. Tanaka, Y. Hagihara and Y. Yoshida, *Anal. Chem.*, 2013, **85**, 6587–6592.
- 32 J. L. Garcia-Cordero, F. Benito-Lopez, D. Diamond, J. Ducleé and A. J. Ricco, *Proc. of IEEE MEMS*, 2009, pp. 439–442.
- 33 J. L. Garcia-Cordero, D. Kurzbuch, F. Benito-Lopez, D. Diamond, L. P. Lee and A. J. Ricco, *Lab Chip*, 2010, **10**, 2680.
- 34 T.-H. Kim, K. Abi-Samra, V. Sunkara, D.-K. Park, M. Amasia, N. Kim, J. Kim, H. Kim, M. Madou and Y.-K. Cho, *Lab Chip*, 2013, **13**, 3747.
- 35 K. Abi-Samra, R. Hanson, M. Madou and R. A. Gorkin III, *Lab Chip*, 2011, **11**, 723.
- 36 A. Kloke, A. R. Fiebach, S. Zhang, L. Drechsel, S. Niekrawietz, M. M. Hoehl, R. Kneusel, K. Panthel, J. Steigert, F. von Stetten, R. Zengerle and N. Paust, *Lab Chip*, 2014, **14**, 1527.
- 37 M. Focke, F. Stumpf, G. Roth, R. Zengerle and F. von Stetten, *Lab Chip*, 2010, **10**, 3210.
- 38 M. Focke, F. Stumpf, B. Faltin, P. Reith, D. Bamarni, S. Wadle, C. Müller, H. Reinecke, J. Schrenzel, P. Francois, D. Mark, G. Roth, R. Zengerle and F. von Stetten, *Lab Chip*, 2010, **10**, 2519.
- 39 O. Strohmeier, S. Laßmann, B. Riedel, D. Mark, G. Roth, M. Werner, R. Zengerle and F. von Stetten, *Microchim. Acta*, 2014, **181**, 1681–1688.
- 40 M. Rombach, D. Kosse, B. Faltin, S. Wadle, G. Roth, R. Zengerle and F. von Stetten, *BioTechniques*, 2014, **57**, 151–155.
- 41 O. Strohmeier, N. Marquart, D. Mark, G. Roth, R. Zengerle and F. von Stetten, *Anal. Methods*, 2014, **6**, 2038.
- 42 A. LaCroix-Fralish, J. Clare, C. D. Skinner and E. D. Salin, *Talanta*, 2009, **80**, 670–675.
- 43 O. Strohmeier, B. Kanat, D. Bär, P. Patel, J. Drexler, M. Weidmann, T. van Oordt, G. Roth, D. Mark, R. Zengerle and F. von Stetten, *Proc. of  $\mu$ TAS*, 2012, pp. 779–881.
- 44 M. C. R. Kong, A. P. Bouchard and E. D. Salin, *Micromachines*, 2012, **3**, 1–9.
- 45 S. Soroori, L. Kulinsky, H. Kido and M. Madou, *Microfluid. Nanofluid.*, 2014, **16**, 1117–1129.
- 46 K. Abi-Samra, L. Clime, L. Kong, R. Gorkin, T.-H. Kim, Y.-K. Cho and M. Madou, *Microfluid. Nanofluid.*, 2011, **11**, 643–652.
- 47 T. H. G. Thio, F. Ibrahim, W. Al-Faqheri, J. Moebius, N. S. Khalid, N. Soin, M. K. B. A. Kahar and M. Madou, *Lab Chip*, 2013, **13**, 3199.
- 48 Z. Noroozi, H. Kido and M. J. Madou, *J. Electrochem. Soc.*, 2011, **158**, P130.
- 49 S. Zehnle, F. Schwemmer, G. Roth, F. von Stetten, R. Zengerle and N. Paust, *Lab Chip*, 2012, **12**, 5142.
- 50 J. L. Garcia-Cordero, L. Basabe-Desmonts, J. Ducleé and A. J. Ricco, *Microfluid. Nanofluid.*, 2010, **9**, 695–703.
- 51 C. Li, X. Dong, J. Qin and B. Lin, *Anal. Chim. Acta*, 2009, **640**, 93–99.
- 52 R. Gorkin, L. Clime, M. Madou and H. Kido, *Microfluid. Nanofluid.*, 2010, **9**, 541–549.
- 53 S. Haeberle, N. Schmitt, R. Zengerle and J. Ducleé, *Sens. Actuators, A*, 2007, **135**, 28–33.
- 54 R. Gorkin, S. Soroori, W. Southard, L. Clime, T. Veres, H. Kido, L. Kulinsky and M. Madou, *Microfluid. Nanofluid.*, 2012, **12**, 345–354.
- 55 W. Al-Faqheri, F. Ibrahim, T. H. G. Thio, J. Moebius, K. Joseph, H. Arof and M. Madou, *PLoS One*, 2013, **8**, e58523.



- 56 D. J. Kinahan, S. M. Kearney, O. P. Faneuil, M. T. Glynn, N. Dimov and J. Ducreé, *RSC Adv.*, 2015, **5**, 1818–1826.
- 57 Y. Ukita, M. Ishizawa, Y. Takamura and Y. Utsumi, *Proc. of  $\mu$ TAS*, 2012, pp. 1465–1467.
- 58 D. C. Duffy, H. L. Gillis, J. Lin, N. F. Sheppard and G. J. Kellogg, *Anal. Chem.*, 1999, **71**, 4669–4678.
- 59 S. Lai, S. Wang, J. Luo, L. J. Lee, S.-T. Yang and M. J. Madou, *Anal. Chem.*, 2004, **76**, 1832–1837.
- 60 M. J. Madou, L. J. Lee, S. Daunert, S. Lai and C.-H. Shih, *Biomed. Microdevices*, 2001, **3**, 245–254.
- 61 F. Schwemmer, S. Zehnle, N. Paust, C. Blanchet, M. Rössle and F. von Stetten, R. Zengerle and D. Mark, *Proc. of  $\mu$ TAS*, 2012, pp. 1450–1452.
- 62 H. Cho, H.-Y. Kim, J. Y. Kang and T. S. Kim, *J. Colloid Interface Sci.*, 2007, **306**, 379–385.
- 63 M. Liu, J. Zhang, Y. Liu, W. M. Lau and J. Yang, *Chem. Eng. Technol.*, 2008, **31**, 1328–1335.
- 64 J. M. Chen, P.-C. Huang and M.-G. Lin, *Microfluid. Nanofluid.*, 2008, **4**, 427–437.
- 65 H. Zhang, H. H. Tran, B. H. Chung and N. Y. Lee, *Analyst*, 2013, **138**, 1750.
- 66 A. LaCroix-Fralish, E. J. Templeton, E. D. Salin and C. D. Skinner, *Lab Chip*, 2009, **9**, 3151.
- 67 A. Kazarine, M. C. R. Kong, E. J. Templeton and E. D. Salin, *Anal. Chem.*, 2012, **84**, 6939–6943.
- 68 M. Focke, R. Feuerstein, F. Stumpf, D. Mark, T. Metz, R. Zengerle and F. von Stetten, *Proc. of  $\mu$ TAS*, 2009, pp. 1397–1399.
- 69 P. Andersson, G. Jesson, G. Kylberg, G. Ekstrand and G. Thorsén, *Anal. Chem.*, 2007, **79**, 4022–4030.
- 70 L. Riegger, M. M. Mielnik, A. Gulliksen, D. Mark, J. Steigert, S. Lutz, M. Clad, R. Zengerle, P. Koltay and J. Hoffmann, *J. Micromech. Microeng.*, 2010, **20**, 045021.
- 71 N. Honda, U. Lindberg, P. Andersson, S. Hoffmann and H. Takei, *Clin. Chem.*, 2005, **51**, 1955–1961.
- 72 Y. Ouyang, S. Wang, J. Li, P. S. Riehl, M. Begley and J. P. Landers, *Lab Chip*, 2013, **13**, 1762.
- 73 D. Mark, T. Metz, S. Haeberle, S. Lutz, J. Ducreé, R. Zengerle and F. von Stetten, *Lab Chip*, 2009, **9**, 3599.
- 74 R. Gorkin III, C. E. Nwankire, J. Gaughran, X. Zhang, G. G. Donohoe, M. Rook, R. O’Kennedy and J. Ducreé, *Lab Chip*, 2012, **12**, 2894.
- 75 D. J. Kinahan, S. M. Kearney and J. Ducreé, *Proceedings of Transducers*, 2013, pp. 2189–2192.
- 76 J. Siegrist, R. Gorkin, M. Bastien, G. Stewart, R. Peytavi, H. Kido, M. Bergeron and M. Madou, *Lab Chip*, 2010, **10**, 363.
- 77 W. Al-Faqheri, F. Ibrahim, T. H. G. Thio, N. Bahari, H. Arof, H. A. Rothan, R. Yusof and M. Madou, *Sensors*, 2015, **15**, 4658–4676.
- 78 J. Hoffmann, D. Mark, R. Zengerle and F. von Stetten, *Proceedings of Transducers*, 2009, pp. 1991–1994.
- 79 H. Hwang, H.-H. Kim and Y.-K. Cho, *Lab Chip*, 2011, **11**, 1434.
- 80 C. T. Schembri, T. L. Burd, A. R. Kopf-Sill, L. R. Shea and B. Braynin, *J. Autom. Chem.*, 1995, **17**, 99–104.
- 81 J. Siegrist, R. Gorkin, L. Clime, E. Roy, R. Peytavi, H. Kido, M. Bergeron, T. Veres and M. Madou, *Microfluid. Nanofluid.*, 2010, **9**, 55–63.
- 82 N. Godino, E. Vereshchagina, R. Gorkin and J. Ducreé, *Microfluid. Nanofluid.*, 2013, **16**, 895–905.
- 83 R. Burger, N. Reis, J. G. Fonseca and J. Ducreé, *Proc. of IEEE MEMS*, 2009, pp. 443–446.
- 84 N. Godino, R. Gorkin III, A. V. Linares, R. Burger and J. Ducreé, *Lab Chip*, 2013, **13**, 685.
- 85 F. Schwemmer, S. Zehnle, D. Mark, F. von Stetten, R. Zengerle and N. Paust, *Lab Chip*, 2015, **15**, 1545–1553.
- 86 D. Kinahan, S. M. Kearney, N. Dimov, M. T. Glynn and J. Ducreé, *Lab Chip*, 2014, **14**, 2249–2258.
- 87 J.-M. Park, Y.-K. Cho, B.-S. Lee, J.-G. Lee and C. Ko, *Lab Chip*, 2007, **7**, 557.
- 88 U. Y. Schaff and G. J. Sommer, *Clin. Chem.*, 2011, **57**, 753–761.
- 89 Y.-K. Cho, J.-G. Lee, J.-M. Park, B.-S. Lee, Y. Lee and C. Ko, *Lab Chip*, 2007, **7**, 565.
- 90 M. Amasia, M. Cozzens and M. J. Madou, *Sens. Actuators, B*, 2012, **161**, 1191–1197.
- 91 L. Swayne, A. Kazarine, E. J. Templeton and E. D. Salin, *Talanta*, 2015, **134**, 443–447.
- 92 T. Brenner, T. Glatzel, R. Zengerle and J. Ducreé, *Lab Chip*, 2005, **5**, 146.
- 93 J. Kim, H. Kido, R. H. Rangel and M. J. Madou, *Sens. Actuators, B*, 2008, **128**, 613–621.
- 94 T. T. Thuy, M. Inganäs, G. Ekstrand and G. Thorsén, *J. Chromatogr. B: Anal. Technol. Biomed. Life Sci.*, 2010, **878**, 2803–2810.
- 95 D. Mark, M. Rombach, S. Lutz and R. Zengerle, *Proc. of  $\mu$ TAS*, 2009, pp. 110–112.
- 96 M. Müller, D. Mark, M. Rombach, G. Roth, J. Hoffmann, R. Zengerle and F. von Stetten, *Proc. of  $\mu$ TAS*, 2010, pp. 405–407.
- 97 M. C. R. Kong and E. D. Salin, *Anal. Chem.*, 2011, **83**, 1148–1151.
- 98 D. Mark, P. Weber, S. Lutz, M. Focke, R. Zengerle and F. Stetten, *Microfluid. Nanofluid.*, 2011, **10**, 1279–1288.
- 99 J. Steigert, T. Brenner, M. Grumann, L. Riegger, S. Lutz, R. Zengerle and J. Ducreé, *Biomed. Microdevices*, 2007, **9**, 675–679.
- 100 J. Steigert, M. Grumann, T. Brenner, L. Riegger, J. Harter, R. Zengerle and J. Ducreé, *Lab Chip*, 2006, **6**, 1040.
- 101 S. O. Sundberg, C. T. Wittwer, C. Gao and B. K. Gale, *Anal. Chem.*, 2010, **82**, 1546–1550.
- 102 G. Li, Q. Chen, J. Li, X. Hu and J. Zhao, *Anal. Chem.*, 2010, **82**, 4362–4369.
- 103 M. Grumann, A. Geipel, L. Riegger, R. Zengerle and J. Ducreé, *Lab Chip*, 2005, **5**, 560.
- 104 Y. Ren and W. W.-F. Leung, *Int. J. Heat Mass Transfer*, 2013, **60**, 95–104.
- 105 Z. Noroozi, H. Kido, M. Micic, H. Pan, C. Bartolome, M. Princevac, J. Zoval and M. Madou, *Rev. Sci. Instrum.*, 2009, **80**, 075102.
- 106 Z. Noroozi, H. Kido, R. Peytavi, R. Nakajima-Sasaki, A. Jasinskas, M. Micic, P. L. Felgner and M. J. Madou, *Rev. Sci. Instrum.*, 2011, **82**, 064303.





- 107 M. M. Aeinehvand, F. Ibrahim, S. W. Harun, W. Al-Faqheri, T. H. G. Thio, A. Kazemzadeh and M. Madou, *Lab Chip*, 2014, **14**, 988–997.
- 108 S. Haeberle, T. Brenner, H.-P. Schlosser, R. Zengerle and J. Ducee, *Chem. Eng. Technol.*, 2005, **28**, 613–616.
- 109 J. Ducee, T. Brenner, S. Haeberle, T. Glatzel and R. Zengerle, *Microfluid. Nanofluid.*, 2006, **2**, 78–84.
- 110 J. Ducee, S. Haeberle, T. Brenner, T. Glatzel and R. Zengerle, *Microfluid. Nanofluid.*, 2006, **2**, 97–105.
- 111 D. Chakraborty, M. Madou and S. Chakraborty, *Lab Chip*, 2011, **11**, 2823.
- 112 Y. Ukita and Y. Takamura, *Microfluid. Nanofluid.*, 2013, **15**, 829–837.
- 113 J.-N. Kuo and L.-R. Jiang, *Microsyst. Technol.*, 2014, **20**, 91–99.
- 114 M. La, S. J. Park, H. W. Kim, J. J. Park, K. T. Ahn, S. M. Ryew and D. S. Kim, *Microfluid. Nanofluid.*, 2013, **15**, 87–98.
- 115 J. Liebeskind, A. Kloke, A. R. Fiebach, F. von Stetten, R. Zengerle and N. Paust, *Proc. of  $\mu$ TAS*, 2013, pp. 967–969.
- 116 M. C. R. Kong and E. D. Salin, *Microfluid. Nanofluid.*, 2012, **13**, 519–525.
- 117 M. Czugala, R. Gorkin III, T. Phelan, J. Gaughran, V. F. Curto, J. Ducee, D. Diamond and F. Benito-Lopez, *Lab Chip*, 2012, **12**, 5069.
- 118 E. J. Templeton and E. D. Salin, *Microfluid. Nanofluid.*, 2014, **17**, 245–251.
- 119 A. Lee, J. Park, M. Lim, V. Sunkara, S. Y. Kim, G. H. Kim, M.-H. Kim and Y.-K. Cho, *Anal. Chem.*, 2014, **86**, 11349–11356.
- 120 R. Martinez-Duarte, R. A. Gorkin III, K. Abi-Samra and M. J. Madou, *Lab Chip*, 2010, **10**, 1030.
- 121 M. Boettcher, M. S. Jaeger, L. Riegger, J. Ducee, R. Zengerle and C. DUSCHL, *Biophys. Rev. Lett.*, 2006, **1**, 443–451.
- 122 R. Burger, P. Reith, G. Kijanka, V. Akujobi, P. Abgrall and J. Ducee, *Lab Chip*, 2012, **12**, 1289.
- 123 D. Kirby, J. Siegrist, G. Kijanka, L. Zavattoni, O. Sheils, J. O'Leary, R. Burger and J. Ducee, *Microfluid. Nanofluid.*, 2012, **13**, 899–908.
- 124 M. Glynn, D. Kirby, D. Chung, D. J. Kinahan, G. Kijanka and J. Ducee, *J. Lab. Autom.*, 2013, **19**, 285–296.
- 125 R. Burger, N. Reis, J. G. da Fonseca and J. Ducee, *J. Micromech. Microeng.*, 2013, **23**, 035035.
- 126 S. Zehnle, M. Rombach, F. von Stetten, R. Zengerle and N. Paust, *Proc. of  $\mu$ TAS*, 2012, pp. 869–871.
- 127 S. Haeberle, T. Brenner, R. Zengerle and J. Ducee, *Lab Chip*, 2006, **6**, 776.
- 128 B.-S. Li and J.-N. Kuo, *NEMS*, 2013, 462–465.
- 129 R. Boom, *et al.*, *J. Clin. Microbiol.*, 1990, 495–503.
- 130 J. H. Jung, B. H. Park, Y. K. Choi and T. Seo, *Lab Chip*, 2013, **13**, 3383–3388.
- 131 B. H. Park, J. H. Jung, H. Zhang, N. Y. Lee and T. S. Seo, *Lab Chip*, 2012, **12**, 3875.
- 132 X. Y. Peng, P. C. Li, H.-Z. Yu, M. Parameswaran and W. L. Chou, *Sens. Actuators, B*, 2007, **128**, 64–69.
- 133 G. Jia, K.-S. Ma, J. Kim, J. V. Zoval, R. Peytavi, M. G. Bergeron and M. J. Madou, *Sens. Actuators, B*, 2006, **114**, 173–181.
- 134 R. Peytavi, F. R. Raymond, D. Gagne, F. J. Picard, G. Jia, J. Zoval, M. Madou, K. Boissinot, M. Boissinot, L. Bissonnette, M. Ouellette and M. G. Bergeron, *Clin. Chem.*, 2005, **51**, 1836–1844.
- 135 B. S. Lee, J.-N. Lee, J.-M. Park, J.-G. Lee, S. Kim, Y.-K. Cho and C. Ko, *Lab Chip*, 2009, **9**, 1548.
- 136 H. Nagai, Y. Narita, M. Ohtaki, K. Saito and S.-I. Wakida, *Anal. Sci.*, 2007, **23**, 975–979.
- 137 B. S. Lee, Y. U. Lee, H.-S. Kim, T.-H. Kim, J. Park, J.-G. Lee, J. Kim, H. Kim, W. G. Lee and Y.-K. Cho, *Lab Chip*, 2011, **11**, 70.
- 138 O. Strohmeier, A. Emperle, G. Roth, D. Mark, R. Zengerle and F. von Stetten, *Lab Chip*, 2013, **13**, 146–155.
- 139 K.-C. Chen, T.-P. Lee, Y.-C. Pan, C.-L. Chiang, C.-L. Chen, Y.-H. Yang, B.-L. Chiang, H. Lee and A. M. Wo, *Clin. Chem.*, 2011, **57**, 586–592.
- 140 S. Haeberle, R. Zengerle and J. Ducee, *Microfluid. Nanofluid.*, 2007, **3**, 65–75.
- 141 D. Chakraborty and S. Chakraborty, *Appl. Phys. Lett.*, 2010, **97**, 234103.
- 142 D. Mark, S. Haeberle, R. Zengerle, J. Ducee and G. T. Vladislavjević, *J. Colloid Interface Sci.*, 2009, **336**, 634–641.
- 143 S. Haeberle, L. Naegele, R. Burger, F. von Stetten, R. Zengerle and J. Ducee, *J. Microencapsul.*, 2008, **25**, 267–274.
- 144 K. Maeda, H. Onoe, M. Takinoue and S. Takeuchi, *Adv. Mater.*, 2012, **24**, 1340–1346.
- 145 F. Schuler, F. Schwemmer, M. Trotter, S. Wadle, R. Zengerle, F. von Stetten and N. Paust, *Lab Chip*, 2015, DOI: 10.1039/C5LC00291E.
- 146 T.-H. Kim, J. Park, C.-J. Kim and Y.-K. Cho, *Anal. Chem.*, 2014, **86**, 3841–3848.
- 147 M. M. Hoehl, E. S. Bocholt, A. Kloke, N. Paust, F. von Stetten, R. Zengerle, J. Steigert and A. H. Slocum, *Analyst*, 2014, **16**, 375–385.
- 148 L. Riegger, M. Grumann, J. Steigert, S. Lutz, C. P. Steinert, C. Mueller, J. Viertel, O. Prucker, J. Ruhe, R. Zengerle and J. Ducee, *Biomed. Microdevices*, 2007, **9**, 795–799.
- 149 M. Grumann, J. Steigert, L. Riegger, I. Moser, B. Enderle, K. Riebeseel, G. Urban, R. Zengerle and J. Ducee, *Biomed. Microdevices*, 2006, **8**, 209–214.
- 150 C. E. Nwankire, G. G. Donohoe, X. Zhang, J. Siegrist, M. Somers, D. Kurzbuch, R. Monaghan, M. Kitsara, R. Burger, S. Hearty, J. Murrell, C. Martin, M. Rook, L. Barrett, S. Daniels, C. McDonagh, R. O'Kennedy and J. Ducee, *Anal. Chim. Acta*, 2013, **781**, 54–62.
- 151 L. Riegger, M. Grumann, T. Nann, J. Riegler, O. Ehlert, W. Bessler, K. Mittenbuehler, G. Urban, L. Pastewka, T. Brenner, R. Zengerle and J. Ducee, *Sens. Actuators, A*, 2006, **126**, 455–462.
- 152 Y. Ukita and Y. Takamura, *Microfluid. Nanofluid.*, 2015, **18**, 245–252.
- 153 A. S. Watts, A. A. Urbas, E. Moschou, V. G. Gavalas, J. V. Zoval, M. Madou and L. G. Bachas, *Anal. Chem.*, 2007, **79**, 8046–8054.
- 154 K. Otsuka, A. Hemmi, T. Usui, A. Moto, T. Tobita, N. Soh, K. Nakano, H. Zeng, K. Uchiyama, T. Imato and H. Nakajima, *J. Sep. Sci.*, 2011, **34**, 2913–2919.



- 155 S. Morais, L. A. Tortajada-Genaro, T. Arnandis-Chover, R. Puchades and A. Maquieira, *Anal. Chem.*, 2009, **81**, 5646–5654.
- 156 R. Burger, M. Kitsara, J. Gaughran, C. Nwankire and J. Ducrée, *Future Med.*, 2014, 72–92.
- 157 Y. Li, L. M. L. Ou and H.-Z. Yu, *Anal. Chem.*, 2008, **80**, 8216–8223.
- 158 S. A. Lange, G. Roth, S. Wittemann, T. Lacoste, A. Vetter, J. Grässle, S. Kopta, M. Kolleck, B. Breitingner, M. Wick, J. K. H. Hörber, S. Dübel and A. Bernard, *Angew. Chem., Int. Ed.*, 2006, **45**, 270–273.
- 159 F. G. Bosco, E.-T. Hwu, C.-H. Chen, S. Keller, M. Bache, M. H. Jakobsen, I.-S. Hwang and A. Boisen, *Lab Chip*, 2011, **11**, 2411–2416.
- 160 K. Abi-Samra, T.-H. Kim, D.-K. Park, N. Kim, J. Kim, H. Kim, Y.-K. Cho and M. Madou, *Lab Chip*, 2013, **13**, 3253–3260.
- 161 T. Li, Y. Fan, Y. Cheng and J. Yang, *Lab Chip*, 2013, **13**, 2634.
- 162 W. Lee, J. Jung, Y. K. Hahn, S. K. Kim, Y. Lee, J. Lee, T.-H. Lee, J.-Y. Park, H. Seo, J. N. Lee, J. H. Oh, Y.-S. Choi and S. S. Lee, *Analyst*, 2013, **138**, 2558–2566.
- 163 C. P. Steinert, J. Mueller-Dieckmann, M. Weiss, M. Roessle, R. Zengerle and P. Koltay, *Proc. of MEMS*, 2007, pp. 561–564.
- 164 C.-L. Chen, K.-C. Chen, Y.-C. Pan, T.-P. Lee, L.-C. Hsiung, C.-M. Lin, C.-Y. Chen, C.-H. Lin, B.-L. Chiang and A. M. Wo, *Lab Chip*, 2011, **11**, 474.
- 165 J. Kim, M. Johnson, P. Hill and B. K. Gale, *Integr. Biol.*, 2009, **1**, 574.
- 166 P.-A. Auroux, Y. Koc, A. deMello, A. Manz and P. J. R. Day, *Lab Chip*, 2004, **4**, 534.
- 167 J. Kim, S. Hee Jang, G. Jia, J. V. Zoval, N. A. Da Silva and M. J. Madou, *Lab Chip*, 2004, **4**, 516.
- 168 H. Kido, M. Micic, D. Smith, J. Zoval, J. Norton and M. Madou, *Colloids Surf., B*, 2007, **58**, 44–51.
- 169 T. Brenner, T. Glatzel, R. Zengerle and J. Ducree, *Proc. of  $\mu$ TAS*, 2003, pp. 903–906.
- 170 S. Wadle, O. Strohmeier, M. Rombach, D. Mark, R. Zengerle and F. von Stetten, *Proc. of  $\mu$ TAS*, 2012, pp. 1381–1383.
- 171 O. Strohmeier, S. Keil, B. Kanat, P. Patel, M. Niedrig, M. Weidmann, F. Hufert, J. Drexler, R. Zengerle and F. von Stetten, *RSC Adv.*, 2015, **5**, 32144–32150.
- 172 J. H. Jung, S. J. Choi, B. H. Park, Y. K. Choi and T. S. Seo, *Lab Chip*, 2012, **12**, 1598.
- 173 S. Furutani, H. Nagai, Y. Takamura and I. Kubo, *Anal. Bioanal. Chem.*, 2010, **398**, 2997–3004.
- 174 Espira Inc., *Espira Inc. Digital PCR*, available at: <http://www.espirainc.com/digital-pcr.html>, accessed 8 May 2014.
- 175 M. Focke, D. Kosse, D. Al-Bamerni, S. Lutz, C. Müller, H. Reinecke, R. Zengerle and F. von Stetten, *J. Micromech. Microeng.*, 2011, **21**, 115002.
- 176 G. Czilwik, I. Schwarz, M. Keller, S. Wadle, S. Zehnle, F. von Stetten, D. Mark, R. Zengerle and N. Paust, *Lab Chip*, 2015, **15**, 1084–1091.
- 177 GenomeWeb, <http://www.genomeweb.com/persample-prep/fda-clears-focus-diagnostics-flu-test-3m-integrated-cycler/>, available at: <http://www.genomeweb.com/persample-prep/fda-clears-focus-diagnostics-flu-test-3m-integrated-cycler/>, accessed 21 October 2013.
- 178 Focus Diagnostics, [http://www.mikrogen.de/uploads/tx\\_oe\\_mikrogentables/dokumente/PI-UM-MOL1101-DE.pdf](http://www.mikrogen.de/uploads/tx_oe_mikrogentables/dokumente/PI-UM-MOL1101-DE.pdf), available at: [http://www.mikrogen.de/uploads/tx\\_oe\\_mikrogentables/dokumente/PI-UM-MOL1101-DE.pdf](http://www.mikrogen.de/uploads/tx_oe_mikrogentables/dokumente/PI-UM-MOL1101-DE.pdf), accessed 21 October 2013.
- 179 L. Wang, P. C. Li, H.-Z. Yu and A. M. Parameswaran, *Anal. Chim. Acta*, 2008, **610**, 97–104.
- 180 L. Wang and P. C. Li, *Anal. Biochem.*, 2010, **400**, 282–288.
- 181 M. M. Hoehl, M. Weißert, A. Dannenberg, T. Nesch, N. Paust, F. Stetten, R. Zengerle, A. H. Slocum and J. Steigert, *Biomed. Microdevices*, 2014, **16**, 375–385.
- 182 G. Czilwik, O. Strohmeier, I. Schwarz, N. Paust, S. Zehnle, F. von Stetten and R. Zengerle and D. Mark, *Proc. of  $\mu$ TAS*, 2013, pp. 1607–1609.
- 183 J. H. Jung, B. H. Park, S. J. Choi and T. S. Seo, *Proc. of  $\mu$ TAS*, 2012, pp. 1966–1968.
- 184 *The 3M™ Integrated Cycler Direct Amplification Disc - International*, available at: <https://www.focusdx.com/3m-integrated-cycler/dad-intl>, accessed 15 July 2014.
- 185 M. Exner, L. Jacky, Y.-P. Chen, H. Mai, J. Chen, M. M. Tabb, M. Aye and E. Eleazar, US20130022963A, 2013.
- 186 P. D. Ludowise, D. A. Whitman and F. D. Smith, US20120291538A1, 2012.
- 187 P. D. Ludowise and J. D. Smith, US2012/0291565A1, 2010.
- 188 R. Peytavi and S. Chapdelaine, WP2012/120463A1, 2012.
- 189 L. Bissonnette, S. Chapdelaine, R. Peytavi, A. Huletsky, G. Stewart, M. Boissinot, P. Allibert and M. G. Bergeron, ed. G. J. Kost and C. M. Corbin, *Global Point of Care - Strategies for Disasters, Emergencies, and Public Health Resilience*, AACCC Press, Washington, DC, 2015, pp. 235–247.
- 190 P. J. Asiello and A. J. Baeumner, *Lab Chip*, 2011, **11**, 1420.
- 191 D. Mark, F. von Stetten and R. Zengerle, *Lab Chip*, 2012, **12**, 2464.
- 192 H. He, Y. Yuan, W. Wang, N.-R. Chiou, A. J. Epstein and L. J. Lee, *Biomicrofluidics*, 2009, **3**, 22401.
- 193 R. D. Johnson, I. H. A. Badr, G. Barrett, S. Lai, Y. Lu, M. J. Madou and L. G. Bachas, *Anal. Chem.*, 2001, **73**, 3940–3946.
- 194 J. Park, V. Sunkara, T.-H. Kim, H. Hwang and Y.-K. Cho, *Anal. Chem.*, 2012, **84**, 2133–2140.
- 195 L. Riegger, J. Steigert, M. Grumann, S. Lutz, G. Olofsson, M. Kayyami, W. Bessler, K. Mittenbuehler, R. Zengerle and J. Ducree, *Proc. of  $\mu$ TAS*, 2006, pp. 819–821.
- 196 G. Welte, S. Lutz, B. Cleven, H. Brahms, C. Gärtner, G. Roth, D. Mark, R. Zengerle and F. von Stetten, *Proc. of  $\mu$ TAS*, 2010, pp. 818–820.
- 197 Gyros AB, *Gyros: Gyrolab*, available at: <http://www.gyros.com/>, accessed 8 May 2014.
- 198 C. Y. Koh, U. Y. Schaff, A. K. Singh and G. J. Sommer,  *$\mu$ TAS*, 2011.
- 199 H. Cho, J. Kang, S. Kwak, K. Hwang, J. Min, J. Lee, D. Yoon and T. Kim, *Proc. of IEEE MEMS*, 2005, pp. 698–701.
- 200 Gyrolab Bioaffy system, *Gyrolab CDs*, available at: <http://www.gyros.com/products/gyrolab-cds/>, accessed 7 May 2015.



- 201 G. P. Zaloga, *Chest*, 1990, **97**, 185S.
- 202 J. Zhang, Q. Guo, M. Liu and J. Yang, *J. Micromech. Microeng.*, 2008, **18**, 125025.
- 203 M. Amasia and M. Madou, *Bioanalysis*, 2010, **2**, 1701–1710.
- 204 T. Li, L. Zhang, K. M. Leung and J. Yang, *J. Micromech. Microeng.*, 2010, **20**, 105024.
- 205 C. A. Burtis, J. C. Mailen, W. F. Johnson, C. D. Scott, T. O. Tiffany and N. G. Anderson, *Clin. Chem.*, 1972, **18**, 753–761.
- 206 C. E. Nwankire, M. Czugala, R. Burger, K. J. Fraser, T. M. O'Connell, T. Glennon, B. E. Onwuliri, I. E. Nduaguibe, D. Diamond and J. Ducreé, *Biosens. Bioelectron.*, 2014, **56**, 352–358.
- 207 C.-H. Lin, C.-H. Shih and C.-H. Lu, *J. Nanosci. Nanotechnol.*, 2013, **13**, 2206–2212.
- 208 C.-H. Lin, C.-Y. Liu, C.-H. Shih and C.-H. Lu, *Biomicrofluidics*, 2014, **8**, 052105.
- 209 C.-H. Lin, K.-W. Lin, D. Yen, C.-H. Shih, C.-H. Lu, J.-M. Wang and C.-Y. Lin, *J. Nanosci. Nanotechnol.*, 2015, **15**, 1401–1407.
- 210 Y. Tanaka, S. Okuda, A. Sawai and S. Suzuki, *Anal. Sci.*, 2012, **28**, 33–38.
- 211 T. L. Burd, *Clin. Chem.*, 1992, **38**, 1665–1670.
- 212 J. Suk-Anake and C. Promptmas, *Clin. Lab.*, 2012, **58**, 1313–1318.
- 213 R. Burger, D. Kirby, M. Glynn, C. Nwankire, M. O'Sullivan, J. Siegrist, D. Kinahan, G. Aguirre, G. Kijanka, R. A. Gorkin and J. Ducreé, *Curr. Opin. Chem. Biol.*, 2012, **16**, 409–414.
- 214 S.-W. Lee, J. Y. Kang, I.-H. Lee, S.-S. Ryu, S.-M. Kwak, K.-S. Shin, C. Kim, H.-I. Jung and T.-S. Kim, *Sens. Actuators, A*, 2008, **143**, 64–69.
- 215 H. Chen, X. Li, L. Wang and P. C. Li, *Talanta*, 2010, **81**, 1203–1208.
- 216 R. Burger, D. Kurzbuch, R. Gorkin, G. Kijanka, M. Glynn, C. McDonagh and J. Ducreé, *Lab Chip*, 2015, **15**, 378–381.
- 217 K.-C. Chen, Y.-C. Pan, C.-L. Chen, C.-H. Lin, C.-S. Huang and A. M. Wo, *Anal. Biochem.*, 2012, **429**, 116–123.
- 218 D. Kirby, G. Kijanka, J. Siegrist, J. Burger, O. Sheils, J. O'Leary and J. Ducreé, *Proc. of  $\mu$ TAS*, 2012, pp. 1126–1128.
- 219 M. Boettcher, M. S. Jaeger, L. Riegger, J. Ducreé, R. Zengerle and C. Duschl, *Biophys. Rev. Lett.*, 2006, **1**, 443–451.
- 220 J. L. Garcia-Cordero, L. M. Barrett, R. O'Kennedy and A. J. Ricco, *Biomed. Microdevices*, 2010, **12**, 1051–1059.
- 221 S. M. Imaad, N. Lord, G. Kulsharova and G. L. Liu, *Lab Chip*, 2011, **11**, 1448.
- 222 U. Schaff, A. Tentori and G. Sommer, *Proc. of  $\mu$ TAS*, 2010, pp. 103–105.
- 223 D. J. Kinahan, M. T. Glynn, S. M. Kearney and J. Ducreé, *Proc. of  $\mu$ TAS*, 2012, pp. 1363–1365.
- 224 J.-M. Park, M. S. Kim, H.-S. Moon, C. E. Yoo, D. Park, Y. J. Kim, K.-Y. Han, J.-Y. Lee, J. H. Oh, S. S. Kim, W.-Y. Park, W.-Y. Lee and N. Huh, *Anal. Chem.*, 2014, **86**, 3735–3742.
- 225 S. Rodriguez-Mozaz, M. J. Lopez de Alda and D. Barceló, *Anal. Bioanal. Chem.*, 2006, **386**, 1025–1041.
- 226 Global Water Intelligence, 2009.
- 227 LaMotte, *WaterLink Spin Lab*, available at: <http://www.lamotte.com/en/pool-spa/labs/3576.html>.
- 228 Y. Xi, E. J. Templeton and E. D. Salin, *Talanta*, 2010, **82**, 1612–1615.
- 229 M. C. R. Kong and E. D. Salin, *Anal. Chem.*, 2012, **84**, 10038–10043.
- 230 J. P. Lafleur and E. D. Salin, *J. Anal. At. Spectrom.*, 2009, **24**, 1511.
- 231 J. P. Lafleur, A. A. Rackov, S. McAuley and E. D. Salin, *Talanta*, 2010, **81**, 722–726.
- 232 D. A. Duford, Y. Xi and E. D. Salin, *Anal. Chem.*, 2013, **85**, 7834–7841.
- 233 Y. Xi, D. A. Duford and E. D. Salin, *Talanta*, 2010, **82**, 1072–1076.
- 234 T. van Oordt, G. B. Stevens, S. K. Vashist, R. Zengerle and F. von Stetten, *RSC Adv.*, 2013, **3**, 22046.
- 235 L. Li and R. F. Ismagilov, *Annu. Rev. Biophys.*, 2010, **39**, 139–158.
- 236 V. Gubala, J. Siegrist, R. Monaghan, B. O'Reilly, R. P. Gandhiraman, S. Daniels, D. E. Williams and J. Ducreé, *Anal. Chim. Acta*, 2013, **760**, 75–82.
- 237 A. Bruchet, V. Taniga, S. Descroix, L. Malaquin, F. Goutelard and C. Mariet, *Talanta*, 2013, **116**, 488–494.
- 238 S.-K. Lee, G.-R. Yi and S.-M. Yang, *Lab Chip*, 2006, **6**, 1171.
- 239 N. R. Glass, R. J. Shilton, P. P. Y. Chan, J. R. Friend and L. Y. Yeo, *Small*, 2012, **8**, 1881–1888.
- 240 Samsung, *Samsung: LABGEO IB10*, available at: [http://www.samsungmedison.de/labgeo\\_ib10.aspx](http://www.samsungmedison.de/labgeo_ib10.aspx), accessed 19 September 2013.
- 241 Focus Diagnostics, *3M INTEGRATED CYCLER*, available at: <http://www.focusdx.com/3m-integrated-cycler>, accessed 8 May 2014.
- 242 Roche, *Roche: COBAS b 101*, available at: <http://www.cobas.com/home/product/cobas-b-101-poc-system.html>, accessed 8 May 2014.
- 243 Capitalbio, *Capitalbio: RTisochip*, available at: [http://www.bioon.com.cn/product/show\\_product.asp?id=284704](http://www.bioon.com.cn/product/show_product.asp?id=284704), accessed 8 May 2014.
- 244 Skyla, *Skyla: VB 1: Veterinary Clinical Chemistry Analyzer*, available at: <http://www.skyla.com/veterinarydetail.php?id=3>, accessed 16 September 2014.
- 245 Biosurfit, *Biosurfit: SpinIt*, available at: <http://www.biosurfit.com/>, accessed 8 May 2014.
- 246 Radisens Diagnostics, *Radisens Diagnostics*, available at: <http://www.radisens.com/>, accessed 8 May 2014.
- 247 Gene POC, *Gene POC*, available at: <http://www.genepoc-diagnostics.com/Home.shtml>, accessed 8 May 2014.
- 248 SpinChip Diagnostics AS, *SpinChip Diagnostics AS*, available at: <http://www.spinchip.no/>, accessed 8 May 2014.
- 249 J. Euske, *Sandia National Laboratories: Licensing/Technology Transfer SpinDx™: Point-of-Care Diagnostics Using Centrifugal Microfluidics*, available at: <https://ip.sandia.gov/technology.do/techID=82>, accessed 8 May 2014.
- 250 N. G. Anderson, *Clin. Chim. Acta*, 1969, **25**, 321–330.
- 251 M. J. Felton, *Anal. Chem.*, 2003, **75**, 302A.
- 252 R. M. Rocco, *Clin. Chem.*, 2006, **52**, 1977.
- 253 O. Strohmeier, M. Rombach, D. Mark, R. Zengerle, G. Roth and F. von Stetten, *Proceedings of Transducers*, 2011, pp. 2952–2955.
- 254 M. Focke, O. Strohmeier, P. Reith, G. Roth, D. Mark, R. Zengerle and F. von Stetten, *Proc. of  $\mu$ TAS*, 2011, pp. 659–661.

